

OPTIMIZATION OF TiO_2 PHOTOCATALYST IN AN ADVANCED OXIDATION
PROCESS FOR THE TREATMENT OF LANDFILL LEACHATE

by

Frank Youngman

A Thesis Submitted to the Faculty of
The College of Engineering and Computer Science
in Partial Fulfillment of the Requirements for the Degree of
Master of Science

Florida Atlantic University

Boca Raton, Florida

May 2013

UMI Number: 1523459

All rights reserved

INFORMATION TO ALL USERS

The quality of this reproduction is dependent upon the quality of the copy submitted.

In the unlikely event that the author did not send a complete manuscript and there are missing pages, these will be noted. Also, if material had to be removed, a note will indicate the deletion.



UMI 1523459

Published by ProQuest LLC (2013). Copyright in the Dissertation held by the Author.

Microform Edition © ProQuest LLC.

All rights reserved. This work is protected against unauthorized copying under Title 17, United States Code



ProQuest LLC.
789 East Eisenhower Parkway
P.O. Box 1346
Ann Arbor, MI 48106 - 1346

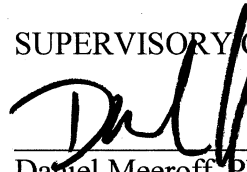
OPTIMIZATION OF TIO₂ PHOTOCATALYST IN AN ADVANCED OXIDATION
PROCESS FOR THE TREATMENT OF LANDFILL LEACHATE

by

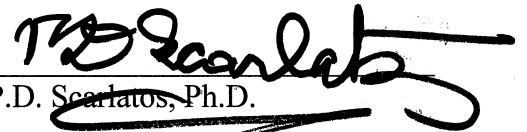
Frank Youngman

This thesis was prepared under the direction of the candidate's thesis advisor, Dr. Daniel E. Meeroff, Department of Civil Engineering, and has been approved by the members of his supervisory committee. It was submitted to the faculty of the College of Engineering and Computer Science and was accepted in partial fulfillment of the requirements for the degree of Master of Science.

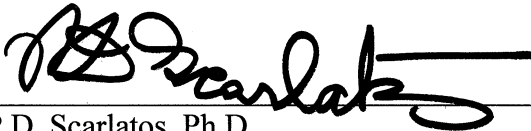
SUPERVISORY COMMITTEE:



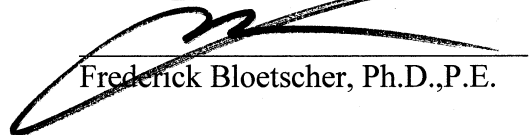
Daniel Meeroff, Ph.D., E.I.
Thesis Advisor



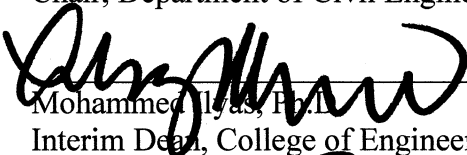
P.D. Scarlatos, Ph.D.



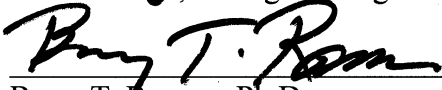
P.D. Scarlatos, Ph.D.
Chair, Department of Civil Engineering



Frederick Bloetscher, Ph.D., P.E.



Mohammed Ilyas, Ph.D.
Interim Dean, College of Engineering and Computer Science



Barry T. Rosson, Ph.D.
Dean, Graduate College

April 12, 2013
Date

ACKNOWLEDGEMENTS

The author wishes to express his recognition to the William W. “Bill” Hinkley Center for Solid and Hazardous Waste Management Council for the funding of this project.

The author wishes to express his sincere thanks to his advisor, Dr. Meeroff, Associate Professor and Director of the Laboratories for Engineered Environmental Solutions, Department of Civil Engineering, for his excellent suggestions, encouragement, review and support.

The author would also thank the other members of his Committee: Dr. Bloetscher, Associate Professor, and Dr. Scarlatos, Department Chair and Professor, for their reviews and suggestions.

Thanks to the members of the Technical Advisory Group for their guidance and help throughout the project.

Thanks to Jeff Roccapiore and Stephen “Leroy” Melton for their assistance collecting samples from Monarch Hill Landfill.

Special thanks are also due to my family and close friends who never stopped believing in me. Without their collective support and encouragement this would not have been possible.

ABSTRACT

Author: Frank Youngman
Title: Optimization of TiO₂ Photocatalyst in an Advanced Oxidation Process for the Treatment of Landfill Leachate
Institution: Florida Atlantic University
Thesis Advisor: Dr. Daniel Meeroff
Degree: Master of Science
Year: 2013

Since the United States Environmental Protection Agency (USEPA) began requiring landfills to implement a leachate collection system in 1991, the proper disposal of leachate has become a growing concern. The potential toxicity of landfill leachate will contaminate groundwater and soil if not managed properly. Research has been made in efforts to manage leachate in a cost-effective, single treatment process. Photocatalytic oxidation is an advanced oxidation process (AOP) which has shown ability to reduce toxicity of an array of leachate constituents including organics, inorganics and heavy metals. The purpose of this manuscript is to scale up the batch scale study of TiO₂ photocatalytic degradation of leachate utilizing a pilot scale falling film reactor. In this research project, the use of UV/TiO₂ for the removal of chemical oxygen demand (COD), ammonia, alkalinity and color will be studied in order to optimize catalyst dosage, determine pH effects and reaction kinetics and develop preliminary cost estimates.

OPTIMIZATION OF TiO_2 PHOTOCATALYST IN AN ADVANCED OXIDATION
PROCESS FOR THE TREATMENT OF LANDFILL LEACHATE

LIST OF TABLES	ix
LIST OF FIGURES	xiii
1.0 INTRODUCTION	1
1.1 Leachate Quality	2
1.2 Pollutants of Concern.....	4
1.3 Leachate Quantities.....	7
1.4 Methods of Leachate Management.....	9
1.5 Advanced Oxidation	13
1.5.1 COD Removal.....	14
1.5.2 Ammonia Removal	16
1.5.3 Heavy Metal Removal	17
1.6 TiO_2 Photocatalyst	19
1.7 TiO_2 Photocatalysis.....	21
1.7.1 Pollutant Removal.....	25
1.7.2 pH Effect.....	30
1.7.3 Catalyst Poisoning	31

1.7.4 Process Modifications	33
1.8 Objectives	36
2.0 METHODOLOGY	38
2.1 Leachate Collection	38
2.2 Pilot Scale Falling Film Reactor	42
2.3 Mechanical Improvements/Additions	47
2.4 Experimental Procedure	56
2.5 UV dosage testing	60
2.6 Analytical Methods for Parameters of Interest	61
2.6.1 COD	61
2.6.2 Ammonia-Nitrogen	63
2.6.3 Alkalinity	65
2.6.4 Color	65
2.6.5 pH	66
2.6.6 Temperature	66
2.6.7 Chloride	66
2.7 Catalyst Recovery	67
3.0 RESULTS AND DISCUSSION	70
3.1 Baseline Leachate Quality Characterization	70
3.2 Preliminary Testing	70

3.3 Preliminary Assessment of Pilot Performance	74
3.4 Experiment 1	77
3.4.1 COD Kinetics.....	79
3.4.2 Alkalinity Kinetics	82
3.4.3 Ammonia Kinetics	86
3.4.4 Color Kinetics	88
3.5 Experiment 2.....	90
3.5.1 COD Kinetics.....	91
3.5.2 Alkalinity Kinetics	94
3.5.3 Ammonia Kinetics	96
3.5.4 Color Kinetics	98
3.6 Experiments 3 - 6.....	100
3.6.1 COD Removal.....	103
3.6.2 Ammonia Removal	106
3.6.3 Alkalinity Removal.....	110
3.6.4 Color Removal	113
3.7 Catalyst Optimization	117
3.8 Catalyst Recovery	118
4.0 CONCLUSIONS AND RECOMMENDATIONS	124
4.1 Summary of Findings.....	124

4.2 Preliminary Cost Analysis	127
4.3 Recommendations.....	130
APPENDIX A: Data for Experiments 1 – 6	135
APPENDIX B: Typical Temperature Recordings	142
APPENDIX C: Prediction Tables.....	151
APPENDIX D: UV data recordings	153
APPENDIX E: MSDS	156
REFERENCES	170

LIST OF TABLES

Table 1: USEPA Effluent limitations for non-hazardous waste landfill (40 CFR 445.21)	2
Table 2: Summary of leachate water quality composition derived from literature review.....	3
Table 3: Broward County sewer use limitations surcharge levels (Sewer Use Ordinance, Broward County Code Chapter 34 Article VI, Ordinance No. 2001-43)	5
Table 4: Leachate generation rates for 31 Florida landfills (Meeroff and McBarnett 2011).....	8
Table 5: Monarch Hill leachate concentration versus Broward County Sewer use limitations	12
Table 6: Advanced Oxidation Processes.....	14
Table 7: Physical Components of Degussa Aeroxide TiO ₂ P-25	20
Table 8: Properties of anatase and rutile forms of titanium dioxide.....	20
Table 9: Chain of oxidative-reductive reactions that occur at the UV activated TiO ₂ surface (Chong et al. 2010).....	22
Table 10: COD removal efficiencies of TiO ₂ photocatalysis	29
Table 11: Rate constant juxtaposition of fresh and regenerated catalysts (Gandhi et al. 2012)	32
Table 12: Summary of experimental data in treatment of paper mill waste water	36
Table 13: Technical data on the falling film reactor.....	60

Table 14: Summary of Leachate Water Quality Testing Results	70
Table 15: Summary of maximum UV intensities recorded and doses calculated	72
Table 16: Summary of all six pilot scale experiments with parameter removal at 24 hours.....	76
Table 17: Removal of parameters from experiment 1 (4 g/L TiO ₂) after 44 hours	77
Table 18: Removal of parameters from experiment 2 (16 g/L TiO ₂) after 40 hours	90
Table 19: COD removal predictions for experiments 1 and 2 using 24 hour k-values from first order kinetics	100
Table 20: Summary of parameter removal at 24 hours for experiments 1 – 6	101
Table 21: Comparison of times to achieve target level COD removal using first order decay rates from six experiments.....	105
Table 22: Comparison of times to achieve target level ammonia removal using first order decay rates from six experiments	108
Table 23: Comparison of pH range and ammonia removal for every 4 hour time interval up to 24 hours	109
Table 24: Comparison of times to achieve 90% alkalinity removal using first order decay rates from six experiments.....	112
Table 25: Color concentration change after adding TiO ₂ to raw leachate insert a column with percent change	114
Table 26: Slopes and R ² values for color comparison graph	115
Table 27: Comparison of times to achieve 90% color removal using zero order decay rates from six experiments	116
Table 28: Summary of results from catalyst recovery experiment	119

Table 29: Preliminary cost analysis based on pilot reactor optimal catalyst dose.....	129
Table 30: Preliminary cost estimate based on batch reactor conditions	130
Table 31: Data for Experiment 1 (4 g/L TiO ₂)	136
Table 32: Data for Experiment 2 (16 g/L TiO ₂)	137
Table 33: Data for Experiment 3 (25 g/L TiO ₂)	138
Table 34: Data for Experiment 4 (40 g/L TiO ₂)	139
Table 35: Data for Experiment 5 (30 g/L TiO ₂)	140
Table 36: Data for Experiment 6 (10 g/L TiO ₂)	141
Table 37: Experiment 1 Day 8 Temperature recordings.....	143
Table 38: Experiment 2 Day 5 Temperature recordings.....	144
Table 39: Experiment 3 Day 5 Temperature recordings.....	145
Table 40: Experiment 4 Day 2 Temperature recordings.....	146
Table 41: Experiment 5 Day 4 Temperature recordings.....	147
Table 42: Experiment 6 Day 1 Temperature recordings.....	148
Table 43: Alkalinity removal predictions for experiments 1 and 2 using 24 hour k-values from first order kinetics	152
Table 44: Ammonia removal predictions for experiments 1 and 2 using 24 hour k-values from first order kinetics	152
Table 45: Color removal predictions for experiments 1 and 2 using 24 hour k-values from zero order kinetics	152
Table 46: Trial 1 of UV measurements.....	154
Table 47: Trail 2 of UV measurements.....	154

Table 48: Trial 3 of UV measurements, taken at 45° angle..... 155

Table 49: Trial 4 of UV measurements, taken at 5.38” from source 155

LIST OF FIGURES

Figure 1: Schematic of sloping trough circulating bed reactor (Liu et. al 2012).....	15
Figure 2: Generalized process of photocatalytic oxidation (Ghaly et al. 2011)	23
Figure 3: Aerial view of Monarch Hill Landfill	39
Figure 4: S.E. Step-up Station Sampling Port.....	40
Figure 5: Aerial photograph of the Broward County North Regional Wastewater Treatment plant	41
Figure 6: Leachate Sampling on 7/18/2012	42
Figure 7: CE 584 Advanced Oxidation Machine.....	43
Figure 8: Photographs of the falling film pilot reactor (left: close up view of the reaction chamber; right: overall view).....	43
Figure 9: Main Components of CE 584 Advanced Oxidation.....	44
Figure 10: Flow Path of Advanced Oxidation Machine	45
Figure 11: Irradiation spectrum for the Strahler NNI 125/84 XL low pressure UV lamp as provided by the manufacturer.....	46
Figure 12: Control Panel for CE584 Advanced Oxidation Machine.....	47
Figure 13: Catalyst settling location in the advanced oxidation machine	48
Figure 14: 3-way valve modification to CE584.....	49
Figure 15: Pump flushing flow path	50

Figure 16: Temperature rise before cooling (left) and after cooling (right)	51
Figure 17: VWR Recirculating Cooler 1150S	52
Figure 18: Recirculating cooler hose surrounding leachate reservoir (left) and Frank Youngman testing the temperature control system provided by the recirculating chiller unit	53
Figure 19: Air pump system	54
Figure 20: Pictorial display of Y-attachment in air pump system	55
Figure 21: 2L of leachate in a 2000 mL graduated cylinder	57
Figure 22: 8L of leachate in CE584 reservoir	58
Figure 23: Leachate containing TiO ₂ photocatalyst	59
Figure 24: UV distance from reactor wall denotation	61
Figure 25: Reagent addition to cuvette for ammonia testing	63
Figure 26: Sample reading from HI 95715 Ammonia Medium Range ISM	64
Figure 27: Nylon monofilament filter bag attached to advanced oxidation machine for catalyst recovery	68
Figure 28: Typical temperature curve collected during one of the 4-hour pilot test runs (January 13, 2012)	71
Figure 29: Time plots for the evaporation experiment. Temperature curve (left) and evaporation loss curve (right)	73
Figure 30: Results of dark reaction for falling film reactor	74
Figure 31: Removal rate comparison of alkalinity, ammonia and COD using 4 g/L TiO ₂	78
Figure 32: Zero order COD kinetics plot for experiment 1 (4 g/L TiO ₂)	79

Figure 33: First order COD kinetics plot for experiment 1 (4 g/L TiO ₂)	80
Figure 34: Second order COD kinetics plot for experiment 1 (4 g/L TiO ₂).....	80
Figure 35: Zero order alkalinity kinetics plot for experiment 1 (4 g/L TiO ₂).....	83
Figure 36: First order alkalinity kinetics plot for experiment 1 (4 g/L TiO ₂).....	83
Figure 37: Second order alkalinity kinetics plot for experiment 1 (4 g/L TiO ₂)	84
Figure 38: Zero order ammonia kinetics plot for experiment 1 (4 g/L TiO ₂).....	86
Figure 39: First order ammonia kinetics plot for experiment 1 (4 g/L TiO ₂).....	87
Figure 40: Second order ammonia kinetics plot for experiment 1 (4 g/L TiO ₂).....	87
Figure 41: Zero order color kinetics plot for experiment 1 (4 g/L TiO ₂)	88
Figure 42: First order color kinetics plot for experiment 1 (4 g/L TiO ₂).....	89
Figure 43: Second order color kinetics plot for experiment 1 (4 g/L TiO ₂)	89
Figure 44: Zero order COD kinetics plot for experiment 2 (16 g/L TiO ₂)	92
Figure 45: First order COD kinetics plot for experiment 2 (16 g/L TiO ₂)	92
Figure 46: Second order COD kinetics plot for experiment 2 (16 g/L TiO ₂).....	93
Figure 47: Zero order alkalinity kinetics plot for experiment 2 (16 g/L TiO ₂).....	94
Figure 48: First order alkalinity kinetics plot for experiment 2 (16 g/L TiO ₂).....	94
Figure 49: Second order alkalinity kinetics plot for experiment 2 (16 g/L TiO ₂)	95
Figure 50: Zero order ammonia kinetics plot for experiment 2 (16 g/L TiO ₂).....	96
Figure 51: First order ammonia kinetics plot for experiment 2 (16 g/L TiO ₂).....	97
Figure 52: Second order ammonia kinetics plot for experiment 2 (16 g/L TiO ₂).....	97
Figure 53: Zero order color kinetics plot for experiment 2 (16 g/L TiO ₂)	98

Figure 54: First order color kinetics plot for experiment 2 (16 g/L TiO ₂).....	99
Figure 55: Second order color kinetics plot for experiment 2 (16 g/L TiO ₂)	99
Figure 56: Comparison plot of first order COD removal after 24 hours for the catalyst dosages from six experiments.....	104
Figure 57: Comparison plot of first order ammonia removal after 24 hours for the catalyst dosages from six experiments.....	107
Figure 58: Comparison plot of first order alkalinity removal after 24 hours for the catalyst dosages from six experiments.....	111
Figure 59: Color comparison for raw leachate (left) vs. leachate w/ TiO ₂ (right).....	113
Figure 60: Comparison plot of zero order color removal after 24 hours for the catalyst dosages from six experiments.....	115
Figure 61: Catalyst optimization curve for COD removal at 24 hours for six experiments.....	117
Figure 62: 5 micron nylon monofilament filter bag filled with treated leachate	120
Figure 63: Interface height vs. Time plot for Talmadge and Fitch method.....	123
Figure 64: Temperature curve for Experiment 1 Day 8.....	143
Figure 65: Temperature curve for Experiment 2 Day 5.....	144
Figure 66: Temperature curve for Experiment 3 Day 5.....	145
Figure 67: Temperature curve for Experiment 4 Day 2.....	146
Figure 68: Temperature curve for Experiment 5 Day 4.....	147
Figure 69: Temperature curve for Experiment 6 Day 1.....	150
Figure 70: MSDS for Titanium Dioxide.....	162

Figure 71: MSDS for COD digestion vials..... 169

1.0 INTRODUCTION

The most widely used form of waste disposal in the U.S. is the sanitary landfill (USEPA 2012). Landfill regulations have been enacted by the U.S. EPA to prevent the spread of leachate contaminants into the groundwater and soil underneath landfills (Qasim and Chiang 1994). Leachate is created when liquid, mostly rain water, percolates through the waste inside the landfill, picking up contaminants along the way. A significant problem with leachate is its high variability. Leachate quantities are directly related to the amount of rain water received by the landfill and the number of open acres being filled. The quality varies according to the waste that the water passes through along the way to the bottom of the landfill liner and collection system. Every landfill's leachate is different and a single landfill's leachate can vary at different points of time.

Because of the potential toxicity of the contaminants in municipal solid waste, leachate will pollute the groundwater and soil underneath and downstream of the landfill if the leachate is not properly managed. The United States Environmental Protection Agency (USEPA) regulations require landfills to implement a leachate collection system to prevent the leachate from being released into the environment: "New Municipal Waste Solid Landfill (MSWLF) units and lateral expansions shall be constructed with a composite liner and a leachate collection system that is designed and constructed to maintain less than a 30-cm depth of leachate over the liner." (40 CFR 258.40). In the

absence of a leachate collection system, the leachate that is released to the environment becomes difficult and/or too expensive to manage because of the widely varying nature of the contaminants (Westlake 1995).

1.1 Leachate Quality

The USEPA (40 CFR 445.21) requires that the effluent from a non-hazardous waste sanitary landfill does not exceed the limitations displayed in Table 1.

Table 1: USEPA Effluent limitations for non-hazardous waste landfill (40 CFR 445.21)

Regulated Parameter	Units	Maximum Daily	Maximum Monthly Average
BOD	mg/L	140	56
TSS	mg/L	88	27
Ammonia	mg/L as N	10	4.9
α -Terpineol	mg/L	0.033	0.016
Benzoic acid	mg/L	0.120	0.071
<i>p</i> -Cresol	mg/L	0.025	0.014
Phenol	mg/L	0.026	0.015
Zinc	mg/L	0.200	0.11
pH	pH units	6 - 9	6 - 9

The USEPA defines the effluent limitations in 40 CFR 122.2 as “any restriction imposed on the quantities, discharge rates and concentrations of pollutants which are discharged into waters of the United States.” When discharging sanitary landfill leachate, meeting these limitations can be challenging. The amount of contaminants in leachate can far exceed these effluent limitations. It is difficult to define a typical landfill leachate because each landfill produces varying compositions of leachate at different times. A review of leachate water quality from 125 sources reported in the literature is

summarized in Table 2. Each of the references cited in Table 2 included the leachate water quality parameters of the leachate used within the study.

Table 2: Summary of leachate water quality composition derived from literature review

Parameter	Units	Concentration	
		Range	Average
Ammonia	mg/L as NH ₃ -N	BDL* – 13,000	1,100
BOD ₅	mg/L as O ₂	BDL* – 80,800	3,100
COD	mg/L as O ₂	0.4 – 152,000	8,750
Conductivity	µS/cm	5.2 – 95,000	15,400
Lead (Pb)	mg/L	BDL* – 5.0	0.41
pH	pH units	2.0 – 11.3	7.73
TDS	mg/L	0.1 – 88,000	11,100
TSS	mg/L	10 – 45,000	1,120
Alkalinity	mg/L as CaCO ₃	3,300 – 11,000	9,640
Color	Platinum-Cobalt Units	3,530 – 40,000	3,630

BDL* = below detectable level

Source: Renou et al. (2008), Akesson and Nilsson (1997), Al-Yaqout et al. (2005), Amokrane et al. (1997), Bekbölet et al. (1996), Bernard et al. (1997), Bila et al. (2005), Calli et al. (2005), Geenens et al. (2000), Gonze et al. (2003), Hickman (2003), Imai et al. (1998), Ince (1998), Kim et al. (1997), Kjeldsen et al. (2002), Lin et al. (2000), Mohammad et al. (2004), Moraes and Bertazzoli (2005), Morais and Zamora (2005), O'Leary and Walsh (1995), Oweis and Kehra (1998), Tammemagi (1999), Tatsi et al. (2003), Tchobanoglous and Kreith (2002), Reinhart and Grosh (1998), Reinhart and Townsend (1998), Silva et al. (2003), Silva et al. (2004), Solid Waste Authority of Palm Beach County (2006), Statom et al. (2004), Steensen (1997), Ward et al. (2002), Westlake and Phil (1995), Wichitsathian et al. (2004), Wu et al. (2004), Youcai et al. (2002), Li et al. (2009), Jia et al. (2011), Iaconi et al. (2010), Kima et al. (2007), Abu Amr and Aziz (2012), Deng and Ezyske (2011), Vilar et al. (2011), Mahmud et al. (2011), Zhao et al. (2010), Anglada et al. (2011), Poblete et al. (2012), Tamrat et al. (2012), Salem et al. (2008), Aziz et al. (2011), Adlan et al. (2011), Kurniawan and Lo (2009), Bashir et al. (2010), Mohajeri et al. (2010), Bouhezila et al. (2011).

The ranges in Table 2 show the extreme concentration values that were reported.

The large ranges reported as the result of the high variability among leachates is the reason that the average values cannot be taken as a typical leachate, there is no such thing. It is important to note that leachate can have very high concentrations of many different constituents, many of which are known to have deleterious impacts in groundwater and soil. Aside from those listed in Table 2, there are numerous other constituents found in leachate ranging from heavy metals (e.g., cadmium, chromium,

mercury, arsenic, nickel, selenium, iron, manganese, silver, copper, lead, thallium, zinc and others), other inorganic components (e.g., ammonium, barium, beryllium, bicarbonate, chloride, magnesium, manganese, nitrate, phosphorus, potassium, sodium, sulfate and others) (Qasim and Chiang 1994), and an array of organic constituents including xenobiotic organic compounds (XOCs) such as: BTEX (benzene, toluene, ethylbenzene, and xylene), antibiotics and other pharmaceuticals, pesticides, herbicides and endocrine disrupting compounds (EDCs) (Baun et al. 2003).

1.2 Pollutants of Concern

This work focuses on the primary pollutants that have been specified to the Broward County, FL effluent limitations. The leachate used here was collected from Monarch Hill Landfill and their specific pollutants of concern pose negative impacts on the environment as well as economic setbacks as a result of fines based upon regulations. These parameters are Chemical Oxygen Demand (COD), ammonia, alkalinity, and color.

COD is a measure of the total quantity of oxygen required to chemically oxidize organic and inorganic matter in water or wastewater (EPA 2012). COD is typically reported as an amount of oxygen in mg/L and COD was chosen as a primary parameter over biochemical oxygen demand (BOD) due to first-hand reported local issues with municipal solid waste disposal sites (Monarch Hill landfill reported exceedance fees incurred on account of elevated COD levels). BOD is a similar parameter which measures the amount of oxygen necessary for microorganisms to degrade the organic material in the water or wastewater. COD is generally higher than BOD because COD includes the oxidation of recalcitrant materials which would not normally be degraded by biological breakdown. A COD test is performed in a matter of hours while a BOD test, in

which bacteria must degrade the organic matter, generally takes 5 days or longer (Masters and Ela 2008). A high concentration of COD present in water causes low dissolved oxygen (DO) level, which can be toxic to all aquatic life. The U.S. government currently has set limitations for BOD (see Table 1), but not for COD. Local sewer use limitations (Sewer Use Ordinance, Broward County Code Chapter 34 Article VI, Ordinance No. 2001-43 for example) typically charge a fine for high strength wastewater if COD concentration exceeds 800 mg/L (see Table 3).

Table 3: Broward County sewer use limitations surcharge levels (Sewer Use Ordinance, Broward County Code Chapter 34 Article VI, Ordinance No. 2001-43)

Parameter	Units	High strength wastewater surcharge can apply if concentrations are:
BOD ₅	mg/L	Greater than 400
COD	mg/L	Greater than 800
TSS	mg/L	Greater than 400
TKN	mg/L	Greater than 30 and not exceeding 100
NH ₃ -N	mg/L	Greater than 25 and not exceeding 70
Total P	mg/L	Greater than 5 and not exceeding 20
O&G (Oil and Grease)	mg/L	Greater than 100 and not exceeding 500

Ammonia (NH₃) is an inorganic form of nitrogen that is created naturally in the environment, especially during the anaerobic degradation of many organics compounds (EPA 2012). Ammonia is a colorless gas which is easily dissolved in water and is used as such in many household cleaners (NYSDOH 2004), although when aqueous ammonia is exposed to open air it rapidly turns to a gas. Ammonia produces a strong odor which is said to be similar to drying urine (Commonwealth of Australia 2010). The concentration of ammonia in water depends on various factors including pH and temperature. The concentration of ammonia is higher in waters with increased temperatures and/or pH

(EPA 1985). Concentrations of ammonia at levels of 0.03 mg/L have been found to be toxic to aquatic life. The LC₅₀ (Lethal Concentration which is fatal to 50% of the subjects) for freshwater fish occurs at 0.068 – 2.00 mg/L as NH₃-N, during a set exposure time of 96 hours (Eddy 2005). Toxicological effects of ammonia in humans are observed at levels greater than 200 mg/kg (WHO 2004). Below that extreme level of ingestion ammonia is not a concern for drinking water standards. Taste and odor issues have been reported at levels of 35 mg/L and 1.5 mg/L, respectively (WHO 2004). Ammonia levels naturally found in groundwater and surface water are usually less than 0.2 mg/L, although anaerobic groundwaters may have levels near 3 mg/L. In the state of Florida, ammonia is identified as a “minimum criteria systemic toxicant” and has a groundwater cleanup target level (CTL) of 2.8 mg/L. The CTL is not a regulation or standard, but rather a suggestion for water quality. The concentrations found in leachate, which were shown in Table 2 (up to 13,000 mg/L as NH₃-N), far exceed these levels, which is one reason that ammonia must be regulated. Broward County sewer use limitations stipulate high strength wastewater surcharges if the NH₃-N is above 25 mg/L as NH₃-N and they do not permit concentrations above 70 mg/L as NH₃-N (refer to Table 3).

Alkalinity is a measurement of the capability for water to accept protons (H⁺ ions) or protons, without a measurable change in pH level. This is the parameter of water which works to retain the pH level in the range of 6.0 - 8.5 pH units. Alkalinity is most often expressed in mg/L as CaCO₃. Alkalinity found in natural waters mostly derives from the carbonate system (Carbonic Acid (H₂CO₃), Bicarbonate (HCO₃⁻), Carbonate (CO₃²⁻), and aqueous Carbon Dioxide (CO_{2(aq)})) (Manahan 2005). The absence of this acid buffering capacity would result in immediate pH change in the presence of any

added acid. The USEPA has a recommended Criterion Continuous Concentration (CCC) for alkalinity set at 20 mg/L as CaCO₃ in their aquatic life criteria table (USEPA 2012). In the USEPA's Human Health Criteria table, alkalinity is simply listed as a Non-Priority Pollutant (NP) and no recommended value is given (USEPA 2012).

Color is usually the first noticeable attribute of water. The presence of color in water can be caused by a number of factors. It can represent dissolved solids, suspended solids or the presence of organic matter and/or inorganic matter. The USEPA has set secondary standards for color in water at 15 platinum-cobalt units (USEPA 2012). As seen previously in Table 2, even the low range value of color in leachate (3,530 – 40,000) has a much higher concentration than this standard, which signifies that a large amount of color must be removed to reach the desired level. The color itself does not impact human health; it is just an issue of aesthetics. However, the presence of color can provide evidence of contamination. Determination of the cause of color is necessary to ascertain whether toxicological effects will be experienced when exposed to or ingesting the water (SWRCB 2010).

1.3 Leachate Quantities

Another challenge to the management of leachate is the variable quantities of this material generated by every landfill. The volume of leachate produced depends on the amount of rain that percolates through the landfill and the exposed surface area. Other factors which influence the volume of leachate include: surface runoff, groundwater intrusion, liquid waste in landfill, irrigation, evapotranspiration, landfill depth and refuse composition (Westlake 1995). A survey was performed by Florida Atlantic University (Meeroff and Teegavarapu 2010) polling 52 landfills in the state of Florida about their

leachate generation rates. For the survey, facilities were divided into four different size classes based on their capacity: small (500,000 MT), medium (5,000,000 MT), large (15,000,0000 MT), and very large or super (> 15,000,000 MT) (USEPA 1999). The results of the survey from the 31 facilities that responded showed flows ranging from less than 100 to nearly 3,000 gpd/acre (refer to Table 4).

Table 4: Leachate generation rates for 31 Florida landfills (Meeroff and McBarnett 2011)

Class	Range (gpd/acre)	Number of landfills
Small	<100	14
Medium	100-300	9
Large	300-850	6
Super	>850	2

The Hydrologic Evaluation of Landfill Performance (HELP) model is a computer program developed by the Waterways Experiment Station (WES), which is the headquarters for the U.S. Army Engineer Research and Development Center (ERDC) (USEPA 2012). The HELP model is used to estimate the generation of leachate from landfills for comparison efforts in the planning and design of the landfill and leachate collection system. The HELP model gives a theoretical value in the South Florida area of 2,000 – 3,000 gpd/acre, which is the design value used for most landfills in the Southeast Florida region. However, most landfills do not have properly calibrated flow meters to record the actual leachate volumes and leachate is also generated in partially lined cells or older systems (Meeroff and McBarnette 2011).

1.4 Methods of Leachate Management

The high strength concentrations along with the highly variable generation rates of leachate create a great deal of difficulty in managing environmentally safe disposal, especially with the growing use of synthetic organic compounds and heavy metals. There are a number of methods currently utilized in leachate management from physical to chemical to biological processes. A review of the currently available treatment processes can provide a basis for the most appropriate leachate management strategies for the future.

One commonly used management option is off-site hauling. Landfills will collect their leachate and send truckloads of the liquid waste to an ultimate disposal site; typically an off-site publicly-owned treatment works (POTW). This method does not address the ultimate disposal of leachate; it simply moves the leachate to another location off-site. For example, Polk County, FL reported a three year contract they signed in July 2009 for the disposal of their landfill leachate at \$130 per thousand gallons (Blandford 2011). Another issue is that not all wastewater treatment plants will accept leachate “as is.” Due to the extremely high concentrations found, large volumes of leachate can upset the normal biological treatment processes at the plant, which may lead to expensive surcharge rates or even rejection. The costs associated with hauling can also vary depending on: the cost of fuel, the distance the leachate needs to travel, and if there is a need to pre-treat the liquid waste prior to wastewater treatment plant acceptance.

Another management practice is deep well injection. The leachate is pumped deep into the ground below the aquifer and between confining layers to assure separation from the groundwater supply. The biggest concern with deep well injection is the risk of

contamination of the drinking water supply. The exact geology thousands of feet underground can be difficult to establish with full certainty. Even a minor leak can cause a substantial problem as groundwater remediation is an incredibly difficult task at these depths. The USEPA has developed specific requirements for Class 1 Municipal Disposal Wells in Florida in areas where wastewater is disposed of underneath underground sources of drinking water (USDW). The requirements emerged in 2005 due to evidence pointing to the upward migration of the injected wastewaters in certain locations (USEPA 2011). The rules required all new waste water discharges to undergo primary and secondary treatment in accordance with Florida Rule 62-600.540 prior to any deep well injection.

Leachate recirculation is another option for managing leachate. This process consists of reintroducing the landfill leachate back into the landfill. The recirculating leachate accelerates the breakdown of organic materials within the landfill (Xing et al. 2012). This leads to increased methane production which must be managed to prevent elevated photochemical ozone formation (Xing et al. 2012). The build-up of head pressure from the increased amount of leachate in the bottom of the landfill creates higher potential for the leachate to escape the landfill into the environment and towards the ground water and soil. Tropical climates make leachate circulation difficult due to high temperatures and elevated levels of evaporation, which lowers the moisture content of the solid waste thereby diminishing the biological activity. One study determined the effect of applying additional water in order to maintain certain levels of moisture, on the methane production and stabilization of the landfill. It was found that supplementing the leachate with water kept elevated levels of methane production and lower time periods of

landfill stabilization (Sanphoti et al. 2006). The implementation of a leachate recirculation system requires high capital and recurring maintenance costs. Also, odor problems from leachate recirculation are common (McBarnette 2011).

Evaporation is another practice used in managing landfill leachate. The primary objective of the evaporation/distillation process is to produce a high quality condensate that can be disposed of in less troublesome ways than conventional leachate. The rate of evaporation depends on the ambient temperature and humidity conditions. It is possible to control the evaporation rate by utilizing a thermal treatment, but this requires additional equipment and energy to generate the heat necessary (Zhao et al. 2012). Evaporation rates change with seasonal variations in temperature and other conditions, making evaporation difficult in areas where excessive humidity and/or rain or excessive cold temperatures are common. The high levels of humidity in Florida diminish evaporation rates and make the evaporation of leachate an inefficient method of leachate management. These limited options point to the need to develop an onsite treatment process.

The Monarch Hill landfill in Pompano Beach, FL currently pumps its leachate directly to the Broward County Regional Wastewater Treatment Facility. When comparing the typical values of the Monarch Hill leachate to the Broward County sewer discharge limits, it can be seen that additional surcharges (which are applied when the limits have been exceeded) are incurred (see Table 5).

Table 5: Monarch Hill leachate concentration versus Broward County Sewer use limitations

Parameter	Units	Broward County Discharge Limitation	Typical Monarch Hill leachate
COD	mg/L	800	5,700
NH ₃ -N	mg/L	25 - 70	1,600
BOD ₅	mg/L	400	700
Copper	µg/L	2.0	2.6
Lead	µg/L	0.8	2.9

Table 5 shows that the concentrations of both the COD and ammonia greatly exceed the regulations, resulting in fines being assessed. The typical leachate from Monarch Hill also exceeds the limit for lead and copper. BOD and COD are generally treated through an activated sludge process and less commonly through ozonation, ion exchange, coagulation/flocculation and adsorption (Qasim et al. 2000). Ammonia is typically removed from wastewater by means of air stripping, ion exchange, breakpoint chlorination, membranes and/or the use of nitrifying bacteria (Hammer and Hammer 2011). Copper and lead are typically removed from waste waters by precipitation processes and/or ion exchange (Hammer and Hammer 2011). Based on those four constituents alone, the leachate would likely require multiple treatment processes to reach the appropriate effluent limitations. Due to the inconsistency of landfill leachate, a universal treatment is difficult to come by. While there are effective treatments available for individual characteristics of leachate, an effective comprehensive treatment process has yet to be established. Removal of individual parameters is possible and the removal processes are performed routinely in wastewater and drinking water treatment. These processes are different for leachate because it has such high concentrations and varied combinations of contaminants that a more universal treatment technique is required to be

cost effective. The development of such a technique is still in the stages of research and experimentation. The main objective of an alternative method of leachate treatment is to find an effective process that can address the multitude of parameters landfill leachate possesses to the point where an acceptable, safe discharge is produced. Recent research suggests that advanced oxidation processes have the potential to solve the leachate management dilemma, with their ability to remove even refractory organics, reduce heavy metals, and oxidize copious amounts of hazardous compounds, including ammonia (Wang and Xu 2012).

1.5 Advanced Oxidation

Advanced oxidation processes (AOPs) are methods that promote the creation of and utilize highly reactive oxidants, such as hydroxyl radicals, ozone and chlorine. These species have oxidation potentials of 2.70, 2.07 and 1.49 electron volts, respectively (Kommineni et al. 2000). Advanced oxidation processes have gained interest and popularity in the past two decades as methods for treating industrial wastewater due to the high removal efficiencies for organic and inorganic contaminants. These oxidation reactions produce radicals which are chemical species that possess an unpaired electron, causing them to be very unstable. The unstable radicals attempt to stabilize themselves by reacting with surrounding species. The radicals will continue to react with substances until stability is reached. Some AOPs focus primarily on the generation of hydroxyl radicals and their reaction with the contaminants in the water. Many different advanced oxidation processes exist. Some of these include a combination of ultraviolet light (UV), hydrogen peroxide (H_2O_2), and/or O_3 . AOPs can be accelerated by using catalysts such as $Fe^{2+/3+}$ and/or TiO_2 . A partial list of commonly used AOPs is shown in Table 6.

Table 6: Advanced Oxidation Processes

Process	Type of Reaction
H_2O_2/Fe^{2+}	Fenton reaction
H_2O_2/Fe^{3+}	Fenton-like reaction
$H_2O_2/Fe^{2+/3+}/UV$	Photo assisted Fenton
H_2O_2/Fe^{3+} -oxalate/UV	Photo assisted Fenton w/ferrioxalate
$H_2O_2/Fe^{2+}/I$ (electric current)	Fered-Fenton method
$Mn^{2+}/O_3/Oxalic\ acid$	Manganese/Ozone/Oxalic acid
O_3/H_2O_2	Ozone/Hydrogen Peroxide
H_2O_2/GAC	Hydrogen Peroxide/Granular Activated Carbon
O_3/UV	Ozone/Ultraviolet Light
H_2O_2/UV	Hydrogen Peroxide/Ultraviolet Light
Fe^{2+}/O_2	Iron Mediated Aeration (IMA)
$Fe^{2+}/O_2/UV$	Photochemical Iron Mediated Aeration (PIMA)
$TiO_2/UV/O_2$	Photocatalysis

Source: Andreozzi et al. (1999), Meeroff et al. (2008), Zhang et al. (2012)

1.5.1 COD Removal

AOPs have shown excellent results in the removal of COD from many types of wastewaters. A study done by Dincer et al. (2007), utilizing a continuously stirred batch reactor, compared the COD removal efficiencies of Fenton, photo Fenton and UV/ H_2O_2 processes in oil recovery industry wastewater. This high strength wastewater had an initial COD concentration of 21,000 mg/L. The Fenton oxidation process delivered 86% removal of COD in one hour. The photo Fenton oxidation of the wastewater exhibited 81% removal of COD. The UV/ H_2O_2 had the lowest removal efficiency (39%) of the 3 processes, but nonetheless, removal was still recorded.

Mandal et al. (2010) attempted to optimize the process parameters (temperature, pH, $FeSO_4$ concentration and H_2O_2 concentration) for a Fenton process for treatment of industrial wastewater. At $FeSO_4$ and H_2O_2 concentrations of 6 mg/L and 277.7 mg/L, respectively, 95% removal of the COD was achieved using a continuously stirred batch

reactor. A study by Liu et al. (2012) showed the results of COD removal from waste activated sludge (WAS) using TiO_2 photocatalytic degradation. At the optimal catalyst value of 3 g/L the maximum COD degradation was 45% using a sloping trough circulating bed photocatalytic reactor (STCBPR). A schematic of the reactor is shown in Figure 1.

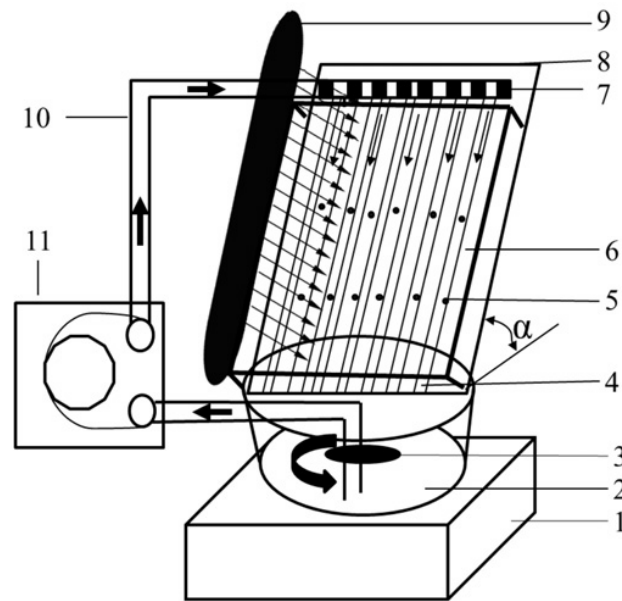


Figure 1: Schematic of sloping trough circulating bed reactor (Liu et. al 2012)

The addition of electrical current to the Fenton process increases the production of hydroxyl radicals and is called the Fered-Fenton method. Zhang et al. (2012) used this method to investigate its effects on the removal of COD from landfill leachate. The reactions were carried out in 0.8 L electrolytic plexiglass batch reactors. The maximum efficiency that was achieved for COD removal 66.4% using concentrations of 0.438 mol/L and 0.037 mol/L of H_2O_2 and Fe^{2+} , respectively.

Another study on the comparison of AOPs for COD degradation was performed by Naumczyk et al. (2012). They compared the COD removal efficiency of four advanced oxidation treatment processes: H₂O₂/UV, O₃/H₂O₂, Modified Fenton and Modified Photo-Fenton. The reactions were all carried out in 1 – 2 L batch reactors for 360 minutes. The raw leachate was subjected to 30 minutes of sedimentation prior to testing. All four processes, the modified Fenton, modified photo-Fenton, H₂O₂/UV and O₃/H₂O₂, exhibited COD destruction at levels of 87.5, 89.9, 91.0 and 92.7%, respectively (Naumczyk et al. 2012). Investigation of the COD removal from wastewater reveals evidence that advanced oxidation processes can be efficient in their removal of refractory organics. Even though excellent COD removal was achieved, none of these studies reported any removal of ammonia in a leachate matrix simultaneously.

1.5.2 Ammonia Removal

Ammonia can also be removed from landfill leachate by means of advanced oxidation processes. Deng and Ezyk (2011) achieved 100% ammonia removal and 79% COD removal when testing the treatment of landfill leachate using a sulfate radical advanced oxidation process (SR-AOP). They tested multiple doses of persulfate and found that increased dose resulted in significantly higher levels of ammonia and COD degradation. When the persulfate concentration was increased from the minimum (S₂O₈²⁻:12COD₀ = 0.1) to the maximum tested dose (S₂O₈²⁻:12COD₀ = 2.0), the ammonia and COD removal increased from 23 – 100% and 39 – 91%, respectively, at the optimal temperature (50°C).

Abu Amr and Aziz (2012) performed comparative tests on the effectiveness of advanced oxidation using ozone, Fenton, Fenton followed by ozone, and the combination of Fenton and ozone simultaneously. The study reported removal rates for ammonia, COD and color ranging from 0 – 12%, 15 – 65%, and 27- 98% removal, the least effective being ozone and the most effective being Fenton and ozone together. Higher ammonia removal was achieved by Zhao et al. (2010) utilizing photoelectrochemical (PEC) oxidation, which combines the processes of electrolysis and photocatalysis. They tested landfill leachate in a 6.5 L capacity continuous flow reactor. Under the optimum conditions, the PEC process removed 94.5% of the ammonia, 74.1% of the COD and 41.6% of the TOC from the landfill leachate.

Sonolysis is another advanced oxidation process used to attack contaminants, utilizing ultrasound to generate hydroxyl radicals. Wenjun et al. (2012) tested the efficiency of combining sonolysis with H_2O_2 . Through the study various pH levels, ultrasonic radiation applications, and hydrogen peroxide concentrations were compared. At the optimum conditions, pH = 11, 1/1 min. intermittent ultrasonic application and 2% H_2O_2 , the ammonia reduction reached 90.4%. At the same conditions removal for COD, hydrazine and urea reached 68%, 60% and 25%, respectively.

1.5.3 Heavy Metal Removal

Dutta et al. (2004) studied arsenic removal from water utilizing photocatalytic reactions with titanium dioxide. The removal efficiencies were tested at a pH range from 3 – 9 in a continuously stirred batch reactor. The study was based on two reactions: first, the oxidation of As(III) to As(V) and then the adsorption of As(V) onto the TiO_2 . The

tests were run until the adsorption equilibrium was established (2 – 3 hours) with 0.05 g/L TiO₂. It was found that adsorption of As(V) is much higher at a pH of 4. Furthermore, they deemed it possible to completely remove arsenic from water in slightly acidic conditions following the oxidation of As(III) to As(V) and subsequent adsorption of the As(V) onto the TiO₂ surface.

Advanced oxidation processes also have been demonstrated to remove Cr(VI) from wastewater. Kebir et al. (2011) combined the process of photocatalysis with adsorption to remove Cr(VI) from water samples in a continuously stirred batch reactor. The advanced oxidation reduces the Cr(VI) to the less harmful form, Cr(III). Under optimum conditions (pH = 2, temperature = 25°C, and CuAl₂O₄/TiO₂ = 1/1), 58% of the Cr(VI) was removed from the waters in 2 hours using the coupled treatment processes.

Multiple heavy metals can be removed from wastewater using multiple processes in concert. Vedrenne et al. (2012) showed this in their study on the treatment of landfill leachate by combining coagulation/flocculation with a photo-Fenton process. Arsenic, lead and mercury removal were all tested in the leachate samples. The combined treatment process achieved 85% removal of Pb, 47% removal of As and 9.1% removal of Hg. Although the mercury removal is low, it still demonstrates the promise of multiple contaminant removal of advanced oxidation processes.

Meeroff et al. (2012) performed batch scale studies of the removal of COD, ammonia, color and lead from simulated and actual landfill leachate utilizing AOPs. The first process evaluated was photochemical iron-mediated aeration (PIMA). The testing of the synthetic leachate achieved 45 – 60% removal of COD with starting concentrations ranging from 1 – 10,900 mg/L. However, the removal of COD from the real leachate only

reached 10% degradation. This was attributed to the high color (>500 PCU) interference of the real leachate. They found that removal of ammonia for the PIMA process was dependent on pH level and the ability for ammonia to escape the reactor. Once the proper adjustments were made, ammonia removal went from 2% to 29% in a 150 minute test. The lead concentrations in the simulated leachate were reduced below detectable limits within 16 hours. The PIMA process demonstrated 88 – 98% removal of color in the real leachate. The second process tested was TiO₂ photocatalysis, which showed higher removal efficiencies in both COD and ammonia. The COD degradation in the simulated leachate reached levels of 94 – 99% removal, while the real leachate exhibited 55 – 86% removal. The photocatalysis showed 23 – 51% removal of ammonia in synthetic leachate and 71% ammonia eradication in the real leachate. The TiO₂ photocatalytic process exhibited >90% color removal in real leachate. Their study shows that these two advanced oxidation processes have the ability to destroy multiple constituents of landfill leachate in one treatment process at laboratory scale. The photocatalytic process showed the promising results which formed the basis of this study.

1.6 TiO₂ Photocatalyst

The focus of this study is photocatalytic oxidation utilizing TiO₂/UV/O₂. Titanium dioxide is a noncombustible, white, crystalline, powder. It is soluble in hydrochloric acid, alcohol, and nitric acid, as well as hot concentrated sulfuric acid, alkali or hydrogen fluoride (Department of Health and Human Services 2011). It exists in the forms of three particular polymorphs: anatase, brookite and rutile. The most stable form is rutile, which is the principal source of TiO₂, followed by anatase (Department of Health and Human Services 2011). A widely used, high quality TiO₂ is the Degussa

Aeroxide TiO₂ P-25. A breakdown of the elements contained in Aeroxide TiO₂ P-25 is shown in Table 7.

Table 7: Physical Components of Degussa Aeroxide TiO₂ P-25

Compound	Unit	Value
Titanium Dioxide	wt. %	≥ 99.5
Al ₂ O ₃	wt. %	≤ 0.300
SiO ₂	wt. %	≤ 0.200
Fe ₂ O ₃	wt. %	≤ 0.010
HCl	wt. %	≤ 0.300
Sieve Residue	wt. %	≤ 0.050

Source: Aeroxide® TiO₂ P 25 Product Information Sheet

The titanium dioxide in the Degussa Aeroxide TiO₂ P-25 is not a pure form of TiO₂. Ohtani et al. (2010) tested the crystalline composition of the Aeroxide P-25 and found that it contained a ratio of anatase, rutile and an amorphous phase of the two. They reported that the Degussa P-25 was 78% anatase, 14% rutile and 8% amorphous phase. Some notable chemical and physical properties of the two pure forms as well as the Aeroxide TiO₂ P-25 (used in this study) are listed in Table 8.

Table 8: Properties of anatase and rutile forms of titanium dioxide

Property	Units	Anatase	Rutile	Aeroxide P-25
Molecular Weight	g/mol	79.88	79.88	79.88
Melting Point	°C	1825	1825	1850
Boiling Point	°C	2500-3000	2500-3000	n/a
Light Absorption	nm	<390	<415	<400
Density	g/cm ³	3.79	4.13	3.8
Crystal Structure	n/a	Tetragonal	Tetragonal	Tetragonal
Refractive Index	n/a	2.55	2.75	2.49
Dielectric Constant	n/a	31	114	78.5

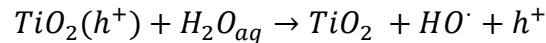
Source: Pelaez et al. (2012), Hong et al. (2005), Faure et al. (2010), Kosmulski et al. (2009), Evonik Industries (2008)

Titanium (IV) oxide is extensively used in products such as: paints and varnishes, floor coverings, roofing granules, most sunscreens and cosmetics, printer inks, ceramics,

plastics, paper coatings, pigments used in numerous foods, toothpastes, medicines, dielectric mirrors and tattoo pigments (Department of Health and Human Services 2011). In 2011, 1.47 million metric tons of TiO₂ pigment was produced in the United States and 6.55 million metric tons worldwide (USGS 2012). TiO₂ was rated as a Group 2B (possibly carcinogenic to humans) substance by the International Agency for Research on Cancer (IARC) in 2006. The health limitations on TiO₂ are only expressed for inhalation, there are none listed for ingestion (DHHS 2011).

1.7 TiO₂ Photocatalysis

Titanium dioxide became a photocatalyst of interest in 1972 when Fujishima and Honda discovered the photoelectrochemical reaction TiO₂ exhibited when combined with the power of UV light (Teh and Mohamed 2011). This resulting reaction was the splitting of a water molecule to generate a hydroxyl radical:



One of the early studies in the photocatalytic properties of titanium dioxide was that of Frank and Bard in 1977, which reported greater than 99% removal of cyanide ion (CN⁻) in water samples treated with sunlight and TiO₂ (Frank and Bard 1977). This piqued the interest of other researchers due to the possibility of air and water decontamination using the free solar energy of the sun (Pelaez et al. 2012). Chong et al. (2010) explained that the oxidative and reductive reactions from titanium dioxide are due to its unique characteristic of possessing a sole electron in its outer orbital. The reaction

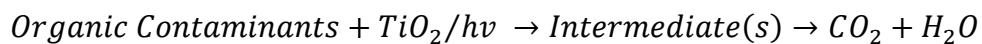
process begins when UV light energy photoexcites that lone electron, which creates an empty outer valence band. The reaction process steps are shown in Table 9.

Table 9: Chain of oxidative-reductive reactions that occur at the UV activated TiO₂ surface (Chong et al. 2010)

Step	Process	Formula
1	Photoexcitation	$TiO_2 + h\nu \rightarrow e^- + h^+$
2	Charge-carrier trapping of e ⁻	$e^-_{CB} \rightarrow e^-_{TR}$
3	Charge-carrier trapping of h ⁺	$h^+_{VB} \rightarrow h^+_{TR}$
4	Electron-hole recombination	$e^-_{TR} + h^+_{VB} (h^+_{TR}) \rightarrow e + \text{heat}$
5	Photoexcited e ⁻ scavenging	$(O_2)_{ads} + e^- \rightarrow O_2^{\bullet -}$
6	Oxidation of hydroxyls	$OH^- + h^+ \rightarrow OH^\bullet$
7	Photodegradation by OH [•]	$R-H + OH^\bullet \rightarrow R^\bullet + H_2O$
8	Direct photoholes	$R + h^+ \rightarrow R^\bullet \rightarrow \text{Intermediate(s)/Final Degradation Products}$
9	Protonation of superoxides	$O_2^{\bullet -} + OH^\bullet \rightarrow HOO^\bullet$
10	Co-scavenging of e ⁻	$HOO^\bullet + e^- \rightarrow HO_2^-$
11	Formation of H ₂ O ₂	$HOO^- + H^+ \rightarrow H_2O_2$

CB = conduction band, VB = valence band, TR = surface trapped

An important precursor to these set of reactions is the absolute necessity of water molecules, without which, hydroxyl radicals could not be created. The formation of not only hydroxyl radicals, but also the superoxide anions (O₂^{•-}) contributes to the formation of hydrogen peroxide. The combination of these two strong oxidants generates a series of mineralization reactions geared toward the destruction of organic contaminants. Chong et al. (2010) simply represented the overall photocatalysis reaction with the following equation:



The organic compounds are mineralized to carbon dioxide and water, given enough irradiation time. A basic visual representation of the photocatalytic mechanism can be seen in Figure 2 which demonstrates the process that occurs when light energy irradiates

TiO₂ particles. The illumination ejects electrons from the valence band resulting in a positively charged area with “holes” (h⁺). These holes primarily react with water molecules to generate hydroxyl radicals, thus creating the dominant destructive component of the photocatalytic process. The free electrons jump to the conduction band where they can react with oxygen molecules in the water to form superoxide radical anions.

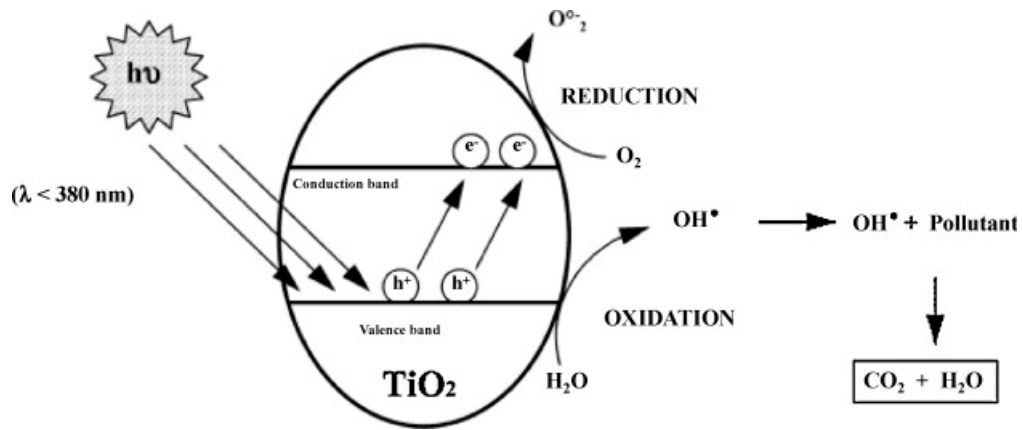
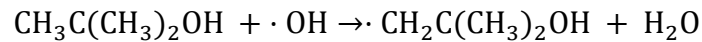


Figure 2: Generalized process of photocatalytic oxidation (Ghaly et al. 2011)

As explained earlier, the photocatalytic process is an array of multi-step reactions (Table 9). The ability of TiO₂ photocatalyst to mineralize such a wide range of pollutants is an attractive quality, but modeling the kinetics of such a complicated process is a difficult task. Sometimes, complex environmental processes allow only for empirical solutions because not all reactions or mechanisms are known. There may be lumped parameters, surrogates, indicators or just overly complex reaction pathways (Hemond and Fechner-Levy 2000). This is why few reviews were found focusing on the kinetics studies of photocatalytic systems.

Due to the complexity, most kinetics evaluations in photocatalytic studies focus on the overall kinetics of the degradation of a certain pollutant. The photocatalytic breakdown of any certain pollutant takes place in a system of reactions (Valencia et al. 2011). Many of which may not necessarily happen in order. Some reactions may occur simultaneously and at different rates. The kinetics can only be modeled to the overall combination of these processes, even though some of these processes may compete with each other to inhibit the photodecomposition. The TiO₂ photocatalyst simply plays a role in initiating the array of reactions; TiO₂ is not in itself a reactant, no matter the overall reaction order (Helali et al. 2012). Also, in the case of COD, multiple hydroxyl radical reactions are required to mineralize the organic material. The initial hydroxyl radical reaction for the destruction of *t*-butanol is as follows:



The initial reaction of one molecule of *t*-butanol with one molecule of hydroxyl radical produces an organic compound, which still registers as COD. After a number of hydroxyl radical attacks, among other reactions, the organic compound eventually will degrade to CO₂ and H₂O. When kinetics are monitored for the destruction of COD, only the final mineralization is measured (Wang and Xu 2012). So, for the purpose of this study the reaction kinetics are reported as overall kinetics. That is to say, for this manuscript, all the kinetics implications within are referring to the overall reaction kinetics, since the true reaction processes are too complex, too numerous, and too unknown to model with any degree of accuracy.

1.7.1 Pollutant Removal

As explained earlier, the generation of mixed radicals in the photocatalytic process makes it possible to decompose an array of contaminants. There are many different configurations of this process that have been tested in the literature. These include continuously stirred batch reactors, continuous flow batch reactors, thin film fixed bed reactors, falling film reactors, sloping trough circulating bed photocatalytic reactors and recirculating parabola cylindrical concentrator solar photoreactors. Some variations adjust the pH, or add hydrogen peroxide, ozone, or oxygen. The simultaneous photocatalytic degradation of COD, dissolved organic carbon (DOC) and color in landfill leachate was demonstrated by Jia et al. (2013). They designed a continuous flow batch reactor which ran at 1.5 L/min and all experiments were run for 72 hours, sampled at 6 hour intervals. Multiple catalyst dosages were tested from 0.0 – 4.0 g/L, with 2.0 g/L being the optimal value for COD removal and 3.0 g/L for color removal. At a pH of 4.0 and TiO₂ concentration of 2.0 g/L, 60% of the COD was mineralized, 72% of the DOC was eliminated and 97% of the color was removed. Vineetha et al. (2012) used TiO₂ photocatalysis to treat highly concentrated effluent with a continuously stirred batch reactor. They reported a removal of 32% of COD and 84% of color from the wastewater at a catalyst dosage of 0.2 g/L and pH 6. To accelerate the hydroxyl radical production, H₂O₂ (0.3 M) was added to the mix.

Specific organic oxygenates were targeted using photocatalytic oxidation with TiO₂ in a falling film reactor. The TiO₂/UV/O₂ process was compared to photocatalytic ozonation (TiO₂/UV/O₃) for the removal of Methyl Tertiary Butyl Ether (MTBE), Ethyl

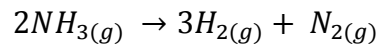
Tert-Butyl Ether (ETBE), Tertiary Amyl Ethyl Ether (TAEE) and Tert-Butyl Alcohol (TBA). The experiment used a flow rate of 0.1 L/min, a UV intensity of 1.0 mW/cm² at a pH of 6-7. The photocatalytic ozonation outperformed the photocatalytic oxidation by removing nearly all contaminants from the solutions within 20 minutes. The TiO₂/UV/O₂ process managed to remove 100% of ETBE and TAEE, 88% of MTBE and 82% of TBA within 50 minutes of treatment (Mehrjouei et al. 2012).

Chemlal (2013) treated landfill leachate using TiO₂ photocatalysis with a 3L Thin Film Fixed Bed Reactor (TFBR), in which the catalyst is fixed onto a sheet that is illuminated, and the contaminated water passes over it. During the testing, the glass reactor plate was illuminated by 3 UVC 15W lamps for 30 – 54 hours. For the leachate containing initial concentrations of 26,000 – 30,000 mg/L COD, pH variations influenced the COD removal from 76 – 92%, with the optimal pH value being controlled at 5 (Chemlal 2013).

Another use of photocatalytic oxidation is to mineralize toxins produced by cyanobacteria. Shephard et al. (2002) utilized a falling film reactor with a fixed sheet impregnated with TiO₂. A total of twelve 15W UV lamps were used to create a 204.5 W/m² UV intensity. The tests were run for 20 minutes. The microcystin degradation was 76.5-84% in 20 minutes, when spiked in natural lake water. The additional natural organic material and inorganic ions from the lake water, competed for photoactivation reaction sites with the contaminants of concern, compared to removal rates in distilled water controls (87% in 8-10 minutes).

Hapeshi et al. (2010) studied the photocatalytic degradation of the antibiotic ofloxacin and the β -blocker atenolol. They tested six commercially available TiO_2 samples. Under 30 minute irradiation time, the Degussa P25 outperformed the other five catalysts by removing 85% of the ofloxacin and 67% of the atenolol. After 240 minutes of UV illumination, both the Degussa P 25 and Hombikat UV 100 destroyed nearly 100% of the ofloxacin (Hapeshi et al. 2010).

TiO_2 photolysis can also be used as a means to degrade ammonia from wastewaters. The photocatalytic process can be used to provide the energy necessary for the conversion of ammonia to hydrogen and nitrogen gases:



The equation shows that 2 moles of ammonia can be converted to 3 moles of hydrogen gas and 1 mole of nitrogen gas. Kominami et al. (2012) tested the formation of H_2 from the photocatalytic destruction of NH_3 . After 30 hours of irradiation, elevated levels of H_2 (160 μmol) were detected when compared to the initial 107 μmol of NH_3 . This 3:2 molar ratio satisfies the above equation and is an indication of substantial, if not full, conversion of ammonia to hydrogen and nitrogen gas (Kominami et al. 2012). Utilizing a 1.1 L batch scale photo-reactor and 0.1 g/L TiO_2 , 56% ammonia removal was observed ($C_0 = 1,250 \text{ mg/L NH}_3$). The study had tested the photocatalytic degradation of ammonia in manure as well and found that although some pretreatment was necessary, 88% of the ammonia was removed. It was also noted that the photocatalysis of the manure samples removed the odor (Altomare et al. 2012).

With regards to certain heavy metals and metallic oxyanions, TiO₂ photocatalysis has demonstrated some success. Since TiO₂ is a metal oxide with a high sorption capacity, it can adsorb various arsenic species, namely As(V) and As(III). Jegadeesan et al. (2010) tested TiO₂ sorption capacities for arsenic in batch solutions, at a pH range of 3 – 11 for 72 hours. They observed TiO₂ sorption capacities for As(III) and As(V) to range from 146 – 392 µg/m² and 46 – 201 µg/m², respectively. Aside from adsorption techniques, the TiO₂ photocatalytic process produces highly reactive radical species which oxidize the arsenic species from the more toxic As(V) to As(III) (Jegadeesan et al. 2010). The ability to remove lead (Pb) from wastewater using TiO₂ photocatalytic oxidation was discussed earlier. The removal of Cr(IV) was also recently studied by Wang et al. (2013) utilizing TiO₂ photosensitized reduction. An amorphous TiO₂ was prepared and compared to the efficiency of Degussa P 25 TiO₂. The amorphous TiO₂ outperformed the regular TiO₂ in the removal of Cr(IV), showing removal efficiencies of 53.5% to 42.1%, for Am-TiO₂ and TiO₂, respectively (Wang et al. 2013). The photocatalytic reduction of copper and selenium was studied by Aman et al. (2011) while testing the efficiencies of various photocatalysts: TiO₂, TiSi and TiZr. Under visible light, the TiZr outperformed the Degussa P25 TiO₂ by removing 86.5 and 75.3% Se and Cu, respectively, compared to TiO₂'s respective removal of 25.9 and 22.1% for Se and Cu. However, under UV light, the Degussa P25 outperformed the synthesized TiZr by removing 90.9 and 81.7% Se and Cu, respectively, compared to TiZn's respective removal of 86.5 and 76.5% (Aman et al. 2011).

TiO₂ photocatalytic oxidation has even been used to deactivate pathogen indicators such as *Escherichia coli* (E.coli). A study in 1996 showed that using 1 g/L TiO₂ led to the

complete inactivation of *E.coli* in 60 minutes (Bekbolet and Araz 1996). A more recent bench scale photoreactor found an optimal dose of 0.1 g/L TiO₂ to inactivate *E.coli* to levels below detectable limits within 33 minutes exposure (Marugan et al. 2012).

In summary, the use of photocatalysis has been employed successfully for the removal of organics, inorganics, nitrogen-based contaminants, xenobiotics, odor and even pathogen indicators at laboratory scale. A summary of research performed using TiO₂ photocatalysis, focusing on the removal of COD is reported in Table 10.

Table 10: COD removal efficiencies of TiO₂ photocatalysis

Water Type	TiO ₂ Dose (g/L)	UV (W)	COD ₀ (mg/L)	pH	Removal (%)	Time (min)	Reference
Grey water	2.0-5.0	nr (TQ 150z1)	3940	10.3	44	150	Sanchez et al. 2010
Simulated wastewater	1% Pt-TiO ₂ immobilized on silica gel	88 W (1.8 mW/cm ²)	62	6.5	86	30	Suri et al. 1999
Simulated wastewater	0.3-1.0	8 W	10	n/a	82	120	Huang et al. 2008
Lagoon wastewater	2.0	Solar radiation	660	8.0	42	120	Araña et al. 2002
Industrial wastewater	0.6	6 x 18 W	3.2	6.0	62	60	Chen et al. 1997
Olive mill wastewater	1.0	Solar radiation (assumed 30 W/m ²)	6,600	2.8	26	1920	Gernjak et al. 2004
Industrial wastewater	4 plates immobilized	4 x 4 W	120 (TOC)	9.0	34	30	Nakamura et al. 2008
Industrial wastewater	1.0	415 W	135	8.0	22 (diluted 1:100 + filtered)	1440	El Hajjouji et al. 2008
Industrial wastewater	0.5	400 W	404	3.0	40	240	Pekakis et al. 2006
Landfill leachate	5.0 (batch) immobilized	16 x 40 W 5.0 – 10.0 mW/cm ²	985	5.0	70	480	Bekbölet et al. 1996
Landfill leachate	3.0	8 W (21 W/cm ²)	1,673	8.7	30	720	Cho et al. 2003
Landfill leachate	1.0-2.0	150 W (0.5 mW/cm ²)	1,200	7.5	35-57	60	Poblete et al. 2011
Landfill leachate	TiO ₂ coated sheet	120 W	26,000 – 30,000	5- 7.6	76-92	150	Chemlal et al. 2013

Water Type	TiO ₂ Dose (g/L)	UV (W)	COD ₀ (mg/L)	pH	Removal (%)	Time (min)	Reference
Industrial wastewater	3.0	7.6 W/m ²	20,000	6.8	36.3	1440	Baransi et al. 2012
Waste Activated Sludge	3.0	1.5 mW/cm ²	16,249	6.83	45	480	Liu et al. 2012
Landfill leachate	2.0	NA	2,440	8.24	60	4320	Jia et al. 2013
Simulated wastewater	3.2 g of TiO ₂ coated on immobilized sheet	38 W/m ²	157,000	7.0	51.6	255	Yahiat et al. 2011
Paper mill wastewater	0.75	35-45 W/m ²	2,075	6.5	70.5	180	Ghaly et al. 2011
Industrial wastewater	0.2	Solar radiation	500	6	32	240	Vineetha et al. 2012

1.7.2 pH Effect

The degradation kinetics for photocatalytic processes are affected by pH (Ghaly et al. 2011, Chong et al. 2010, Nemoto et al. 2007). More specifically, the process removal efficiency is reported to increase with decreasing pH. The point of zero charge for TiO₂ is between pH = 5.6 – 6.4 (Chemlal et al. 2013). Below that range results in a positive charge on the catalyst surface, and above that range results in a negative surface charge. The surface charge plays a role in the adsorption and desorption processes between the contaminant molecule and the catalyst. The pH can change the structure of a pollutant, thereby affecting its interaction with the catalyst. For example, at low pH conditions, higher COD degradation is reported, while a high pH increases the destruction of ammonia (Chemlal 2013). Rocha et al. (2011) studied this phenomenon by comparing the photocatalytic degradation of leachate with and without pH adjustment. The study found that reducing the landfill leachate to a pH of 4 gave 10 times the degradation of DOC compared to the samples that were not adjusted. Hapeshi et al. (2010) also tested the

effect of pH on TiO₂ photodegradation from pH = 3 – 10. The results showed that an increase in pH led to a decrease in the degradation kinetics for atenolol. At pH values of 3, 6 and 10 the degradation constant decreased from 1.49 to 1.24 to 0.95 min⁻¹, respectively. Nemoto et al. (2007) studied the pH effect on the photodecomposition of ammonia and found only minimal destruction at pH values below 9 and maximum pollutant breakdown at pH 11. Helali et al. (2013) reported that the photocatalytic decay of methylamine, like ammonia, proved to be more efficient at higher pH values (pH = 11.7).

1.7.3 Catalyst Poisoning

One serious drawback of TiO₂ that has been discussed in recent years is the deactivation of the catalyst due to adsorption of partially oxidized intermediates on the surface of the TiO₂ during the photocatalytic degradation process, thus changing the effective shape of the TiO₂ particles (Carneiro et al. 2010). Gandhi et al. (2012) tested the regeneration of spent Degussa P25 from the photocatalytic degradation of phthalic acid by using three notably prominent regeneration techniques: washing with methanol, thermal treatment, and treating with hydrogen peroxide. The spent TiO₂ was collected and the samples were regenerated using the three different methods and subsequently used again for a second and third treatment cycle. Within 40 minutes the new TiO₂ degraded >99% of the phthalic acid. The spent catalyst was used again in a second cycle which resulted in 49% removal of the contaminant. The second cycle using regenerated TiO₂ via the wash method, thermal treatment, and H₂O₂ treatment showed ≈ 55, 87, and 99% degradation, respectively. The third cycle showed lower degradation for the wash

method and thermal treatment, while the H₂O₂ treatment exhibited similar removal to fresh leachate. The change in the degradation rate constants from the different regeneration methods and their cycles can be seen in Table 11.

Table 11: Rate constant juxtaposition of fresh and regenerated catalysts (Gandhi et al. 2012)

Catalyst	Rate Constant (min ⁻¹)	
	2 nd Cycle	3 rd Cycle
Fresh catalyst	0.104	
Regenerated catalyst using wash method	0.021	0.014
Regenerated catalyst using thermal treatment	0.048	0.044
Regenerated catalyst using H ₂ O ₂ treatment	0.103	0.099

The full regeneration of the catalyst was achieved by treating the used TiO₂ with a 30% hydrogen peroxide solution (10mL per gram of catalyst) for a one hour period. This shows that the life of the catalyst can be extended through multiple uses by chemical desorption or surface oxidation.

The reuse of titanium dioxide not only depends on the regeneration, but also on the recovery efficiency. Suryaman and Hasegawa (2010) studied the reuse of recovered TiO₂ in the treatment of various chlorophenols in water. The recovery method involved simple sedimentation of the catalyst after each run was performed. They discovered that using tap water instead of deionized water led to higher coagulation of TiO₂ particles which delivered greater catalyst settling for reuse, but resulted in lower degradation efficiency of the catalyst. The additional electrolytes in the tap water neutralized charged species on the catalyst surface and diminished repulsion. The study showed that the settled catalyst particles were used at least 3 times before a drop in efficiency was noted.

Another study confirmed the theory of pollutant adsorption being the primary inhibitor of

TiO₂, but also found that an increase in alkalinity also plays an inhibitory role. The carbonates, just like the NOM, act as competing OH[•] scavengers. Also, the excess alkalinity in the water led to the formation of large TiO₂ aggregates. The destruction of metaldehyde using UV/TiO₂ dropped from 93% to 45% in the presence of alkalinity. Furthermore, when testing the destruction of methaldehyde in the presence of alkalinity background organics were introduced into the wastewater but had no effect on the degradation (Autin et al. 2013). However, this is contradicted by Meeroff and McBarnette (2011) which found that complete mineralization of KHP in laboratory tests required alkalinity.

1.7.4 Process Modifications

Recent studies focus on the combination of processes and/or the doping of TiO₂ to enhance the photocatalytic oxidation process. Teh and Muhammed (2011) suggested that TiO₂ doped with holmium could greatly reduce the recombination of excited electrons and the holes, leading to more hydroxyl radical production. Pan et al. (2013) show that non-metal doping of TiO₂ increases the photocatalytic activity of the catalyst. TiO₂ doped with nitrogen and fluorine exhibited 6.8 times higher activity than plain TiO₂. Also, they found that calcination of the doped catalyst improves degradation efficiency 1.5-2.7 fold (Pan et al. 2013). Nitrogen and carbon doped TiO₂ was reported to have higher degradation in the visible light spectrum than TiO₂ alone. After 1 hour of light exposure, N,C-TiO₂ removed 69% of phenol from the water, while the Degussa P25 control removed only 26% although, the Degussa P25 outperformed the doped catalyst when exposed to one hour of UV irradiation 76% to 33% degradation (Gorska et al. 2009).

Another study showed promising results from combining the TiO₂ with iron and carbon. After 3 hours of UV irradiation with the Fe-C-TiO₂ 100% of the phenol concentration in the water was destroyed, as reported Grabowska et al. (2012). Platinum doping of TiO₂ was studied by Ma et al. (2011). They tested the efficiencies of doping the TiO₂ with 0.005, 0.025 and 0.20 wt.% Pt/TiO₂ and found the highest efficiency with the 0.005% Pt/TiO₂ combination. Treating a wastewater stream having dichloromethane (DCM) inlet concentrations of 50, 100, 200, and 300 mg/L with TiO₂ resulted in 99.0%, 82.7%, 55.2% and 57.9% removal efficiency, respectively. The respective removal efficiency of the Pt/TiO₂ was 99.3%, 79.7%, 76.5% and 73.4%. The platinum addition showed greater photodegradation assistance at higher pollutant levels (Ma et al. 2011). The combination of TiO₂ and AgCl powders calcined together was studied by Sangchay et al. (2012). The powders were calcined together 400, 500 and 600° C and those 3 new catalysts were tested against Degussa P25. The most efficient photocatalytic activity was exhibited by the calcined TiO₂-AgCl at 400°C. Under UV and visible light irradiation TiO₂-AgCl showed a 92% and 50% degradation of methylene blue, while Degussa P25 showed 47% and 32%, respectively. While doping TiO₂ has shown to be somewhat effective in improving the photocatalytic process, there are disadvantages. TiO₂ is a low cost, nontoxic substance, but adding to the cost to create a new more expensive, potentially more toxic catalyst has its drawbacks. Also, research indicates that doping blocks some of the surface reactive sites for photocatalytic activity (Teh and Mohamed 2011), which would increase the amount of photocatalyst needed.

Combining processes has been studied as another method of enhancing contaminant degradation. Selvam et al. (2007) combined the Fenton reaction with TiO₂

photocatalysis, utilizing a UV/ferrioxalate/H₂O₂/TiO₂ process. Within 10 minutes of reaction 93.0% decolorization and 60.0% degradation of reactive orange 4 was observed. The TiO₂ photocatalysis alone resulted in 22% decolorization and 9.7% degradation and the solo ferrioxalate process exhibited 9.7% and 2.8%, respectively (Selvam et al. 2007). Potassium persulfate (K₂S₂O₈), which promotes the production of sulfate radicals, can potentially increase the concentration of oxidants in the matrix. Hazime et al. (2013) tested this additive on the removal of imazalil. Without the potassium persulfate the photocatalytic process took 21 minutes to degrade 90% of the contaminant. The addition of K₂S₂O₈ brought the reaction time down 5 minutes for 90% pollutant destruction. The process of photocatalysis in the presence of TiO₂ was studied by Ghaly et al. (2011). The study focused on the removal of COD in highly polluted paper mill wastewater. A catalyst loading experiment was performed with samples ranging from 0.25 to 1.5 g/L with a resulting optimum catalyst load of 0.75 g/L. Using the optimum amount of catalyst, the effects of pH were tested in four samples at a range of 3 – 10 pH units. The final series of tests dealt with the investigation of additional hydrogen peroxide concentration. The experiments were conducted with four samples, utilizing the optimum TiO₂ value (0.75 g/L), pH of 6.5 and the addition of varying volumes of hydrogen peroxide: from 1 – 4 ml/L. The concentration of hydrogen peroxide addition resulted in COD removal efficiencies ranging from 62.0% - 77.9%, with 2 ml/L being the optimum amount. One final note in this experiment was that the reaction was deemed to obey pseudo-first-order kinetics. The results of the testing are shown in Table 12.

Table 12: Summary of experimental data in treatment of paper mill waste water

Run no.	Catalyst loading (g/L)	pH	Solar radiation	H ₂ O ₂ (ml/L)	k ₀ (min ⁻¹)	φ180(%)
1	0	6.5	+	0	0.0003	4.70
2	0.75	6.5	-	0	0.0007	12.0
3	0.75	6.5	+	0	0.0066	70.5
4	0.25	6.5	+	0	0.0036	46.3
5	0.5	6.5	+	0	0.0043	55.1
6	1	6.5	+	0	0.0060	67.3
7	1.25	6.5	+	0	0.0049	57.5
8	1.5	6.5	+	0	0.0038	48.4
9	0.75	3	+	0	0.0032	43.1
10	0.75	5	+	0	0.0039	50.6
11	0.75	8	+	0	0.0068	72.1
12	0.75	10	+	0	0.0076	74.7
13	0.75	6.5	+	1	0.0073	73.9
14	0.75	6.5	+	2	0.0087	77.9
15	0.75	6.5	+	3	0.0065	68.0
16	0.75	6.5	+	4	0.0053	62.0

k₀ is the pseudo-first-order reaction rate constants in min⁻¹.

φ180 is the efficiencies of %COD removals within 180 min reaction time.

+ means with or in the presence of.

- means without.

Source: Ghaly et al. (2011)

Chemical additives show some promise for the enhancement of photocatalytic oxidation process removal efficiency, but further research needs to be performed on the basic TiO₂ process before enhancements should be made. Again, one of the most attractive features of the TiO₂ photocatalyst is its economic efficiency. This is why the basic process should be studied with minimal adjustments or chemical additions.

1.8 Objectives

The main purpose of this study is to test UV/TiO₂ photocatalytic degradation of selected pollutants (COD, ammonia, alkalinity, and color) in landfill leachate using a pilot scale falling film reactor. It is hypothesized that the degradation rate of the contaminants will follow overall first-order reaction kinetics. The primary objective of this study is to determine an optimum dosage of catalyst using a falling film reactor

without the use of any pretreatment or chemical addition methods. The secondary objective is to determine the collection efficiency of three filter bag sizes (5, 10 and 20 micron) used to recover the catalyst once the leachate has been through the treatment process.

2.0 METHODOLOGY

2.1 Leachate Collection

Leachate was collected from the Monarch Hill Class 1 sanitary landfill in Pompano Beach, FL. The facility was opened by Waste Management Inc. in 1965 and was formerly known as Central Disposal Sanitary Landfill (CDSL). The site has a mass-burn facility rated at 2000 tons per day and receives between 10,000 tons (2007 data) to 4000 tons (2010 data) of municipal solid waste (MSW) per day. The site has a footprint of approximately 300 acres, of which about 80 acres is being landfilled currently. The landfill is located at 2700 Wiles Road, Pompano Beach, FL. The property spans east to west from S. Powerline Rd. to Florida's Turnpike and north to south from Wiles Rd. to Sample Rd. as shown in Figure 3.



Figure 3: Aerial view of Monarch Hill Landfill

Approval and permission to obtain samples of raw leachate was obtained from Jeff Roccapiore, District Manager, Broward County Central Disposal, Waste Management Inc. of Florida. Samples were collected with the assistance of Stephen “Leroy” Melton, Landfill Technician. Figure 3 shows the location of the main sampling point for the southeast corner of the landfill, which is known as the “South East Step-up Station.” This is the station where all the leachate in this work was collected from. A small pressure monitoring valve installed at the port allows for manual leachate sampling. A closer look at this sampling port is shown in Figure 4. It is possible to collect other samples from various locations on the property such as: the NW corner (old leachate), SW corner (new leachate), SE corner (Waste-To-Energy condensate), or from the wastewater treatment plant sump (combined leachate).



Figure 4: S.E. Step-up Station Sampling Port

The leachate from this facility is discharged to a sanitary sewer collection system and sent directly to the Broward County North Regional Wastewater Treatment Plant (Figure 5) located at the intersection of Powerline Road and Copans Road. Waste Management, Inc., who owns the landfill facility, has a 5-year agreement with Broward County to accept its leachate provided it meets the industrial pretreatment criteria (see Table 3), but most notably: $TSS < 400 \text{ mg/L}$, $BOD_5 < 400 \text{ mg/L}$, and $COD < 2 \times BOD_5$. According to Jeff Roccapiore (District Manager), the county assesses a surcharge on the order of \$350,000 per year for leachate disposal fees. The facility records approximately 3.5 million gallons per month of leachate generation, but the treatment plant flowmeter reads 5-6 million gallons per month, typically.



Figure 5: Aerial photograph of the Broward County North Regional Wastewater Treatment plant

The first leachate sampling for these experiments took place on September 30th, 2011. Three gallons of leachate was taken from the site at this time, in a five-gallon bucket. The second sampling took place on March 9th, 2012. Five gallons of leachate was secured from the site during the March landfill visit, in a five-gallon gas can (used to minimize spilling). The third sampling date was July 18th, 2012. Another five gallons of leachate was acquired using the five gallon gas can (shown in Figure 6). The collected leachate was stored in a refrigerator at 4°C until treated in the laboratory.



Figure 6: Leachate Sampling on 7/18/2012

2.2 Pilot Scale Falling Film Reactor

The experiments for this pilot scale study were conducted using a falling film reactor: CE 584 Advanced Oxidation, which is part of the 2E – Energy and Environment product range. 2E is a sector owned by G.U.N.T. Gerätebau GmbH; a company based in Barsbuettel, Germany. The advanced oxidation machine is shown in Figure 7 and Figure 8.



Figure 7: CE 584 Advanced Oxidation Machine



Figure 8: Photographs of the falling film pilot reactor (left: close up view of the reaction chamber; right: overall view).

The test rig measures 1510 mm x 790 mm x 1990 mm and weighs approximately 330 lbs. The main components of the advanced oxidation machine are labeled in Figure 9. The unit is equipped with a 10 L reservoir, temperature sensor (0-50°C), 260 Lph circulating centrifugal pump (at 29.5 feet of head), flow meter with regulating valve, sampling port with three-way valve, a weir compartment for distributing flow in the reaction zone, and a 120 W low pressure, ultraviolet lamp with power source (30-35% efficiency).

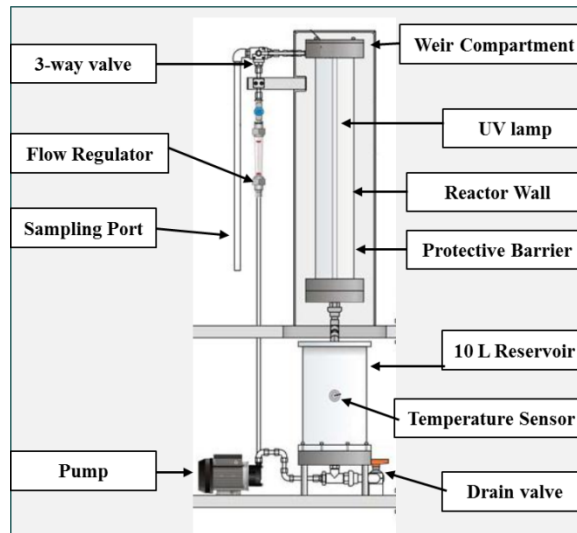


Figure 9: Main Components of CE 584 Advanced Oxidation

This device is designed to oxidize contaminants in water using UV radiation. The process begins by adding the desired liquid to the 10 L reservoir. The liquid is then pumped up through the flow regulator, which allows a flow range of 30 – 320 L/hour. Following the flow regulator, there is a three-way valve which leads to either the sampling port or the weir compartment. The liquid builds up in the weir compartment until it falls over the weir onto the cylindrical reactor wall, which surrounds the UV lamp.

While the liquid runs down the reactor wall it is exposed to ultraviolet emittance before it falls back into the reservoir. Underneath the reservoir is a drain valve to remove the desired liquid from the machine. A schematic drawing displaying the flow path(s) of the machine is shown in Figure 10.

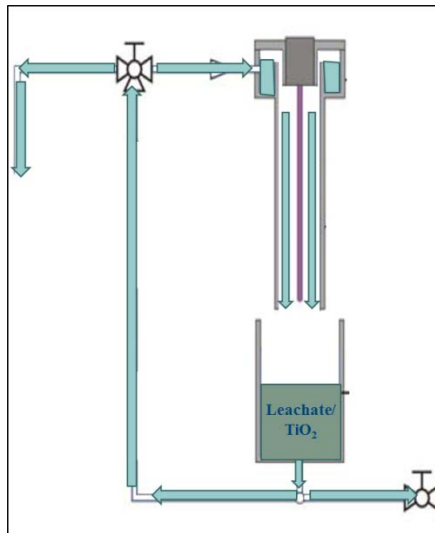


Figure 10: Flow Path of Advanced Oxidation Machine

The UV lamp (Strahler NNI 125/84 XL) was purchased from Heraeus Noblelight (Hanau, Germany). The irradiation spectrum (Figure 11) shows that the lamp provides most of its intensity from 250-260 nm in the UVC germicidal range. Inside the falling film reactor zone, there is an inner protective tube for the lamp. This tube is made of quartz glass (transmittance = 80-90%) with diameter 43 mm. The reactor wall is made of borosilicate glass (transmittance = 80-90%) with diameter 110 mm, and the glass tubing is protected with an external tube made of polymethyl methacrylate (PMMA XT) at 140 mm diameter. The borosilicate glass and the PMMA both block the transmittance of UV light at wavelengths less than 300 nm.

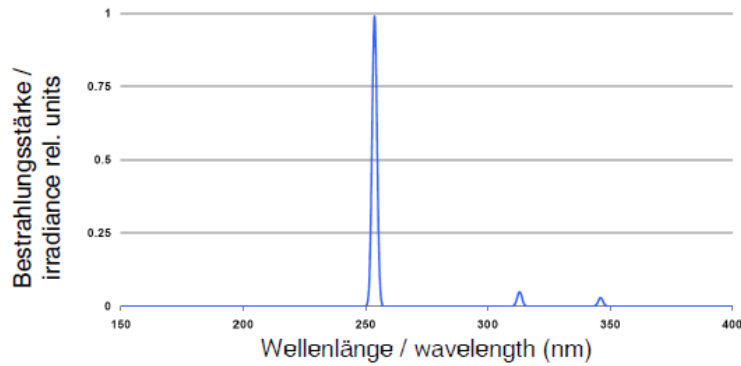


Figure 11: Irradiation spectrum for the Strahler NNI 125/84 XL low pressure UV lamp as provided by the manufacturer

The unit's power options are accessed through the control panel. The power supply for the advanced oxidation unit is a standard 120V outlet. The controls on the panel are shown in Figure 12. The main power switch is in the off position in the image, a quarter turn in the clockwise direction will power up the unit. The pump control and UV lamp control can be used, when the main power switch is in the "on" position. Pushing the green button turns them on and pushing the red button turns them off. Next to those controls is a digital temperature output, which displays the temperature in degrees Celsius.

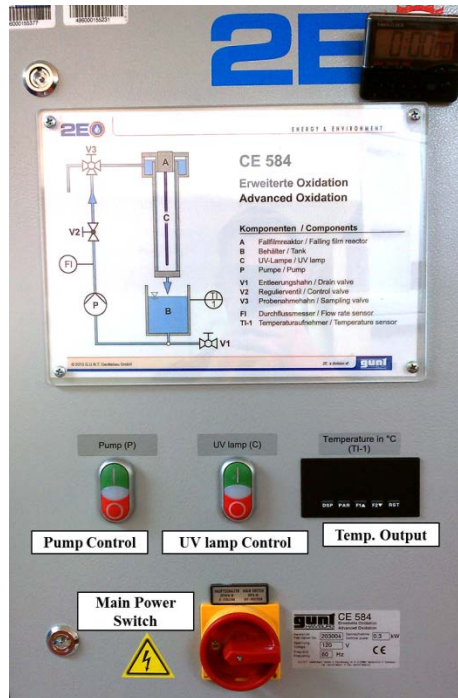


Figure 12: Control Panel for CE584 Advanced Oxidation Machine

2.3 Mechanical Improvements/Additions

Before testing the machine with leachate, some mechanical improvements had to be made. The first alteration to the advanced oxidation machine was the addition of a 3-way valve between the reservoir and the pump. The necessity of this modification arose from trouble encountered priming the pump. Using a tap water test with TiO_2 particles, the heavy catalyst particles would settle in the pump cavity, dry up and harden around the impeller in the pump head. This hardening of the catalyst in the pump led to a dry start (see location in Figure 13), such that the pump did not have enough initial torque to break up the dried particles, so it needed to be primed.

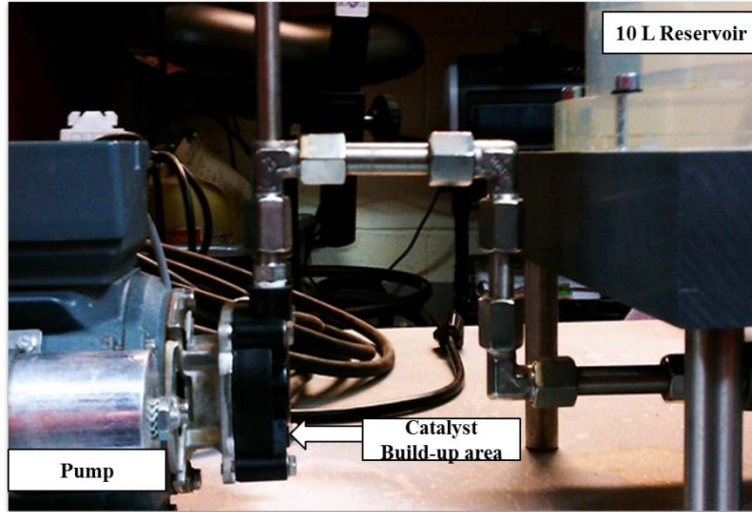


Figure 13: Catalyst settling location in the advanced oxidation machine

A new stainless steel 3-way valve was installed so that the pump could be flushed out after every use, limiting the amount of TiO_2 build-up and maintaining proper pump operation. The 3-way valve can be seen in Figure 14. The valve allows one to stop the unit, drain the pump, and recirculate the catalyst so that it will not collect in the pump cavity or in the weir above the falling film reaction zone during long term kinetics experiments in which the unit is started and stopped overnight for cooling.

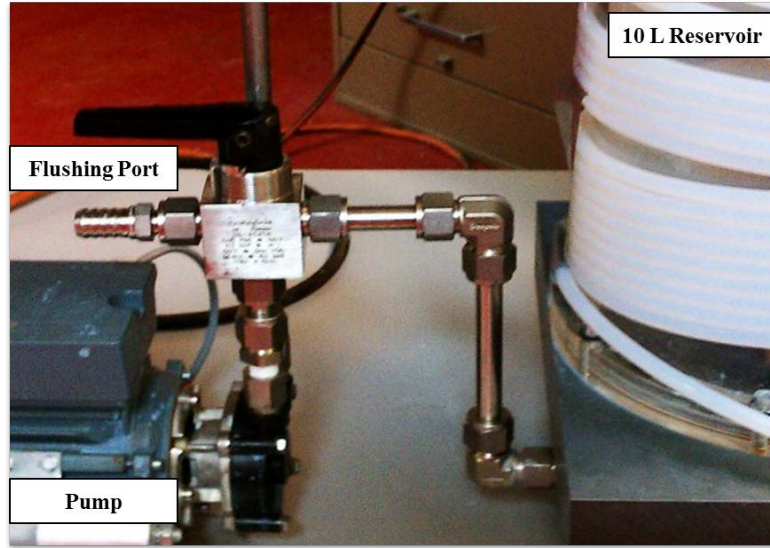


Figure 14: 3-way valve modification to CE584

After each experiment, a hose from a bucket of clean tap water is connected to the flushing port. The pump is turned on, and the pump pulls water from the bucket. By opening the 3-way valve (V3) just before the weir compartment, the wash water can be disposed of. A flow diagram of the flushing process is shown below in Figure 15 with the 3-way valves circled.

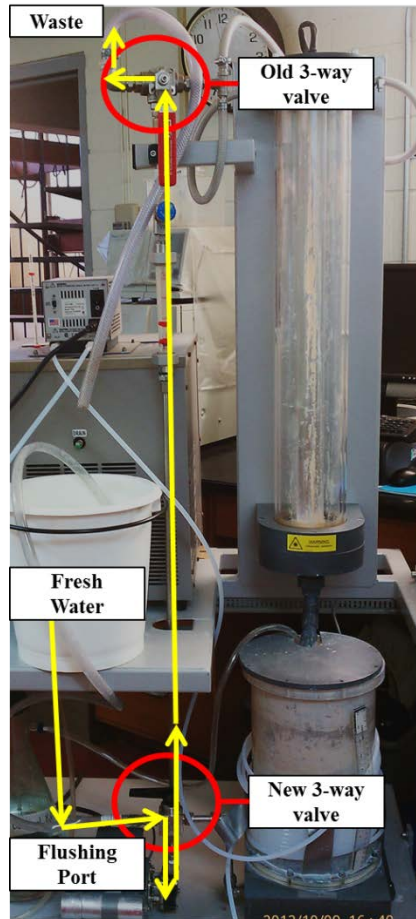


Figure 15: Pump flushing flow path

A second modification to the unit was required to try to maintain constant temperatures throughout the duration of kinetics testing. In tests performed by previous students, it was found that the temperature kept rising over the course of each trial. The temperatures would reach nearly 50°C in four hours' time. To counteract this rising temperature, a cooling system was installed to limit the heating of liquid in the reservoir. The cooling system limited the increase of the sample temperature to a maximum of 35°C as shown in Figure 16.

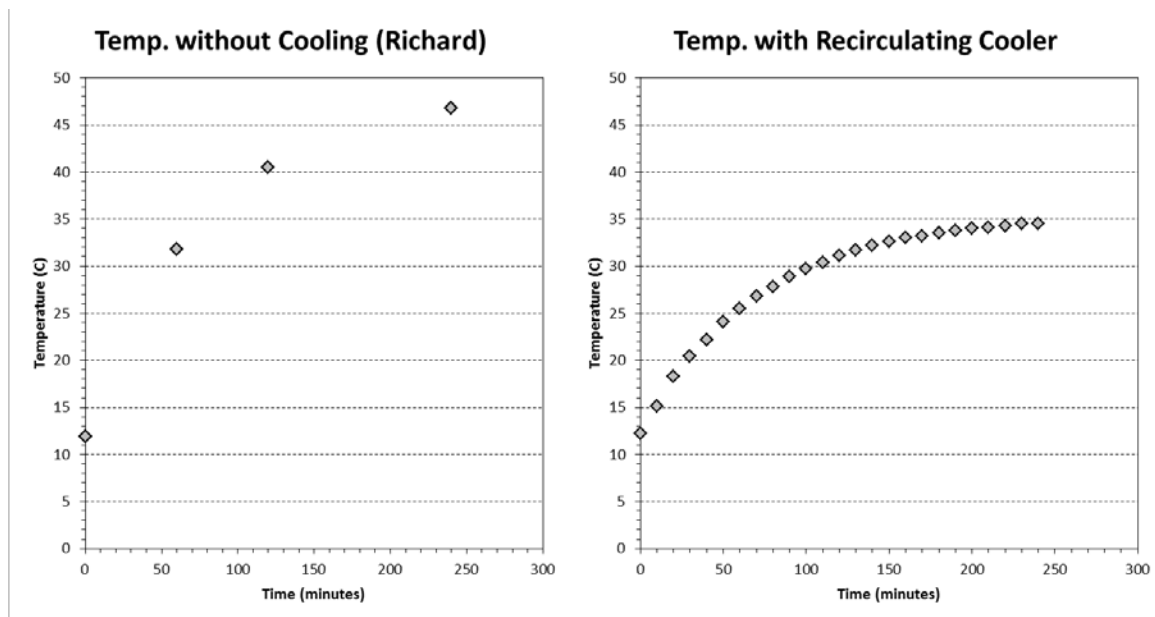


Figure 16: Temperature rise before cooling (left) and after cooling (right)

A VWR Recirculating Chiller 1150S with a 13-L capacity was purchased. The chiller unit can circulate fluid at a temperature range of -30°C to 150°C. The circulating fluid used was Dynalene HC-50 (hydrocoolant), which is an aqueous based heat transfer fluid. Dynalene HC-50 works efficiently between a temperature range of -50°C to 218°C. The silicone-based Dynalene HC-50 bath fluid was selected to maximize our heat transfer to provide the best thermal stability for the reactor, as possible given the technological limitations. The recirculating cooler has inlet and outlet ports located at the rear of the unit which lead to the 13-L reservoir as shown in Figure 17.

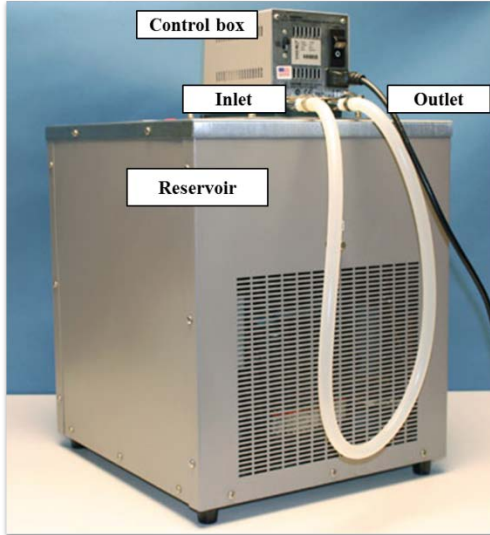


Figure 17: VWR Recirculating Cooler 1150S

The hose in Figure 17 was replaced with a 50 ft long, 3/8-inch OD polytetrafluoroethylene (PTFE) tubing, which was attached to the inlet port and then wrapped around the reservoir of the advanced oxidation unit multiple times (see Figure 18) before the opposite end was connected to the outlet port of the cooler to close the loop. As shown, crystalline ice formation occurred on the outside of the tubing due to the temperature of the liquid cycling through it. It can also be seen that duct tape was applied to secure the tubing to the reservoir.



Figure 18: Recirculating cooler hose surrounding leachate reservoir (left) and Frank Youngman testing the temperature control system provided by the recirculating chiller unit

A third modification was an air pump. Specifically, the Sweetwater SL22 linear air pump was utilized in conjunction with a large flask of deionized water (to saturate the air with moisture to limit evaporation) and an air stone in the shape of a rectangular prism to add air directly into the leachate reservoir (see Figure 19).

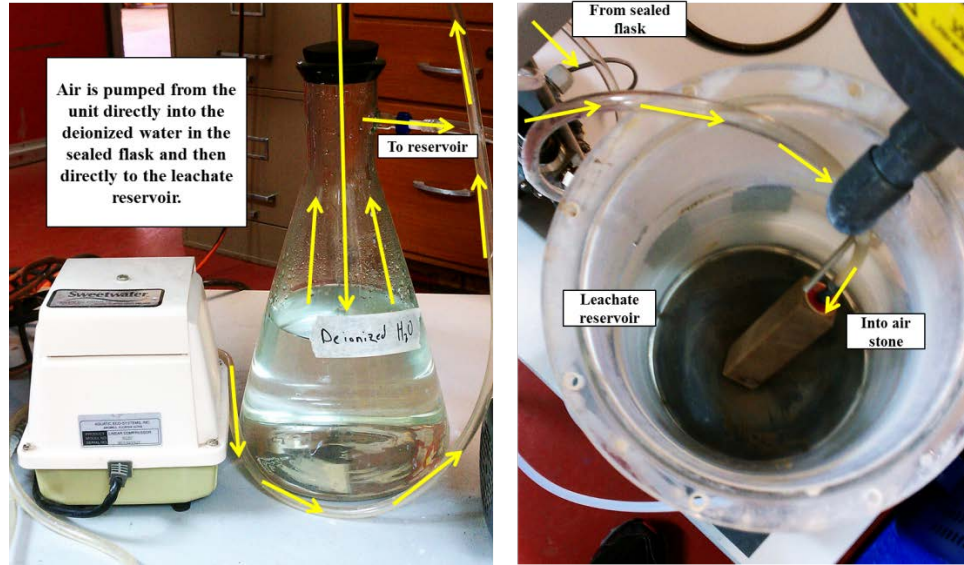


Figure 19: Air pump system

A Y-attachment and two-way valve was installed onto the tubing which the air is pumped through (See Figure 20).

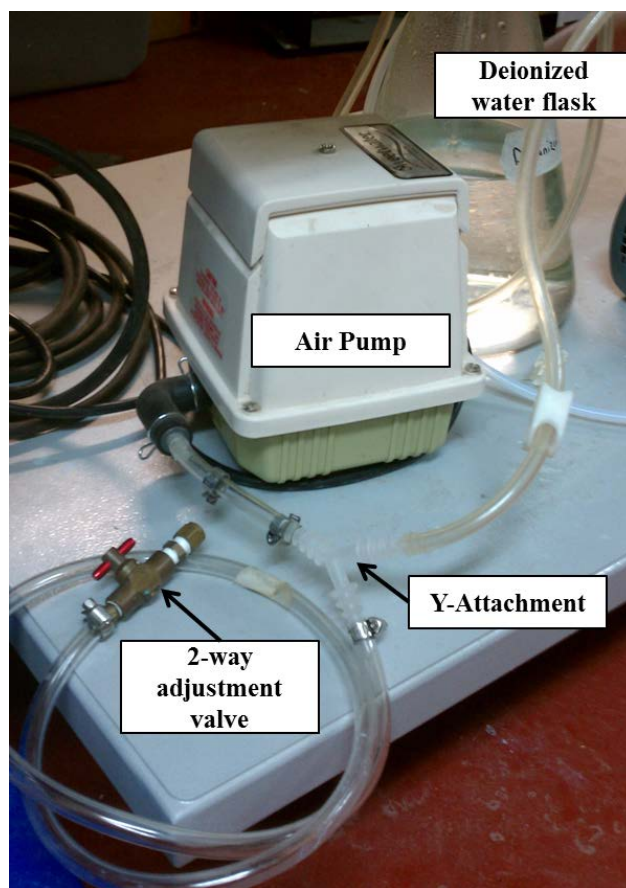


Figure 20: Pictorial display of Y-attachment in air pump system

Opening the valve allowed a portion of the pressurized air to escape into the open environment, thus reducing the amount of air introduced into the leachate, permitting agitation in the reservoir without causing overflow. No attempt was made to measure the flowrate of air added to the reservoir. There are two main purposes to the addition of the air pump system. The first is to agitate the leachate sample to prevent settling of the heavy TiO_2 particles. The second function is to accelerate oxygenation of the sample. One issue found in prior research was that when the air was pumped into the leachate, the mixture would immediately foam up and overflow the reservoir. So the valve was adjusted mid-experiment, as needed, to limit foaming.

2.4 Experimental Procedure

Before beginning the experiments, a review of the work performed by previous students using the falling film reactor was executed. This review led to the initial determination of running the leachate through the advanced oxidation machine in 4-hour segments to limit the increase in reaction temperature. This was to be performed until acceptable temperature control was achieved and then longer test segments would be possible. The full length of each experiment was unknown in the beginning because the amount of removal that would occur was to be determined. From the literature and data review, it was found that a process that took longer than 24 hours to break down the contaminants in the leachate was inefficient. For completeness, some experiments were carried out for periods well in excess of 24 hours. Prior to each experiment, a sample would be taken from the raw leachate to determine the initial levels of the parameters of interest.

To begin each experiment, the leachate was removed from storage and then 8L was measured out, 2 liters at a time, using a 2L graduated cylinder as shown in Figure 21



Figure 21: 2L of leachate in a 2000 mL graduated cylinder

The 8 liters of raw leachate was then added to the advanced oxidation unit's reservoir (Figure 22). Once the raw leachate was added to the machine, a sample of 30-40 mL was taken from the leachate for testing. Approximately 7 mL of this sample was permanently removed from the leachate, as the unused remainder of the sample was poured back into the reservoir.



Figure 22: 8L of leachate in CE584 reservoir

The next step in the process was to add the titanium dioxide photocatalyst. Through analysis of the previous batch scale work, it was determined to add 4 grams of TiO_2 per liter of leachate for the first experiment. Further amounts of catalyst were to be determined by the results of the previous experiment to arrive at an optimum dose at this scale. The catalyst was gathered in a 1000mL HDPE beaker and weighed using Mettler-Toledo's XS204 DeltaRange Analytical Balance. Once the correct amount of catalyst was measured out, the advanced oxidation machine was turned on, and the centrifugal pump and the air pump were started to begin circulating the leachate. After about 5 minutes, the TiO_2 was slowly added to the leachate allowing it to thoroughly mix into the liquid and prevent clogging of the system. After the catalyst appeared to be well mixed (about 5-10 minutes) with the leachate, the pump and air pump were shut off so that a 30-40 mL sample could be obtained from the mixture (see Figure 23).



Figure 23: Leachate containing TiO₂ photocatalyst

After the second initial sample (leachate plus catalyst) was taken, the machine's pump, the UV lamp, the air pump, the recirculating cooler, and a digital timer were all activated. At this point, the temperature was recorded from the digital output on the control box of the advanced oxidation machine. Initially, the temperature was inscribed every five minutes to gain an understanding of the temperature control exhibited by the recirculating cooler. Once the behavior pattern of the temperature was established, recording at 5 minute intervals was determined to be unnecessary. Thereafter the interval increased to 10 minutes and then 30 minutes. The advanced oxidation machine was run until the timer reached 4 hours, at which point the machine's pump, the UV lamp, the air pump, the recirculating cooler, and a digital timer were all stopped or switched off. Another 30-40 mL sample was taken for parameter testing. Then the drain valve was opened to allow the leachate to drain into the desired container so that it could be put

back in refrigeration to limit any further breakdown or biological growth from high temperatures. Once the leachate was stored, a bucket full of 8-9 liters of tap water was poured into to the leachate reservoir and cycled through the system to collect any catalyst or other constituents remaining in the machine. That flushing process was repeated 3-5 times depending on the clarity of water when it was drained out of the system. After flushing the main system, the pump was flushed as described earlier.

2.5 UV dosage testing

The power of the UV lamp was tested using a Fisher Scientific Traceable UV Light Meter. To perform the measurement, the ultraviolet lamp had to be removed from the unit, away from the protective barriers. The diameter of the UV bulb itself, the protective quartz glass tube and the borosilicate glass reactor wall were all measured and compared to the specifications given in the CE584 Advanced Oxidation manual, shown in Table 13.

Table 13: Technical data on the falling film reactor

Falling film reactor	Material	Diameter (mm)
Inner protective tube	Quartz glass	43
Reactor wall	Borosilicate glass	110
Outer protective tube	PMMA XT	-

To determine the distance between the UV source and the reactor tube (i.e. the distance to the leachate), the radius of the UV bulb was subtracted from the radius of the borosilicate glass reactor wall. This distance was found to be 1.84 inches.

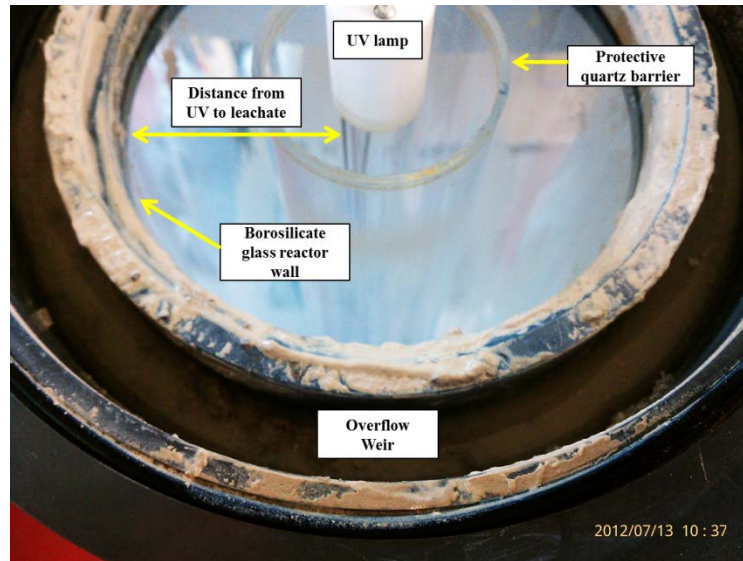


Figure 24: UV distance from reactor wall denotation

Once the distance from the UV source was determined, the UV lamp was taped to the back of the oxidation machine. The sensor was then placed at the correct distance from the bulb for 5 – 10 minute readings. The UV sensor showed that the UV lamp reached maximum power output after the lamp had been on for five minutes.

2.6 Analytical Methods for Parameters of Interest

The advanced oxidation unit was used to test the removal efficiency of the following constituents: COD, ammonia, alkalinity, color, and pH.

2.6.1 COD

For chemical oxygen demand (COD) testing the Reactor Digestion Method for the Hach DR4000U (Loveland, CO) was used with the High Range COD digestion vials (20 to 1,500 mg/L as O₂). The main reaction concerned in this method is the reduction of the dichromate ion (Cr₂O₇²⁻) to chromic ion (Cr³⁺). These can be analyzed

colorimetrically because the two species of chromium are colored (Cr^{6+} (orange), and Cr^{3+} (green)) and absorb visible light. Theoretically, since each dichromate ion accepts 6 electrons per molecule and each molecule of dioxygen accepts 4 electrons, the COD of 1 g of $\text{Cr}_2\text{O}_7^{2-}$ is equal to 1.5 g of dioxygen. The COD was tested prior to treatment and then after every subsequent 4 hours of treatment. At least 2 duplicate samples were created for each COD test. After centrifugation at 6000 rpm to separate the photocatalyst particles, samples were diluted to 2.0 mL using 18.2M Ω -cm deionized water. Throughout the pilot scale testing, a dilution of 1:10 was used. Briefly, 2 mL samples were inverted 20 times to mix and placed in a heating block at 150°C to digest for 2 hours. Samples were removed from the heating block and inverted another 20 times before being allowed to cool for one hour in the dark. At this point, samples were wiped clean using a Kim-Wipe and analyzed using a Hach DR/4000U UV-Vis spectrophotometer. The COD value in mg/L was recorded. A certified reference material (Total Organic Carbon Std. 1,000ppm (Prepared to EPA Method 415-1) Aqua Solutions, Deer Park, TX) was used to check the instrument calibration. This value varied from 0.1-14.7% error. One calibration check standard was analyzed per COD test. It was discovered that high levels of chloride in the samples can work as an interferent in this test method. When accelerated levels of chloride (>2,000 mg/L) are present in the sample, the chlorides can be quantitatively oxidized by the dichromate, consequently displaying erroneous levels of oxidizable organic compounds. For this reason, the chlorides were tested in the leachate as described in the chloride section.

2.6.2 Ammonia-Nitrogen

For ammonia-nitrogen, the EPA Method # 350.2 (Detection of Ammonia by Colorimetry), Nessler spectrophotometric method was used. An ammonia (Medium Range: 0.00 to 9.99 mg/L as $\text{NH}_3\text{-N}$) ion specific meter from Hanna Instruments (Woonsocket, RI) was used. The test began by adding 10 mL of sample to a 10 mL cuvette. The cuvette was cleaned with a Kim-wipe and placed in the instrument to be zeroed out. Next, four drops of the first reagent were added to the cuvette. The cuvette was then swirled and then four drops of the second reagent were added (see Figure 25) and the sample was swirled again.



Figure 25: Reagent addition to cuvette for ammonia testing

The cuvette was cleaned once more before being placed back into the instrument. The recommended reaction time of 3.5 minutes was allowed to pass before the reading was

taken. The instrument directly displayed the concentration in mg/L of ammonia-nitrogen ($\text{NH}_3\text{-N}$) on the liquid crystal display (see Figure 26).



Figure 26: Sample reading from HI 95715 Ammonia Medium Range ISM

To convert the reading to mg/L of ammonia (NH_3), ammonia-nitrogen values can be multiplied by a factor of 1.216. For the purpose of these experiments conversion was not necessary since the Broward County Sewer Use Limitations specify a limit of 25 mg/L as $\text{NH}_3\text{-N}$. Dilution was necessary to lower the concentrations of known interferences, such as organics, sulfides, color, chloramines, aldehydes, and hardness above 1 g/L as CaCO_3 . Due to the potency of the ammonia in real leachate a 0.4 – 1% dilution was used.

2.6.3 Alkalinity

For the total alkalinity measurements, SM 2320B was used. A Hach digital titrator was loaded with a 1.600 N H₂SO₄ titrant cartridge for all analyses. First the sample was diluted to 0.4 – 1%, then phenolphthalein indicator was added to the sample. Titrant was added until the phenolphthalein endpoint was reached (pink to clear), if necessary. The reading on the digital titrator was recorded as corresponding to the phenolphthalein alkalinity in mg/L as CaCO₃ by multiplying the dilution factor by the number of digits. No phenolphthalein alkalinity was measured during any of the experiments. Then the bromocresol green-methyl red indicator was added to the sample, and again titrant was added until the second endpoint was reached (blue-green to light pink). This is the bromocresol green methyl-red alkalinity. When the phenolphthalein alkalinity and bromocresol green methyl-red alkalinity values were added together, this corresponded to the total alkalinity value.

2.6.4 Color

The color parameter was monitored with a color wheel comparison method in order to determine the magnitude of color removal. The procedure for this analysis was taken according to SM2120B using a Hach Model C0-1 color comparator (2234-00; lot number: A7984). For each sample, 5.0 mL was placed into the 15 mL sample viewing tube. Leachate samples were diluted 1:25 with deionized water. Samples were compared to deionized water using a color comparator wheel that was rotated against a light source until a color match was obtained. Values were reported in APHA platinum cobalt units.

2.6.5 pH

For all experiments, pH was recorded during, prior, and at the end of every experiment using pH Indicator Strips (Whatman Inc., Clifton, NJ), a Hach SensIon 3 pH meter, or a Hach MP-6 multiparameter unit, or a HQ40d Portable pH, Conductivity, Dissolved Oxygen (DO), ORP with ISE Multi-Parameter Meter, with the latter being used for nearly all of the measurements reported. Probes were calibrated periodically with standard pH buffers (4, 7, and 10). Sensors were rinsed with deionized water and dried with kimwipes in between sample readings.

2.6.6 Temperature

The temperature was recorded prior to and during all pilot scale experiments. The advanced oxidation machine has a built in temperature probe in the 10L reservoir. The temperature was recorded from the digital output located on the control box of the unit. Initially, the temperature was recorded every five minutes to gain an understanding of the temperature control exhibited by the recirculating cooler. Once the behavior pattern of the temperature was established, recording at 5 minute intervals was determined to be unnecessary. Thereafter the interval was increased to 10 minutes and then to 30 minutes.

2.6.7 Chloride

The chloride levels of the leachate needed to be tested due to the possibility of interference with the COD measurements. The test performed was Hach Silver Nitrate Method 10246. This method has the ability to test levels of chloride within the range of 100 to 200,000 mg/L as Cl⁻. Before the sample could be tested, an estimation procedure

was performed to determine the sample size and dilution necessary for the test. Consequently 1mL of sample was to be diluted into approximately 100 mL deionized water. A Hach digital titrator was loaded with a 1.128 N Silver Nitrate titrant cartridge for the analyses. The contents of one Chloride 2 Indicator Powder Pillow was added to the sample and mixed thoroughly. The titrant was added to the sample until the end point was reached (yellow to red-brown). The digits added to reach the end point was recorded. The chloride concentration (in mg/L as Cl⁻) was determined by multiplying the number of digits by the given multiplier (determined from Table 2 in the Chloride test procedure). An interference of concern for the chloride test was sulfide. For this reason, a test was run using a Sulfide Inhibitor Reagent Powder Pillow to remove this possible interference from the sample. The results of the sulfide inhibitor showed that sulfide was not present at a level which would cause interference. Accuracy checks were performed using Chloride Voluette® Ampule Standard Solution, 12,500 mg/L Cl⁻. The error derived from the standard ranged from 1.3 – 8%.

2.7 Catalyst Recovery

An experiment was run in an attempt to collect the used catalyst from the treated leachate for reuse. Nylon monofilament filter bags were purchased from Aquatic Eco-Systems for the experiment. The three sizes purchased were 5 micron (BAG5), 10 micron (BAG10) and 20 micron (BAG20). The leachate used for the experiment was diluted with tap water. Five liters of leachate was mixed with 3 L of water and added to the reservoir of the advanced oxidation machine. A catalyst dosage of 5 grams per liter was added to the leachate. The leachate was treated for 8 hours continuously in the machine. Prior to collecting the leachate, the bag was placed in an oven at 100° C for 45 minutes and

subsequently placed in a desiccator for 1 hour. The dried, empty filter bag was placed in a 1000mL HDPE beaker and weighed using Mettler-Toledo's XS204 DeltaRange Analytical Balance. Once the 8 hour treatment of the leachate was completed, the machine was shut down so the filter bag could be attached to the spigot above the 10 L reservoir. Once the bag was attached using a single cable tie the machine was powered back up so the leachate could flow into and through the bag (Figure 27).



Figure 27: Nylon monofilament filter bag attached to advanced oxidation machine for catalyst recovery

After all the leachate passed through the filter bag, the bag was removed and placed into an oven at 100° C for one hour and subsequently placed in the desiccator for one hour. The dried filter bag containing the used catalyst was placed in a 1000mL HDPE

beaker and weighed on the balance. The weight of catalyst recovered was determined to be the difference between the weight of the empty bag and the weight of the bag containing the used catalyst.

3.0 RESULTS AND DISCUSSION

3.1 Baseline Leachate Quality Characterization

Table 14 characterizes the Monarch Hill leachate samples for pH, COD, alkalinity, color, and ammonia. Supporting the fact that leachate quality has high variability, the parameter concentrations varied for each sample, even though 3 of the samples were collected in the same year. The COD ranged from 5,270 – 6,560 mg/L. The alkalinity varied from 3,560 – 4,688 mg/L as CaCO₃. The ammonia levels ranged from 1,310 – 1,855 mg/L as NH₃-N and the color ranged from 750 – 1125 PCU.

Table 14: Summary of Leachate Water Quality Testing Results

Parameter	Units	SE step up station 09/30/2011	SE step up station 03/09/2012	SE step up station 07/18/2012	SE step up station 11/02/2012
Alkalinity	mg/L as CaCO ₃	4625	3560	4125	4688
pH	pH units	7.8	7.4	7.7	7.7
Color	PCU	1125	950	760	750
Ammonia	mg/L as NH ₃ -N	1855	1310	1635	1700
COD	mg/L as O ₂	6250	5270	6560	6180

3.2 Preliminary Testing

Initial screening experiments were conducted to test the efficacy of hydraulic modifications to the pilot testing unit which allowed for longer term experiments. In

previous work (Meeroff and McBarnette 2011), testing was limited to only 4 hours before the temperatures became excessive ($T > 60^{\circ}\text{C}$). The modifications were described in the previous methodology section. After running the pilot unit for a total of 44 hours over an 11-day period, reaction temperatures below $20 - 35^{\circ}\text{C}$ were maintained, consistently, as shown in Figure 28. For each experiment, the maximum temperature was recorded as described previously.

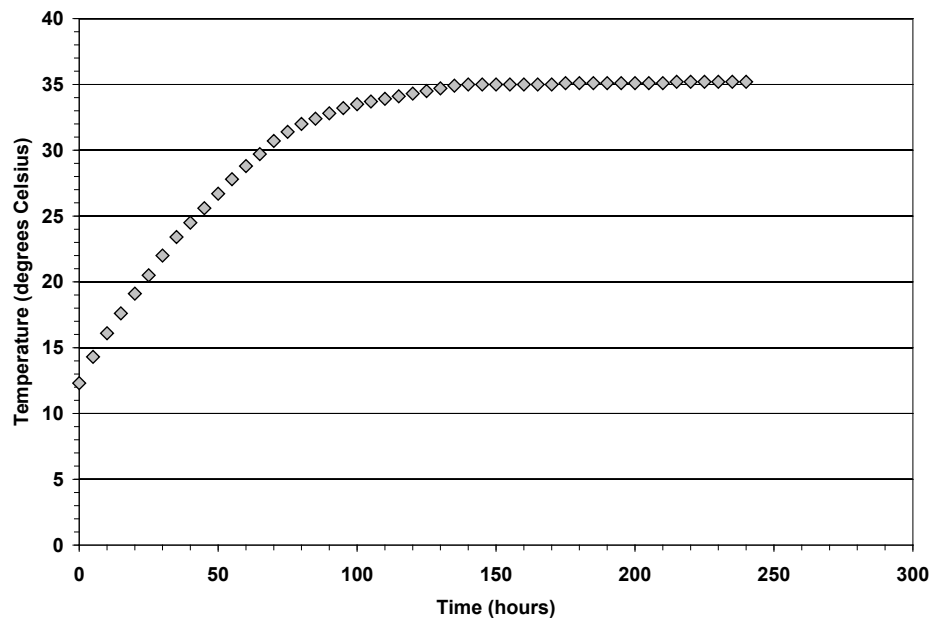


Figure 28: Typical temperature curve collected during one of the 4-hour pilot test runs (January 13, 2012)

The UV dosage was tested in July of 2012 by removing the UV lamp from the advanced oxidation machine. A Fisher Scientific UV light meter was used to measure the intensity of the lamp. Measurements were recorded for approximately ten minutes or once the lamp had stabilized at maximum intensity. The lamp reached maximum intensity at 5-6 minutes. The measurements were taken at two distances from the lamp:

1.84” and 5.38”. The actual distance from the lamp to the reactor wall is 1.84”. Previous UV intensity measurements for the same machine conducted by Kelly Horner were performed at a distance of 5.38”, so this distance was used to compare data results. A summary of the trial results and comparison to Kelly’s data is shown in Table 15.

Table 15: Summary of maximum UV intensities recorded and doses calculated

	Trial 1	Trail 2	Trial 3	Kelly H.
Measurement Distance (in)	1.84	1.84	5.38	5.38
Sample distance from reactor wall (in)	1.84	1.84	1.84	1.84
Measured Intensity (mW/cm ²)	0.34	0.37	0.14	0.21
Calculated UV dose @ 1.84" (mW/cm ²)	0.34	0.37	1.17	1.78
$I_{(IR),z^*}$ (mW/cm ²)	1.16	1.25	4.03	6.12

$I_{(IR),z^*}$ = Intensity of incident radiation entering the inner wall of the annulus at $z^* = 0.5$

The intensity measured in July 2011 was higher than the intensity measured one year later. This suggests a decrease in UV intensity over the life of the lamp. The calculated dose was the result of applying the inverse square law by multiplying the measured intensity (mW/cm²) by the measurement distance squared and then dividing by the sample distance squared. The distances did not need to be converted to centimeters because their units cancel each other out. Measuring from the actual reactor distance resulted in much lower calculated intensities than measuring from far away. This was unexpected since increased light scattering should occur over longer distances in air. During the measurements, the only interference between the UV lamp and UV meter was air. Also, these measurements assumed that the full power of the lamp was being recorded. This was not the case due to the limitation of the UV light meter, which can only measure wavelengths between 320 – 390 nm. The UV lamp in the falling film reactor emits most of its intensity in the 250 – 260 nm range, which was not recorded by the UV light meter. Previous UV testing conducted by André McBarnette on the batch

scale reactor UV dose resulted in calculated intensities as high as 130 mW/cm^2 . The UV doses from the various UV/TiO₂ experiments in Table 10 ranged from 1.8 – 10 mW/cm^2 . Compared to these and the batch scale UV intensities, the UV dose is relatively low for this falling film reactor unit.

The application of UV radiation to the leachate causes the water to heat up, which could theoretically lead to evaporation losses and difficulties for kinetics experiments. Testing for evaporation losses from the falling film reactor were conducted by previous FAU researchers (Meeroff and McBarnette 2011). The experiment used 8.0-L of deionized water instead of leachate. Temperature and evaporation were recorded during the experiment and the results were plotted (Figure 29).

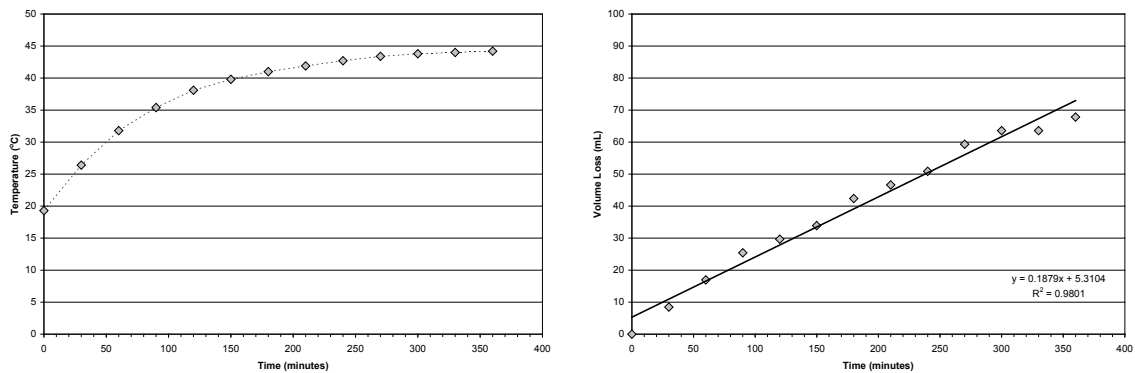


Figure 29: Time plots for the evaporation experiment. Temperature curve (left) and evaporation loss curve (right)

The temperature rose to a maximum of 44.2°C in six hours. The average evaporation rate determined by the data was found to be 11.5 mL/hr . The total volume loss for the six hour period was 70 mL , which equates to 0.9% . It was determined that evaporation losses can be neglected when losses are less than 2% , so the evaporation losses for the falling film reactor can be ignored.

A previous FAU research assistant, Richard Reichenbach, performed a dark test with the falling film reactor. The experiment was performed with 8.0-L of leachate collected from the Monarch Hill landfill SE step up station. A catalyst dosage of 36.7 g/L TiO₂ was used. The experiment was run for 6 hours with no application of UV radiation. The results of the dark reaction showed no change in pH or removal of COD (Figure 30) (Meeroff and McBarnette 2011).

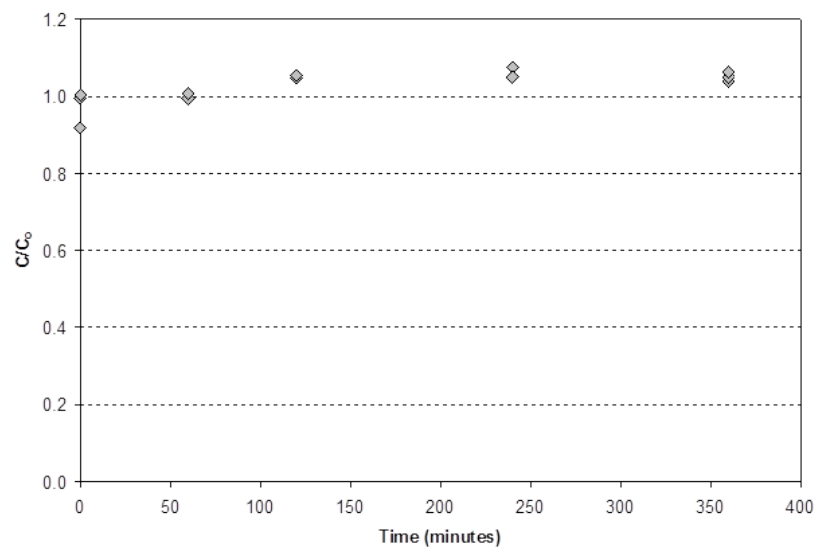


Figure 30: Results of dark reaction for falling film reactor

3.3 Preliminary Assessment of Pilot Performance

Preliminary experiments were designed to attempt to optimize the catalyst dosage, understand more about the alkalinity dependence, and learn more about the reaction order kinetics, if possible. During operation of the preliminary testing pilot unit, measurements of COD, ammonia, color, alkalinity, and pH were recorded to investigate system performance. Experiments were run at 4-hour intervals at which time the leachate was

removed from the unit to cool back down to room temperature and flush any suspended materials from the pump housing. This was repeated after each 4-hour period. Samples were collected at $t=0$ and $t=4$ hours for each daily run as described in the previous methodology section. The starting point for the catalyst dosage optimization experiments was derived from previous bench scale experiments (Merroff and McBarnette 2011) which gave 100% COD removal using 4 g/L TiO_2 .

A summary of all the pilot scale experiments performed is presented in Table 16. The experiments were run over the course of approximately one year. Table 16 clearly displays the catalyst doses used and the parameters measured throughout the testing.

Table 16: Summary of all six pilot scale experiments with parameter removal at 24 hours

Exp.	Date started	TiO ₂ (g/L)	Max Temp. (°C)	pH (pH units)		Alkalinity (mg/L as CaCO ₃)		Ammonia (mg/L as NH ₃ -N)		COD (mg/L as O ₂)		Color (PCU)	
				range	mean	Alk ₀	Alk _f	Amm ₀	Amm _f	COD ₀	COD _f	Color ₀	Color _f
1	12/29/11	4	36.7	8.35 – 9.26	8.89	4625	875	1713	306	6246	4890	1125	750
2	05/16/12	16	35.7	7.63 – 9.18	8.84	3560	1375	1310	602	5268	3780	825	575
3	06/18/12	25	36.0	7.54 – 8.96	8.72	3563	1875	1380	700	5360	3540	788	525
4	08/08/12	40	36.7	7.59 – 9.06	8.74	4313	1130	1523	842	6990	4530	756	325
5	09/20/12	30	36.3	7.70 – 9.20	8.87	4125	1013	1635	845	6135	4322	756	425
6	12/10/12	10	37.1	7.66 – 9.09	8.73	4375	700	1700	470	6064	5343	813	600

3.4 Experiment 1

For the first long time trial, real leachate from the SE step up station collected on September 30, 2011 was used, with an initial COD concentration of 6,250 mg/L and 4 g/L of TiO₂ photocatalyst (0.6:1 TiO₂:COD ratio). The results of the first experiment after 44 hours of treatment showed various removal rates among the parameters of interest. Table 17 summarizes the results of the first experiment.

Table 17: Removal of parameters from experiment 1 (4 g/L TiO₂) after 44 hours

Parameter	Units	C ₀	C ₄₄	Removal (%)
COD	mg/L as O ₂	6250	3910	37.4
Ammonia	mg/L as NH ₃ -N	1710	172	89.9
Alkalinity	mg/L as CaCO ₃	4630	500	89.2
Color	PCU	1130	525	55.5

The ammonia and alkalinity degraded at nearly an identical rate until the end of the experiment at which time both constituents approached 90% removal. Slightly more than half of the color was removed in 44 hours. The lowest removal percentage came from the COD at only 37.4%, but 2,350 mg/L of COD was destroyed. The wide difference in removal percentages prompted an investigation of which of the water quality parameters may be the limiting parameter. This was done by comparing the removal rates of COD, alkalinity and ammonia. A graphical display of the comparison is shown in Figure 31.

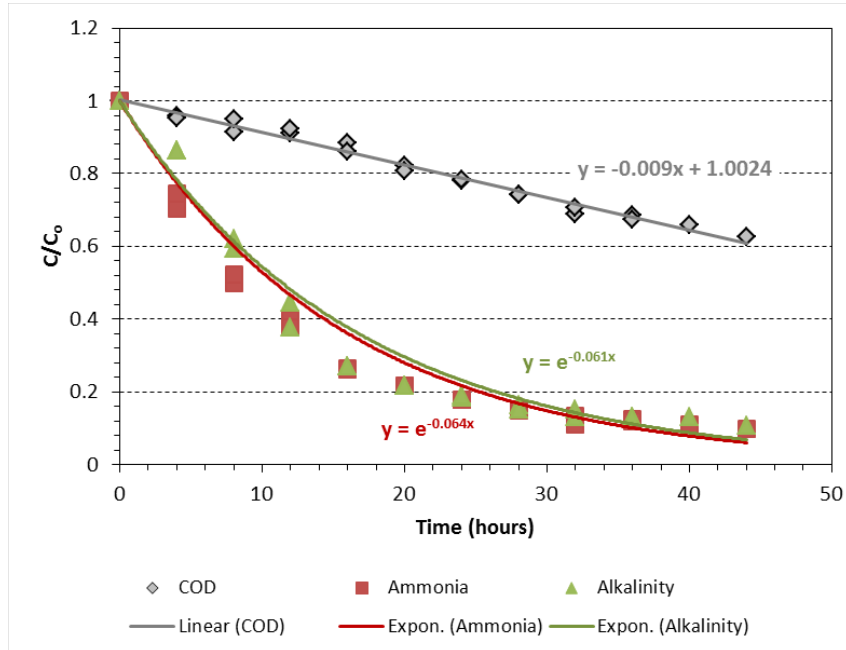


Figure 31: Removal rate comparison of alkalinity, ammonia and COD using 4 g/L TiO₂

Figure 31 clearly shows a more rapid degradation rate for ammonia and alkalinity when compared to the oxidation of COD. It can be deduced that once all of the COD has been oxidized, the ammonia and alkalinity will likely have already been degraded as well. Also, it appears that the destruction of COD follows a linear trend while the degradation of ammonia and alkalinity follow a more complex trend. This difference in degradation patterns and rates beckons for the investigation of the reaction kinetics for all parameters of interest. Assuming first order kinetics for the same comparison of parameters in Figure 31 results in a clear distinction as well. The COD exhibits a slope of -0.011 ($R^2 = 0.984$) while the ammonia and alkalinity have slopes of -0.053 ($R^2 = 0.944$) and -0.053 ($R^2 = 0.922$), respectively. This shows that initially, the first order rate of

degradation of alkalinity and ammonia is five times that of COD removal. This, again, clearly indicates COD to be the limiting parameter.

3.4.1 COD Kinetics

Since the limiting parameter was determined to be COD, the first kinetics investigation experiment was focused on COD removal. Kinetics data was plotted for zero order (Figure 32), first order (Figure 33) and second order (Figure 34).

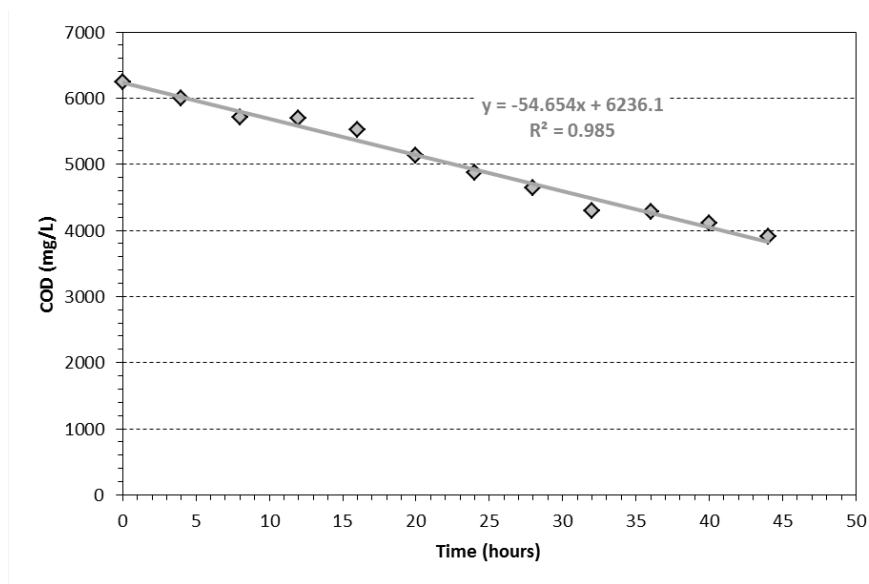


Figure 32: Zero order COD kinetics plot for experiment 1 (4 g/L TiO₂)

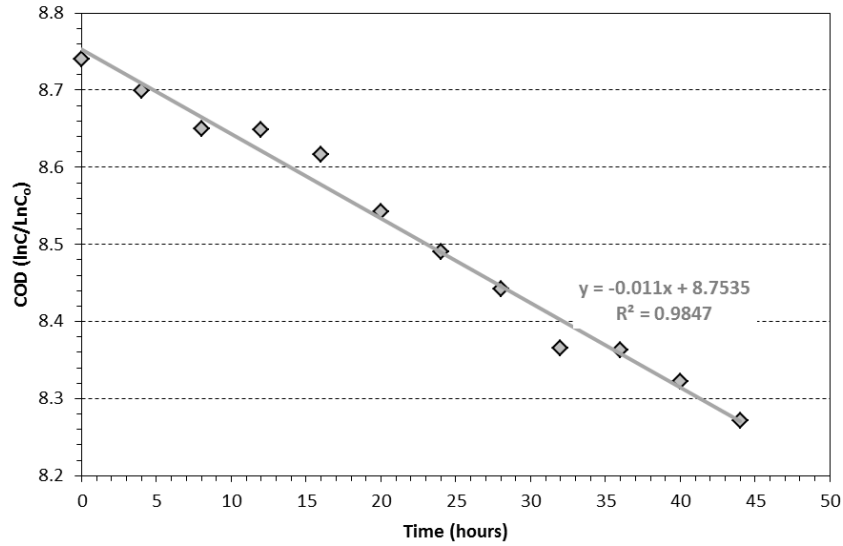


Figure 33: First order COD kinetics plot for experiment 1 (4 g/L TiO₂)

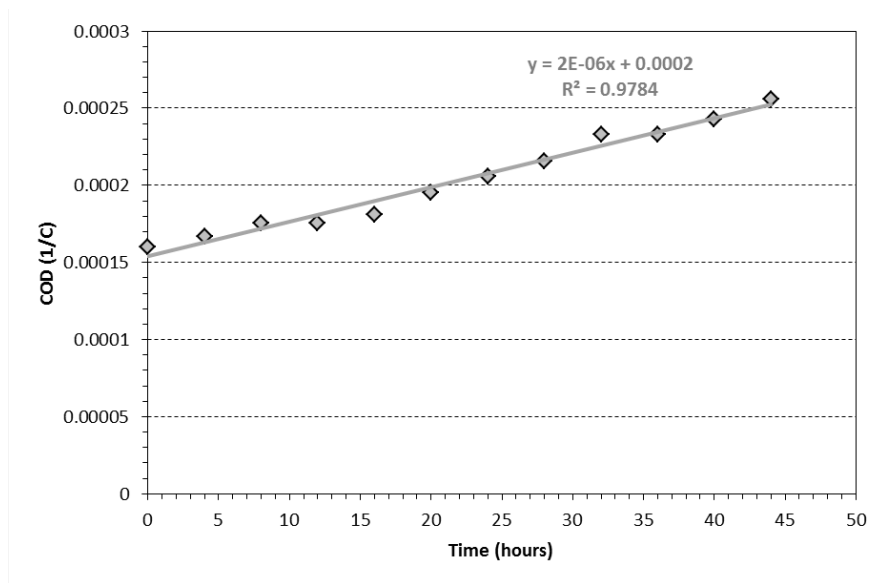


Figure 34: Second order COD kinetics plot for experiment 1 (4 g/L TiO₂)

As shown in previous testing by the FAU Laboratories for Engineered Environmental Solutions (Lab.EES) (Meeroff and McBarnette 2011) and in other

literature (Chong et al. 2010), the kinetics could follow either zero or first order. Though, zero order assumes that the degradation rate is constant with time, which does not seem to be possible since the catalyst has reported issues with deactivation, which slows down the reaction process (Carneiro et al. 2010). First order reactions assume that degradation rate is concentration dependent, which fits with the experimental results and follows a behavior of multiple reactions taking place. For example, adsorption of organics on the TiO₂ surface reduces the active area for UV radiation to penetrate and excite the catalyst, which in turn decreases the reaction rate. Initially there is a high concentration of COD in the complex leachate matrix, which increases the probability that free radicals will collide with COD molecules as opposed to competing compounds. As the COD concentration is decreases, it can be assumed that the likelihood of free radicals and/or photons colliding with COD particles in the matrix is decreased as well. From inspection of the data collected in this experiment, the coefficient of determination (R²) is ≈ 0.985 for both zero and first order reactions suggesting an equal possibility of either zero or first order kinetics for COD degradation. Rearranging the kinetics equations to solve for the time needed for the actual removal percentage can give further insight on the reaction time. The estimated time for target removal of COD (800 mg/L COD) using zero order kinetics is calculated by:

$$t = \frac{C_t - C_0}{-k} = \frac{6246 - 800}{-56.23} = 96.9 \text{ hours}$$

The estimated time for target removal using first order kinetics is calculated by:

$$t = \frac{\ln\left(\frac{C_t}{C_0}\right)}{-k} = \frac{\ln\left(\frac{800}{6246}\right)}{-0.0102} = 201.5 \text{ hours}$$

The estimated time for target removal using second order kinetics is calculated by:

$$t = \frac{\left(\frac{C_0}{C_t} - 1\right)}{kC_0} = \frac{\left(\frac{6246}{800} - 1\right)}{0.000002 \times 6246} = 545 \text{ hours}$$

The time for the target achievement of 800 mg/L COD using 4 g/L TiO₂ under these conditions are estimated by zero order and first order calculations as 97 and 202 hours, respectively. Further investigation of the reaction order can be done by fitting the data to the three models. If the data follows the zero, first or second order model, then it can be said that the data are consistent with that particular reaction rate, within the limits of observation (Hemond and Fechner-Levy 2000). The actual COD removal in 44 hours was 37.4%. Solving the zero order reaction equation for 37.4% removal results in a time of 41.5 hours (5.7% error). The times calculated for first and second order are 45.9 hours (4.3% error) and 47.8 hours (8.6% error), respectively. The data appear to more closely follow first order reaction kinetics.

3.4.2 Alkalinity Kinetics

The same process was conducted for alkalinity, ammonia and color. The reaction kinetics plots for alkalinity can be seen in Figure 35 (zero order), Figure 36 (first order) and Figure 37 (second order).

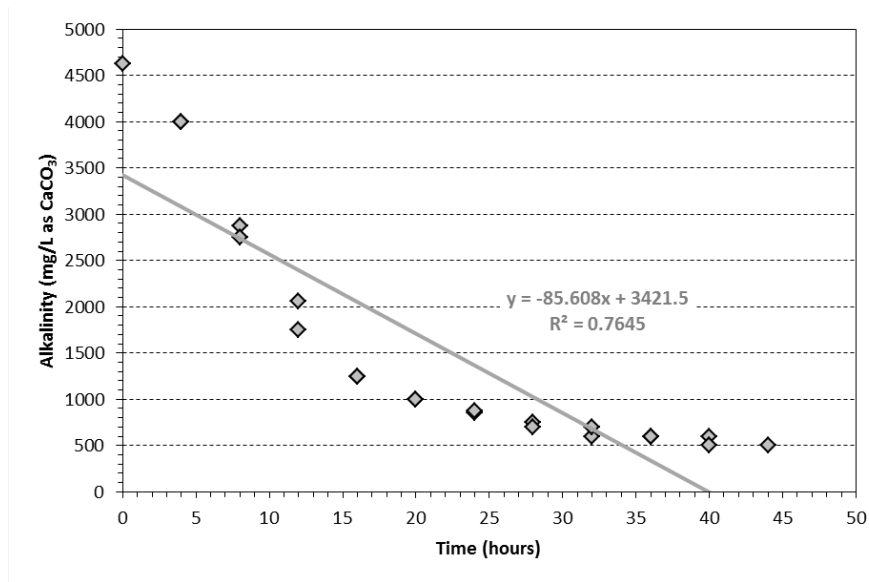


Figure 35: Zero order alkalinity kinetics plot for experiment 1 (4 g/L TiO₂)

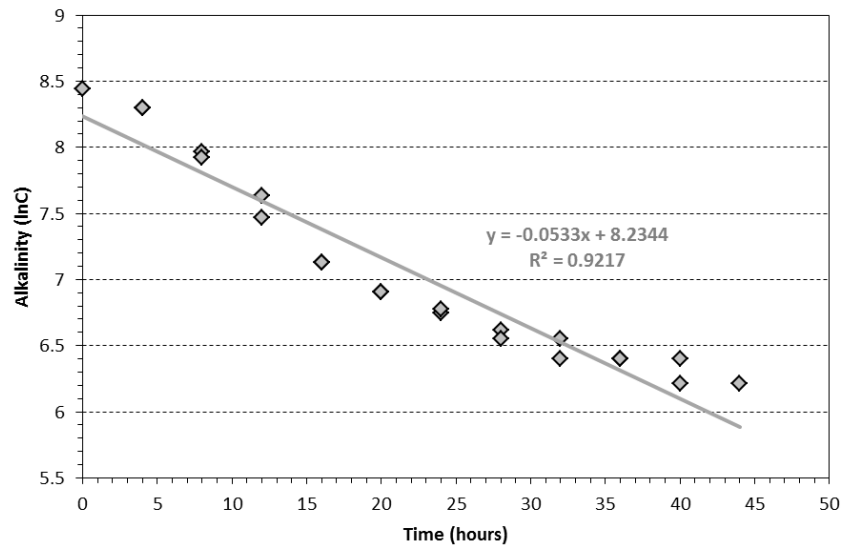


Figure 36: First order alkalinity kinetics plot for experiment 1 (4 g/L TiO₂)

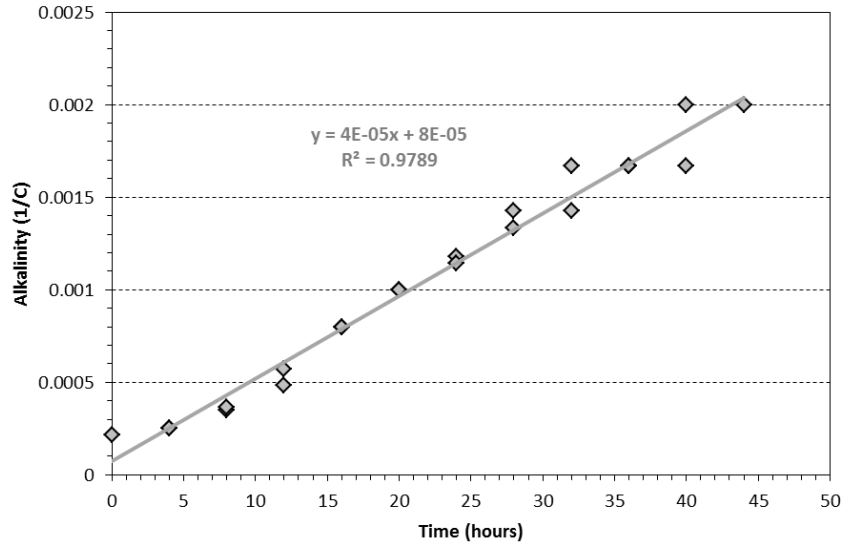
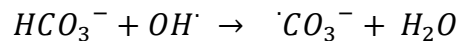


Figure 37: Second order alkalinity kinetics plot for experiment 1 (4 g/L TiO₂)

Inspection of the data presented above shows that the largest coefficient of determination lies in the second order kinetics plot ($R^2 = 0.979$) followed by the first order reaction ($R^2 = 0.922$). The zero order can be ruled out since the shape of data points clearly do not follow an acceptable linear relationship ($R^2 = 0.765$) and appear to create an exponential curve. Due to the high R^2 value of the first order plot, it is difficult to rule out first order even though the data points appear to have a slight curve to them as well. Following these data sets, it would take approximately 30 hours for 90% removal of alkalinity using first order kinetics and 43 hours modeling the second order reaction. Since the experiment actually showed 89% removal at 44 hours, the second order plot is most likely to fit. Kwon et al. (2000) suggested that hydroxyl radical reactions follow second order reaction kinetics for organic compounds and alkalinity in the form of carbonate and bicarbonate. They compared their experimental rate constant to reported rate constants and found similar results. They found a bicarbonate rate constant of $1.93 \times$

$10^7 \text{ M}^{-1}\text{s}^{-1}$ versus the expected value of $8.5 \times 10^6 \text{ M}^{-1}\text{s}^{-1}$. By converting the k-value from Figure 37 to the same units the k constant comes out to $7.6 \times 10^4 \text{ M}^{-1}\text{s}^{-1}$, which is approximately 10 magnitudes difference. A major difference is that Kwon et al. (2000) studied the reaction constants strictly for hydroxyl radical attack of a laboratory solution of bicarbonate in pure water. In the photocatalytic degradation of landfill leachate, the sample matrix is substantially more complex. Bicarbonate alkalinity is known to be a hydroxyl radical scavenger (Kishimoto et al. 2007). Also, the relatively fast degradation of alkalinity could also be a result of the aeration acting as an air stripping mechanism to release CO_2 from the leachate (Kishimoto et al. 2007), but this should only be significant at low pH, which was not the case in these experiments ($\text{pH} > 7.54$).

The specific component of concern of alkalinity is the bicarbonate ions. The range of pH throughout all six experiments stayed within the pH range ($\text{pH} > 6.35$ and < 10.33) where the bicarbonate species dominates the carbonate system. When the bicarbonate species scavenges hydroxyl radicals, the theoretical reaction that occurs is as follows:



The bicarbonate ions react with hydroxyl radicals to form a significantly less effective carbonate radical and water. Due to the scavenging effects, Jia et al. (2011) suggests that removing alkalinity prior to photocatalytic treatment is necessary to increase degradation efficiency for other parameters. The alkalinity plays a role in the rate-determination step for photocatalytic degradation due to its hydroxyl radical scavenging, inhibition of reactions at catalyst surface on account of an increase in negative charge, pH effects, and promotion of catalyst aggregation (Autin et al. 2013).

Also, in strongly alkaline waters, OH^- is rapidly converted to its conjugate base O^- (Buxton et al. 1988).

3.4.3 Ammonia Kinetics

The reaction kinetic plots for ammonia can be seen in Figure 38 (zero order), Figure 39 (first order) and Figure 40 (second order).

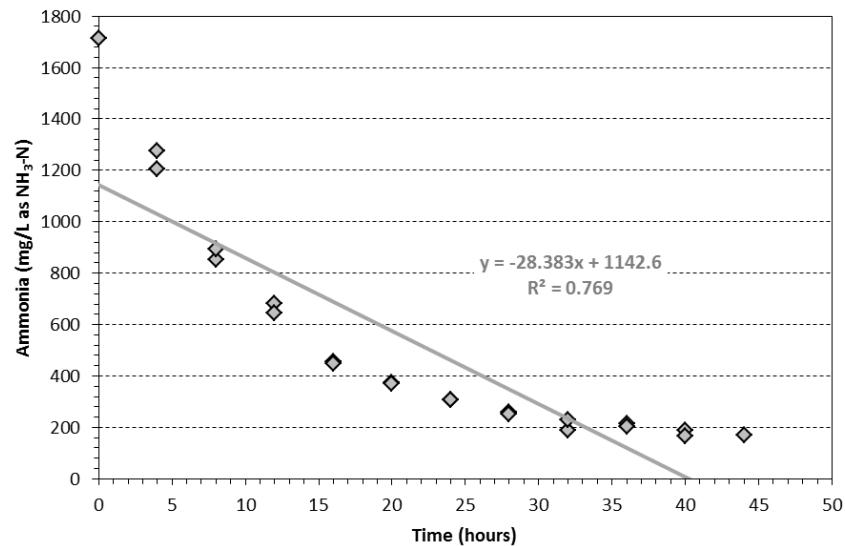


Figure 38: Zero order ammonia kinetics plot for experiment 1 (4 g/L TiO₂)

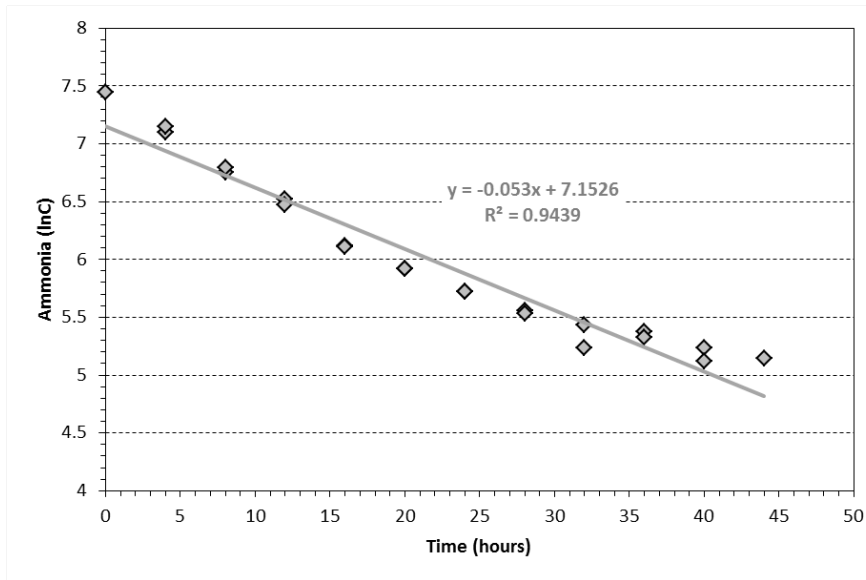


Figure 39: First order ammonia kinetics plot for experiment 1 (4 g/L TiO₂)

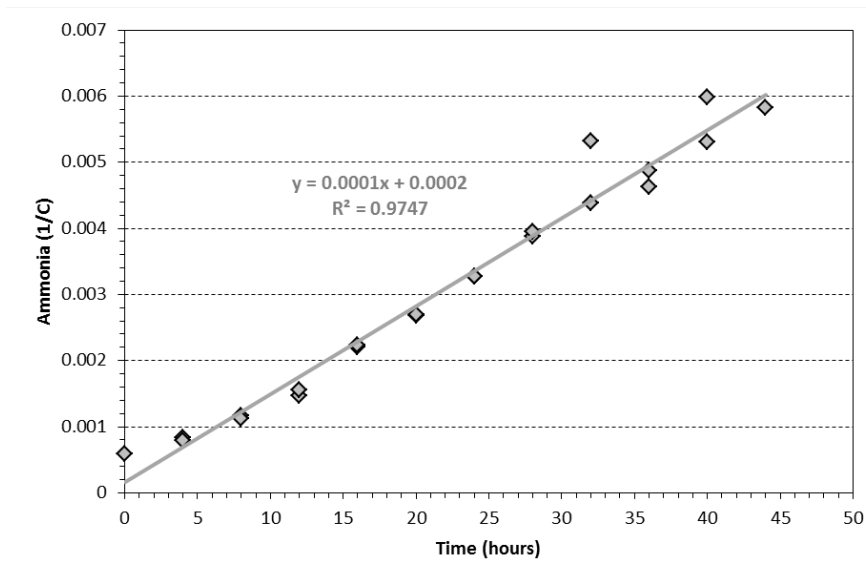


Figure 40: Second order ammonia kinetics plot for experiment 1 (4 g/L TiO₂)

Inspection of the data presented above shows that the ammonia degradation closely mimics the alkalinity degradation. Again, the largest coefficient of determination lies in the second order kinetics plot ($R^2 = 0.975$) followed by the first order reaction (R^2

= 0.944). The zero order can be ruled out since the shape of data points clearly do not follow an acceptable linear relationship ($R^2 = 0.769$) and appear to create an exponential curve. Similar to the alkalinity, the high R^2 value of the first order plot makes it difficult to rule out first order even though the data points appear to have a slight curve to them. Following these data sets, it would take approximately 58 hours to achieve hours to achieve the 25 mg/L $\text{NH}_3\text{-N}$ target for sewer disposal using first order kinetics and 331 hours using second order kinetics.

3.4.4 Color Kinetics

The reaction kinetic plots for color can be seen in Figure 41 (zero order), Figure 42 (first order) and Figure 43 (second order).

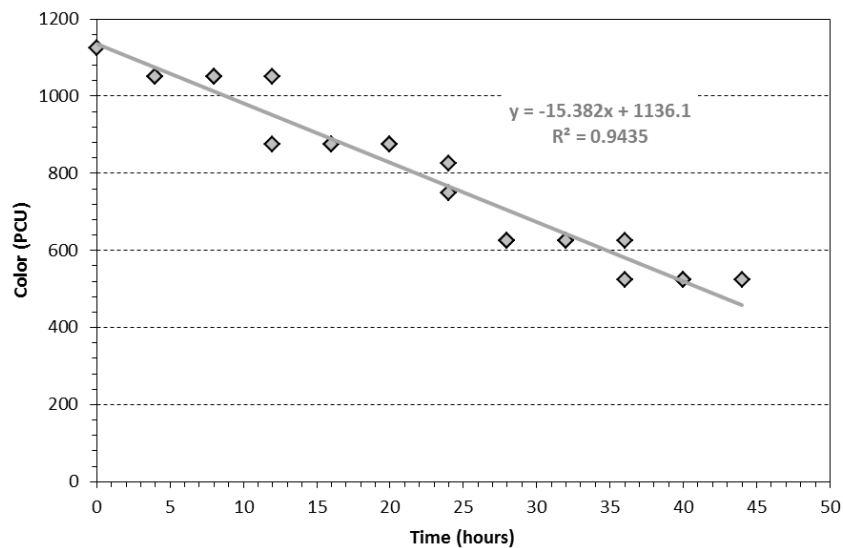


Figure 41: Zero order color kinetics plot for experiment 1 (4 g/L TiO_2)

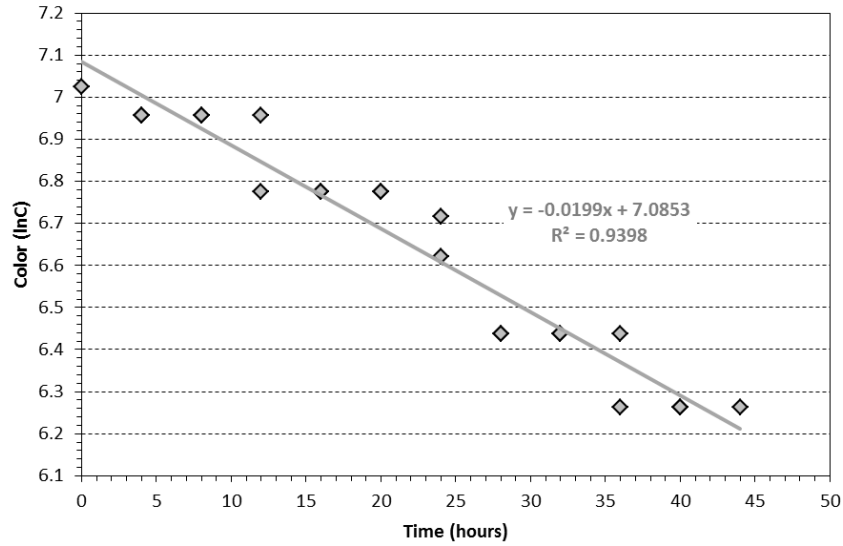


Figure 42: First order color kinetics plot for experiment 1 (4 g/L TiO₂)

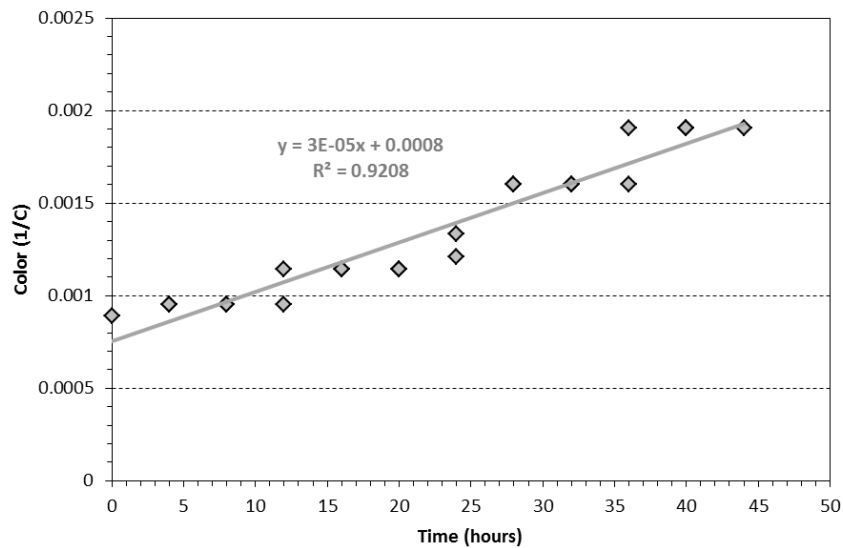


Figure 43: Second order color kinetics plot for experiment 1 (4 g/L TiO₂)

Analysis of the color removal data shows close linear trends for zero, first and second order ($R^2 = 0.944, 0.940$ and 0.921 , respectively). This does not allow the elimination of any order reaction which means that the first experiment does not provide

any progress on the reaction kinetics for color removal. Following these trends, 90% color removal is delivered at approximately 74 hours for zero order, 158 hours for first order and 500 hours for second order reactions.

3.5 Experiment 2

After the first 44 hour test (Experiment 1), the next step was increasing the TiO_2 dosage incrementally to attempt to improve efficiency. The starting point was the 4 g/L dose that gave 100% removal in 4 hours at the bench scale in previous testing (Meeroff and McBarnette 2011), but as described earlier, the pilot reactor has a lower UV intensity and much lower contact time in the reaction zone compared to the bench scale testing conditions. Previous pilot testing conducted in FAU's laboratory with 28 g/L TiO_2 did not show promising results in respect to COD removal (Meeroff and McBarnette 2011). It was hypothesized that increasing the TiO_2 dose to 16 g/L would improve the process efficiency.

This second long-time experiment used leachate from Monarch Hill south east step-up station collected on March 9, 2012. The initial COD was 5,270 mg/L. Samples were collected for parameter measurement at $t=0$ and $t=4$ for each daily run for a total of 10 days (or 40 hours). The results of the first experiment after 40 hours of treatment showed various removal rates among the parameters of interest, which are summarized in Table 18.

Table 18: Removal of parameters from experiment 2 (16 g/L TiO₂) after 40 hours

Parameter	Units	C ₀	C ₄₀	Removal (%)
COD	mg/L as O ₂	5270	3160	40.0
Ammonia	mg/L as NH ₃ -N	1310	408	68.9
Alkalinity	mg/L as CaCO ₃	3560	1000	71.9
Color	PCU	825	425	48.5

Similar to experiment 1, the ammonia and alkalinity degraded at a comparable rate (within 3%), achieving approximately 70% removal. Slightly less than 50% of the color was removed in 40 hours. Again, the lowest removal percentage came from the COD at 40%, which represents 2,110 mg/L of COD that was destroyed. The high removal percentage of alkalinity and ammonia compared to the lower degradation rate of COD supports the limiting parameter hypothesis from experiment 1.

3.5.1 COD Kinetics

Kinetics data for COD was plotted for zero order (Figure 44), first order (Figure 45) and second order (Figure 46).

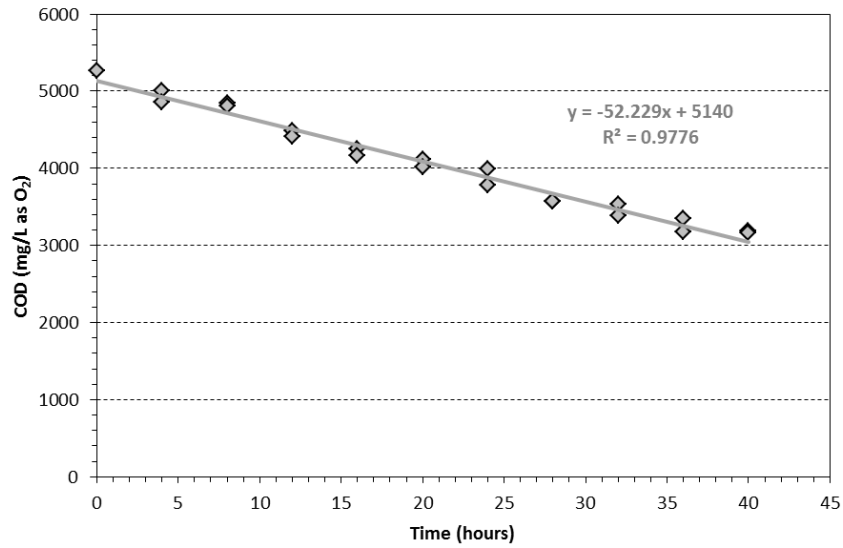


Figure 44: Zero order COD kinetics plot for experiment 2 (16 g/L TiO₂)

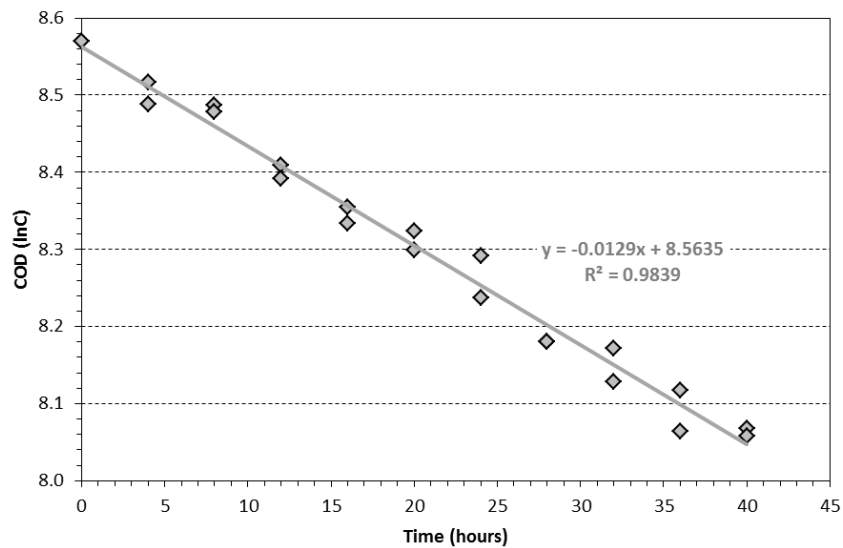


Figure 45: First order COD kinetics plot for experiment 2 (16 g/L TiO₂)

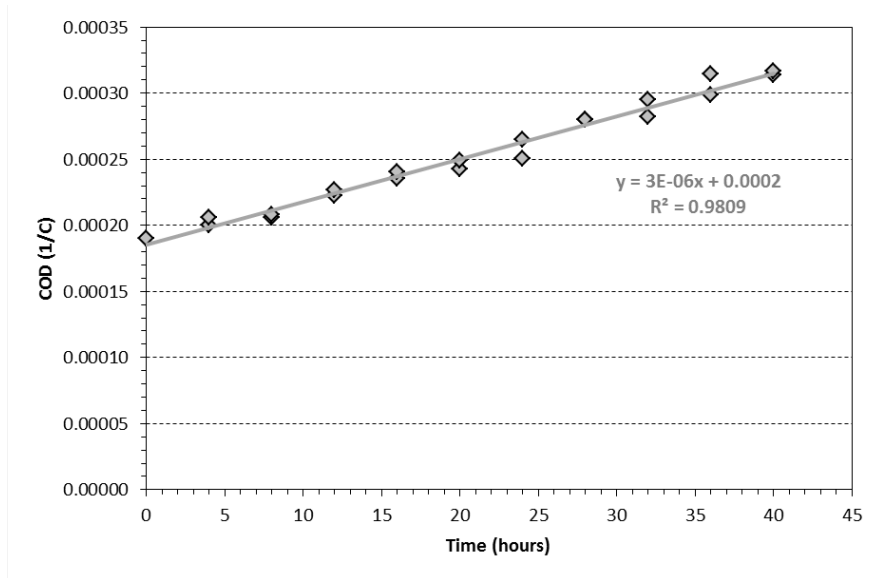


Figure 46: Second order COD kinetics plot for experiment 2 (16 g/L TiO₂)

The kinetics from this experiment appear to follow first order, since it has the highest coefficient of determination ($R^2 = 0.984$). However, zero and second order still seem to follow a linear relationship. Using this data the removal time to achieve 800 mg/L COD is estimated to take 78 hours for zero order, 148 hours for first order and 353 hours for second order kinetics.

The actual removal of COD was 40% in 40 hours. Using the kinetics equations to solve for the time needed to achieve the actual removal percentage can provide more information on the reaction kinetics. Solving the first order reaction for time to remove 40% COD results in 40.2 hours (0.5% error). The zero order and second order estimations result in times of 36.9 hours (7.8% error) and 42.2 hours (5.5% error), respectively. As seen in experiment 1, the first order estimation equates better to the actual removal, strongly supporting COD degradation as a first order reaction.

3.5.2 Alkalinity Kinetics

Further investigation of the kinetics for alkalinity was conducted by plotting the zero order (Figure 47), first order (Figure 48) and second order (Figure 49) data.

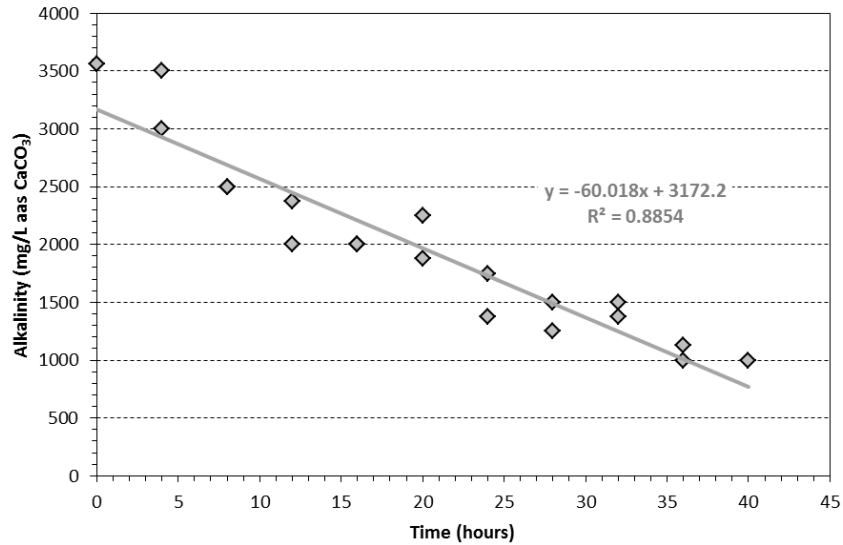


Figure 47: Zero order alkalinity kinetics plot for experiment 2 (16 g/L TiO₂)

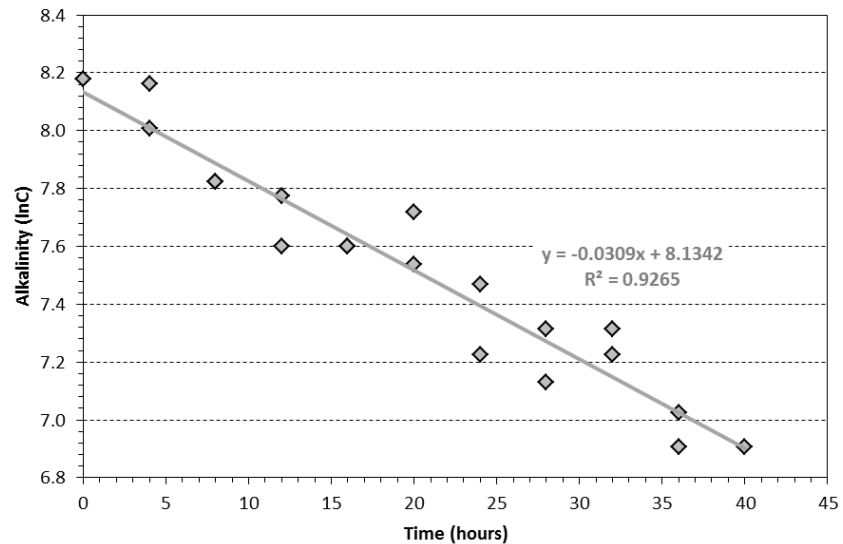


Figure 48: First order alkalinity kinetics plot for experiment 2 (16 g/L TiO₂)

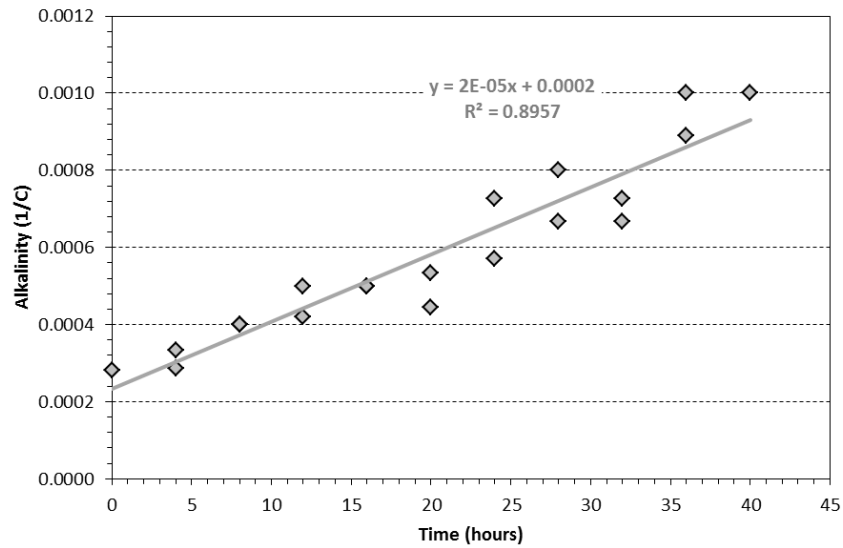


Figure 49: Second order alkalinity kinetics plot for experiment 2 (16 g/L TiO₂)

The data show the highest coefficient of determination lies with the first order reaction kinetics ($R^2 = 0.927$) followed by second order reaction ($R^2 = 0.896$). The zero order reaction has a higher linear correlation in this test than in experiment 1 ($R^2 = 0.885$ vs. $R^2 = 0.765$, respectively). However, the zero order reaction plot appears to have a slight curve, whereas the data for the second order plot appears to be randomly scattered from the mean. Using the second order kinetics formulas to solve for 71.9% removal (actual removal achieved by the experiment) of alkalinity, the time was found to be 51 hours which is 11 hours above the actual time. Following first order kinetics, 71.9% removal was estimated to be 40 hours, which coincides with the experimental value. This highly supports alkalinity degradation following first order kinetics. Using the same first order kinetics, the time for 90% removal is approximately 72 hours.

3.5.3 Ammonia Kinetics

The reaction kinetics of ammonia removal was further studied by plotting the zero order (Figure 50), first order (Figure 51) and second order (Figure 52) kinetics data.

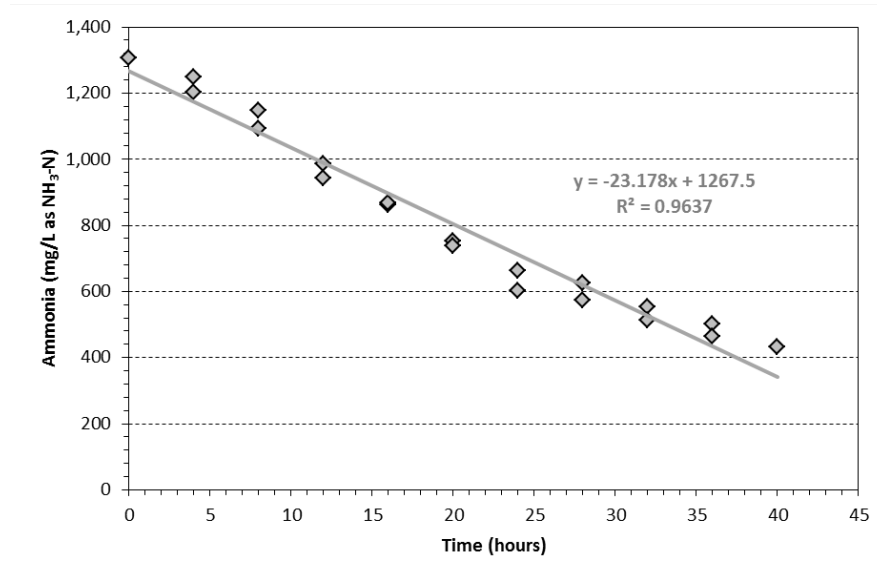


Figure 50: Zero order ammonia kinetics plot for experiment 2 (16 g/L TiO₂)

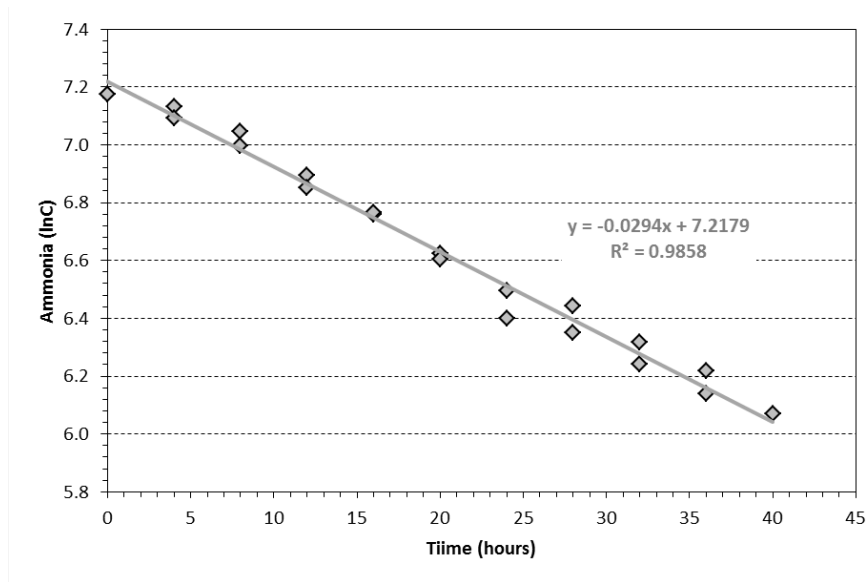


Figure 51: First order ammonia kinetics plot for experiment 2 (16 g/L TiO₂)

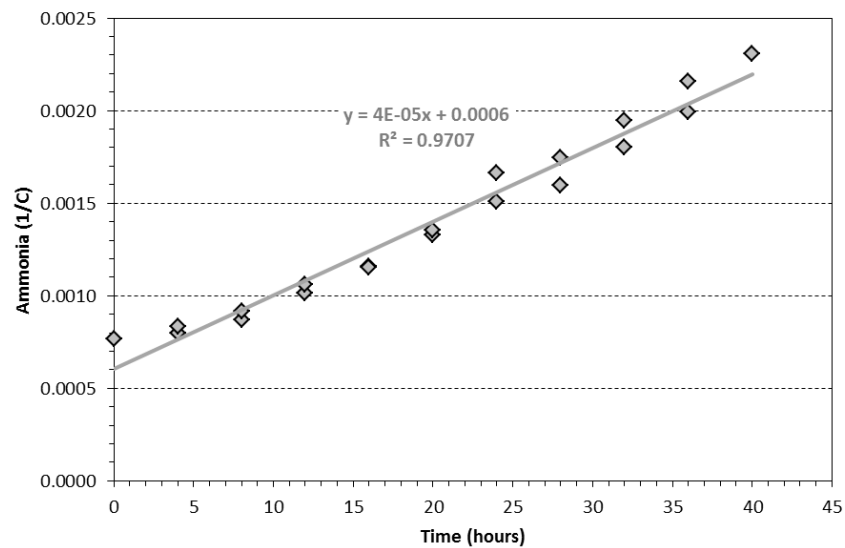


Figure 52: Second order ammonia kinetics plot for experiment 2 (16 g/L TiO₂)

Similar to the alkalinity, the ammonia degradation shows the highest linear relationship with first order kinetics ($R^2 = 0.986$) followed by second order ($R^2 = 0.971$).

The zero order plot shows the data following a slight curve, while the first order and second order show a trendline characterized by more randomized scatter about the mean. The actual removal of ammonia achieved in 40 hours was 68.9%. Modeling second order kinetics to estimate the time necessary for 68.9% removal returns a value of 48 hours, which is 8 hours higher than the actual time. For 68.9% removal using first order kinetics, only 37 hours was estimated, which is just 3 hours shy of the actual value. Ammonia appears to primarily follow first order kinetics. Using the first order kinetics, achieving the 25 mg/L goal is estimated to be 125 hours.

3.5.4 Color Kinetics

The reaction order kinetics plots for color can be seen in Figure 53 (zero order), Figure 54 (first order) and Figure 55 (second order).

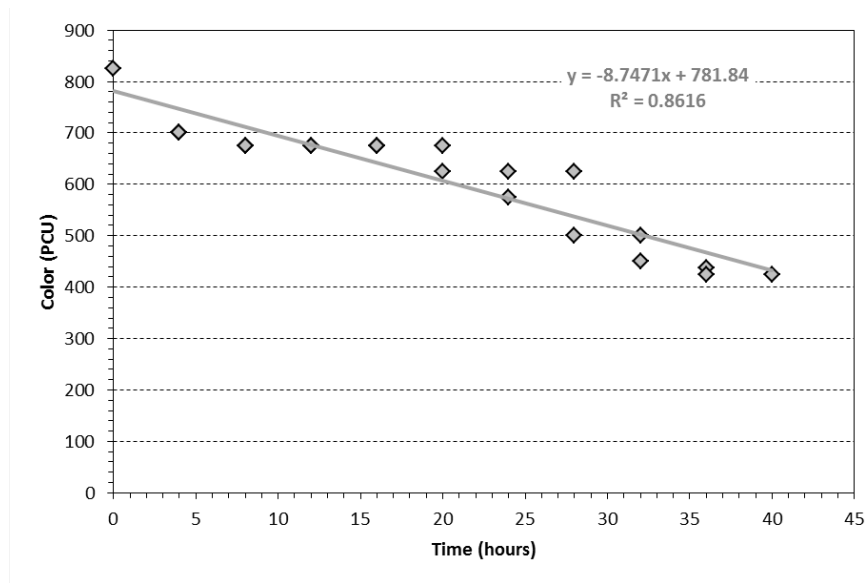


Figure 53: Zero order color kinetics plot for experiment 2 (16 g/L TiO₂)

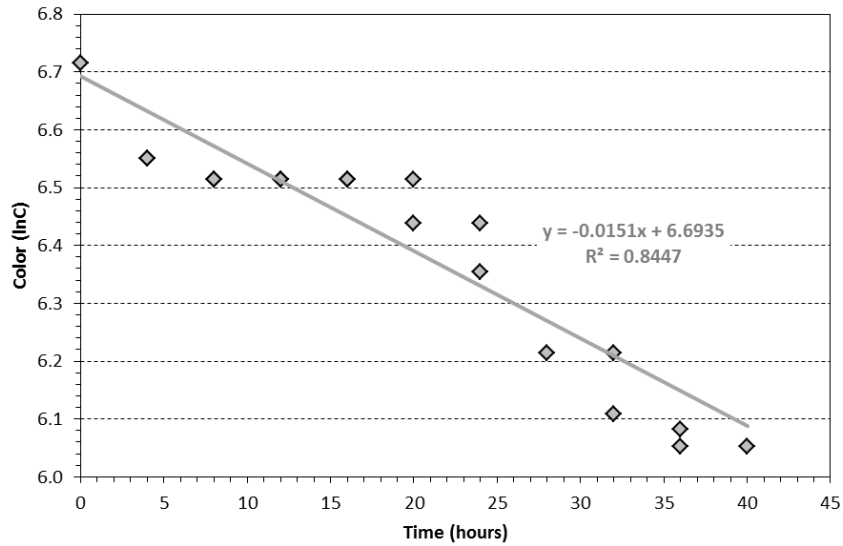


Figure 54: First order color kinetics plot for experiment 2 (16 g/L TiO₂)

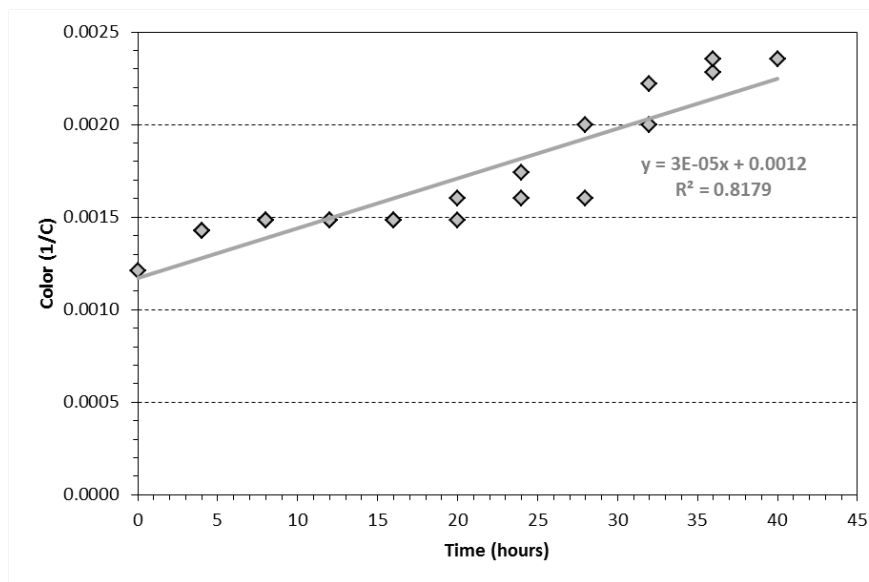


Figure 55: Second order color kinetics plot for experiment 2 (16 g/L TiO₂)

The strongest linear relationship for color falls on the zero order plot ($R^2 = 0.862$) followed by the first order plot ($R^2 = 0.845$). The second order reaction kinetics have the

smallest coefficient of determination ($R^2 = 0.818$), suggesting the color degradation is not second order. In 40 hours 48.5% of the color was removed. Using the zero, first and second order kinetics equations to solve for the time to remove 48.5% of the color it would take 46, 44, and 38 hours, respectively. None of these times correlate with the actual data, making the reaction kinetics difficult to determine. This is attributed to the limitation of the color testing method, which relies on the perception of color from the naked eye. Also, the color wheel markings were spaced too far away too allow for accurate estimates to be made at the dilution levels used (1:25). Cortes et al. suggests that color removal from a TiO_2/UV AOP follows a zero order decolorization reaction rate (2008); however, this pilot testing cannot confirm this relationship.

3.6 Experiments 3 - 6

Experiments 1 and 2 allowed for the reaction kinetics determination for ammonia, alkalinity, COD and color. These parameters were all found to follow either zero or first order kinetics and were modeled using first order for the remainder of testing. Prior to beginning experiment 3 calculations, using the kinetics equations, were made using the removal data for each parameter to predict the removal at any given time. The results showed that using the k-value from the experiments at 24 hours provided an accurate representation of the actual removal at the end of the experiments (40 – 44 hrs) using first order kinetics. The results of the COD prediction model are shown in Table 19.

Table 19: COD removal predictions for experiments 1 and 2 using 24 hour k-values from first order kinetics

TiO ₂ (g/L)	k-value (hr ⁻¹)	C ₀ (mg/L as O ₂)	t (hr)	Concentration (mg/L)		% Removal		% error
				calculated	actual	calculated	actual	
4	-0.0102	6246	44	3990	3910	36.2	37.4	1.98
16	-0.0127	5268	40	3170	3160	39.8	40.0	0.32

Table 19 shows that using the 24 hour k-values for first order reactions allows for prediction of the COD concentration with less than 2% error. This demonstrates that the removal pattern does not effectively change after 24 hours. Similar prediction tables were made for the other parameters (Appendix C). Since the results were similar, subsequent experiments were performed for a total of 24 hours, rather than 40 or more.

Experiments 3 – 6 investigated removal efficiencies at various catalyst dosages, varying from 10 – 40 g/L TiO₂. The results of each experiment determined the catalyst dosage for the next experiment. The removal efficiencies for all the parameters of interest for all six experiments can be seen in Table 20, in order of increasing TiO₂ dose.

Table 20: Summary of parameter removal at 24 hours for experiments 1 – 6

	Experiment	1	6	2	3	5	4
	TiO₂ (g/L)	4	10	16	25	30	40
	Max Temp. (°C)	36.7	37.1	35.7	36.0	36.3	36.7
pH	Min	8.35	7.66	7.63	7.54	7.70	7.59
	Max	9.26	9.09	9.18	8.96	9.20	9.06
	Mean	8.89	8.73	8.84	8.72	8.87	8.74
	C₀ (mg/L as O₂)	6,250	6,060	5,270	5,360	6,140	6,990
COD	C₂₄ (mg/L as O₂)	4,880	4,510	3,890	3,540	4,320	4,560
	Removal (%)	22	26	26	34	30	34
	k-value (hr⁻¹)	-0.0102	-0.0125	-0.0127	-0.0167	-0.0146	-0.0160
Ammonia	C₀ (mg/L as NH₃-N)	1,710	1,700	1,310	1,380	1,640	1,520
	C₂₄ (mg/L as NH₃-N)	306	470	602	700	850	850
	Removal %	82	72	52	49	48	44
	k-value (hr⁻¹)	-0.0726	-0.0580	-0.0316	-0.0271	-0.0275	-0.0227
Alkalinity	C₀ (mg/L as CaCO₃)	4,630	4380	3,560	3,560	4,130	4,310
	C₂₄ (mg/L as CaCO₃)	860	700	1,560	1,940	1,010	1,190
	Removal (%)	81	84	56	46	75	72
	k-value (hr⁻¹)	-0.0780	-0.0794	-0.0319	-0.0228	-0.0585	-0.0496
Color	C₀ (PCU)	1,130	813	825	788	756	756
	C₂₄ (PCU)	788	600	600	525	450	325
	Removal (%)	30	26	27	33	40	57
	k-value (PCU/hr)	-13.735	-5.9390	-7.0910	-16.809	-9.2500	-8.8170

As shown in Table 20, the COD removal generally increased with increasing TiO₂ dose, but for the other water quality parameters, this was not the case. The ammonia removal actually decreased with an increase in catalyst concentration. The overall pH range throughout all the experiments was 7.54 – 9.26. The mean pH values for each experiment were within 0.2 pH units of each other. Comparing the pH to the removal of each individual parameter does not show any obvious trend. Even in the high destruction of alkalinity, it was expected to see relatively greater changes in pH, but this was not the case. As the literature suggested, higher pH levels demonstrated greater destruction of ammonia compared to COD, which is reported to degrade faster in acidic conditions (Chemlal 2013).

3.6.1 COD Removal

The six experiments showed a range of COD destruction from 22% to 34%, only a 12% difference between the highest and lowest removal percentage. The highest removal for COD is observed using 25 g/L and 40 g/L of catalyst, which both achieved 34% removal. More mass of COD was removed with the 40 g/L dose (2430 mg/L vs. 1820 mg/L), but the final concentration for the 25 g/L dose was lower (3540 mg/L vs. 4560 mg/L). The removal efficiency was increasing with catalyst dosage until the 25 g/L dose. Catalyst doses in excess of 25 g/L demonstrated similar removal efficiency but a cost of using much more TiO₂. To compare the first order destruction rates for each catalyst dosage, a plot was created (Figure 56). Figure 56 shows that the highest degradation rate takes place at the TiO₂ dose of 25 g/L ($k = -0.0167 \text{ hr}^{-1}$), followed closely by 40 g/L ($k = -0.0160 \text{ hr}^{-1}$). The slowest rate of COD destruction was from the first experiment using 4 g/L TiO₂ ($k = -0.0102 \text{ hr}^{-1}$).

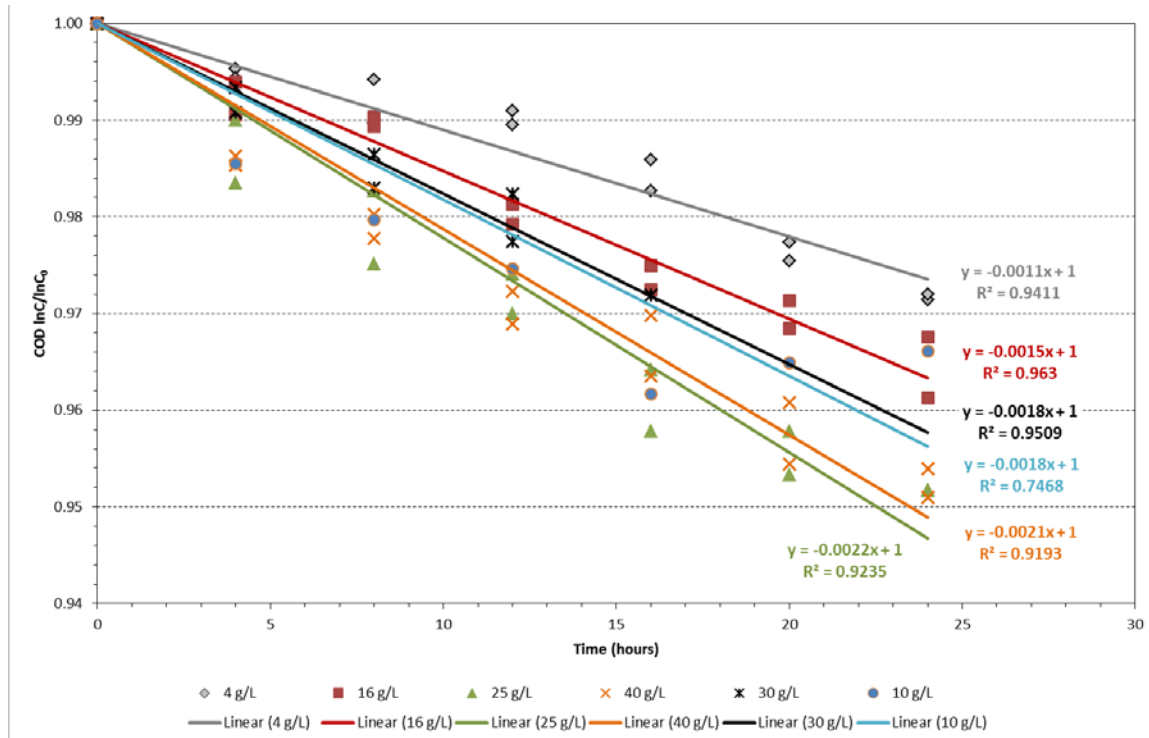


Figure 56: Comparison plot of first order COD removal after 24 hours for the catalyst dosages from six experiments

Since the removal target for COD (800 mg/L) was not achieved by any of the experiments so far, based on the 24 – 44 hour tests, predictions for the time necessary to reach 800 mg/L COD were made. Using the first order kinetic plots to get a k-value for each experiment, the times to achieve the target COD (800 mg/L as O₂) were compared in Table 21.

Table 21: Comparison of times to achieve target level COD removal using first order decay rates from six experiments

Experiment	TiO ₂ (g/L)	k-value (hr ⁻¹)	C ₀ (mg/L as O ₂)	C _t (mg/L as O ₂)	t (hr)
1	4	-0.0102	6246	800	201.5
2	16	-0.0127	5268	800	148.4
3	25	-0.0167	5360	800	113.9
4	40	-0.0160	6980	800	135.4
5	30	-0.0146	6135	800	139.5
6	10	-0.0125	6064	800	162.0

Just as the comparison plot (Figure 56) demonstrated, Table 21 displays that the catalyst dosage of 25 g/L achieved the fastest degradation rate ($k = -0.0167 \text{ hour}^{-1}$) and therefore had the lowest time ($t = 113.9$ hours) to reach the target COD. The k-values ranged from -0.0102 to -0.0167 hr^{-1} . These values were less than the k-values from the batch scale reactor with real leachate experiments performed by André McBarnette. McBarnette observed k-values ranging from -0.0266 to -0.1252 hr^{-1} , double to nearly 10 times the rates from this pilot study. The most rapid degradation ($k = -0.1252 \text{ hr}^{-1}$) took place in a six-hour experiment with an initial COD concentration of 5,218 mg/L and used 35.5 g/L TiO₂ plus lime and sulfuric acid addition. Also, the maximum temperature reached nearly 60°C. In six hours of treatment, 55% of the COD was mineralized. Using the first order kinetics for the batch scale reactor, the lowest estimated time to achieve the target COD (800 mg/L) was 15 hours or about one tenth of the fastest pilot scale time. Literature review revealed photocatalytic destruction of COD had first order k-values ranging from -0.026 hr^{-1} to -0.456 hr^{-1} (Vineetha et al. 2012, Ghaly et al. 2011, Chemlal et al. 2013). Although the study which showed the lowest k values (-0.026 hr^{-1} to -0.061 hr^{-1}) was the only one conducted with real landfill leachate, indicating lower removal

rates in the treatment of leachate versus other wastewaters and solutions. From inspection of Table 21, the pilot scale degradation rates are similar in value and do not show a clear correlation between the rate of removal and initial concentration of COD.

3.6.2 Ammonia Removal

The six experiments showed a range of ammonia destruction from 44% to 82%, with a 38% difference between the highest and lowest removal percentage (see Table 20). Experiment #1 (4 g/L TiO₂) demonstrated the greatest efficiency with 82% removal in 24 hours. The lowest removal was exhibited by the highest catalyst dose (40 g/L). The removal efficiency of ammonia consistently decreased as the catalyst dosage increased. A graphical comparison for the ammonia destruction in all six experiments is shown in Figure 57.

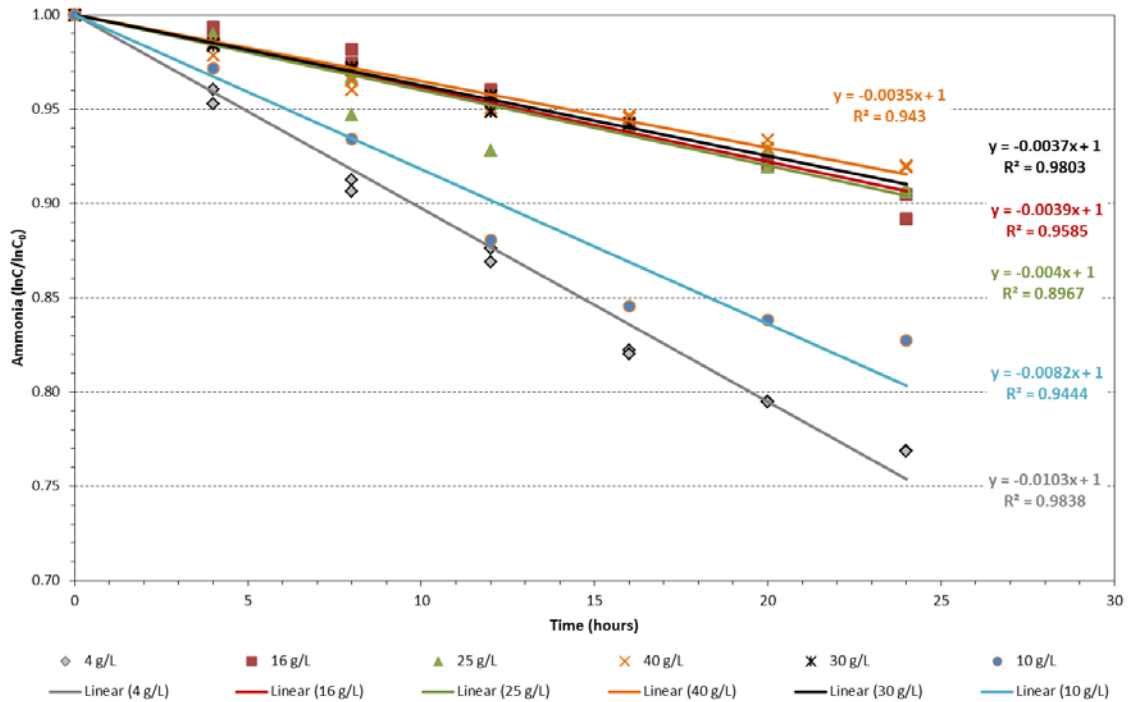


Figure 57: Comparison plot of first order ammonia removal after 24 hours for the catalyst dosages from six experiments

Inspection of Figure 57 shows that the highest ammonia removal rate takes place at the lowest TiO₂ dose of 4 g/L ($k = -0.0726 \text{ hr}^{-1}$), followed by 10 g/L ($k = -0.0580 \text{ hr}^{-1}$). These two doses exhibited removal rates much higher than the other four experiments. All catalyst doses above 10 g/L showed comparable degradation rates. The slowest rate of ammonia destruction ($k = -0.0227 \text{ hr}^{-1}$) came from the highest amount of catalyst application (40 g/L TiO₂).

The Broward County Sewer Use Limitations state that ammonia levels need to be less than or equal to 25 mg/L as NH₃-N to avoid exceedance fees. Since none of the experiments were able to achieve this goal, the time necessary to do so had to be

estimated from kinetics data. Using the first order kinetics plots to get a k-value for each experiment, the times to achieve the target ammonia (25 mg/L as NH₃-N) were compared in order of increasing catalyst (Table 22).

Table 22: Comparison of times to achieve target level ammonia removal using first order decay rates from six experiments

Experiment	TiO ₂ (g/L)	pH range (pH units)	k-value (hr ⁻¹)	C ₀ (mg/L as NH ₃ -N)	C _t (mg/L as NH ₃ -N)	t (hr)
1	4	8.35 – 9.26	-0.0726	1713	25	58.2
6	10	7.66 – 9.09	-0.0580	1700	25	72.7
2	16	7.63 – 9.18	-0.0316	1310	25	125.3
3	25	7.54 – 8.96	-0.0271	1380	25	148.0
5	30	7.70 – 9.20	-0.0275	1635	25	152.0
4	40	7.59 – 9.06	-0.0227	1523	25	181.0

Just as Figure 57 displayed, Table 22 demonstrates that the catalyst dosage of 4 g/L achieved the fastest degradation rate ($k = -0.0726 \text{ hr}^{-1}$) and therefore had the lowest time ($t = 58.2$ hours) to reach the target ammonia concentration. Also, it can be seen that an increase in catalyst dosage results in a decrease of ammonia removal efficiency. The slowest rate of ammonia reduction was executed by the highest dose of TiO₂, resulting in an estimation of 181 hours for target removal. The degradation rates appear to have no observable correlation to the initial concentration. However, since the degradation of ammonia decreased with increasing levels of catalyst it can be noted that the optimum catalyst dose for ammonia removal may be ≤ 4 g/L.

Ammonia removal is highly dependent on the pH (Yuzawa et al. 2012). The dissociation of the ammonium ion (NH₄⁺) to free ammonia (NH₃) occurs at a high pH (pKa = 9.24). The most rapid photodecomposition of ammonia occurs when it exists in

the form of NH_3 (Nemoto et al. 2007). The first experiment exhibited a maximum pH of 9.26 and also showed the fastest degradation rate of ammonia. So to further investigate the relationship between ammonia and pH a table was made comparing the pH range for each time interval up to 24 hours for the three lowest catalyst doses (Table 23).

Table 23: Comparison of pH range and ammonia removal for every 4 hour time interval up to 24 hours

t	$\text{TiO}_2 = 4 \text{ g/L}$		$\text{TiO}_2 = 10 \text{ g/L}$		$\text{TiO}_2 = 16 \text{ g/L}$	
	pH	$\text{NH}_3\text{-N}$ % removal	pH	$\text{NH}_3\text{-N}$ % removal	pH	$\text{NH}_3\text{-N}$ % removal
0 – 4	8.35 – 9.20	29.63	7.66 – 9.07	19.00	7.63 – 8.85	29.64
4 – 8	9.04 – 8.98	20.55	9.07 – 9.04	19.66	8.97 – 8.88	7.79
8 – 12	9.26 – 9.10	10.03	9.04 – 9.09	20.25	9.01 – 8.99	12.44
12 – 16	9.22 – 9.03	13.21	9.09 – 9.01	9.41	9.16 – 9.02	9.39
16 – 20	9.18 – 8.91	4.82	9.01 – 8.61	1.62	9.12 – 9.01	8.32
20 – 24	9.09 – 8.91	3.87	8.61 – 8.62	2.39	9.18 – 9.01	6.95
Total	–	82.13	–	72.33	–	74.53

It was expected that the time intervals with the highest pH ranges would provide the most removal, but that was not the case. For example, the highest amount of removal was expected to be the 8-12 hour time interval for the 4 g/L experiment since the pH ranged from 9.10 to 9.26, but the table shows it only achieved about 1/3 of the maximum removal for any of the 4-hour time periods. Table 23 shows that the majority of the degradation actually occurs in the first 12 hours of treatment, regardless of pH. This is another indicator of first order reaction kinetics since the removal decreases at lower total concentration. Although it is known that ammonia removal is greater at higher pH, the data collected in this study did not support an observable trend.

3.6.3 Alkalinity Removal

The alkalinity in all six experiments existed primarily as bicarbonate species since the pH extremes ranged from 7.4 – 9.3, which are levels where bicarbonate is the dominant species of the carbonate system. The destruction of alkalinity for the six experiments ranged from 46% to 84%, with a 36% difference between the highest and lowest removal percentage (see Table 20). Experiment #6 (10 g/L TiO₂) demonstrated the greatest efficiency by removing 84% of the alkalinity in 24 hours. The lowest removal was exhibited in the third experiment (25 g/L TiO₂) with 46% removal. The removal efficiency of alkalinity did not seem to correlate with the catalyst dosage as there were high amounts of alkalinity reduction with higher and lower dosages of TiO₂. A graphical comparison for the alkalinity destruction in all six experiments is shown in Figure 58.

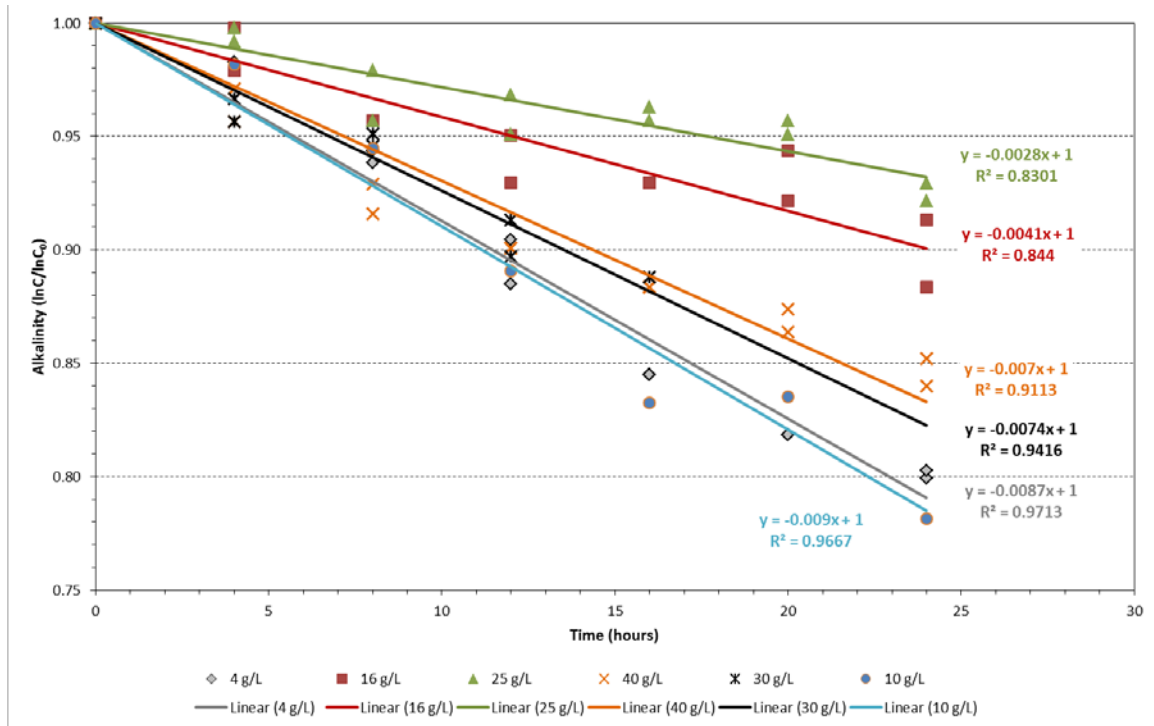


Figure 58: Comparison plot of first order alkalinity removal after 24 hours for the catalyst dosages from six experiments

Figure 58 shows that the fastest alkalinity removal rate occurs at a catalyst dosage of 10 g/L ($k = -0.0794 \text{ hr}^{-1}$), closely followed by 4 g/L ($k = -0.0780 \text{ hr}^{-1}$). The slowest reduction rate of alkalinity came from the experimental catalyst dose of 25 g/L ($k = -0.0228 \text{ hr}^{-1}$). There does not appear to be any clear relationship between the catalyst dosage and removal rate of alkalinity.

Experiment 1 nearly achieved a 90% reduction in alkalinity in 44 hours of treatment. None of the other experiments approached 90% removal although it is likely that experiment 6 would have exceeded 90% if run for 44 hours. To estimate the time required for this experiment, as well as the other five experiments, to achieve 90%

alkalinity reduction a table was made using first order degradation constants (see Table 24).

Table 24: Comparison of times to achieve 90% alkalinity removal using first order decay rates from six experiments

Experiment	TiO ₂ (g/L)	k-value (hr ⁻¹)	C ₀ (mg/L as CaCO ₃)	C _t (mg/L as CaCO ₃)	t (hr)
1	4	-0.0780	4625	462.5	29.5
2	16	-0.0319	3560	356	72.2
3	25	-0.0228	3562.5	356.25	101.0
4	40	-0.0496	4312.5	431.25	46.4
5	30	-0.0585	4125	412.5	39.4
6	10	-0.0794	4375	437.5	29.0

Table 24 demonstrates that the catalyst dosage of 10 g/L achieved the fastest degradation rate ($k = -0.0794 \text{ hr}^{-1}$) and therefore had the lowest time ($t = 29$ hours) to reach 1-log removal of alkalinity. The slowest rate of alkalinity reduction ($k = -0.0228 \text{ hr}^{-1}$) was exhibited by the experimental dosage of 25 g/L TiO₂, resulting in an estimation of 101 hours for target removal. The removal of alkalinity to the goal of 90% has the lowest removal times of all the measured parameters, which may show a preferential reaction with bicarbonate species, which act as hydroxyl radical scavengers (Holmes 2003), even though alkalinity was needed to initiate the reaction in laboratory tests of artificial leachates containing KHP and water (Meeroff and McBarnette 2011). The two samples that had initial alkalinity concentrations under 4,000 mg/L as CaCO₃ had lower degradation rates and lower overall percentage removal compared to the samples with higher initial alkalinity. This suggests that the degradation of alkalinity has some dependence on the initial concentration, which is an indicator of first-order reaction kinetics.

3.6.4 Color Removal

The six main experiments in the study returned decolorization efficiencies ranging from 26 - 57%, as seen in Table 20. The highest removal of color in 24 hours was achieved with the largest amount of catalyst (40 g/L). However, this may be pseudo removal attributed to a whitening (or lightening) effect the catalyst has on the leachate. Figure 59 shows the comparison of color between raw leachate and the leachate mixed with TiO₂.



Figure 59: Color comparison for raw leachate (left) vs. leachate w/ TiO₂ (right)

The raw leachate has the appearance of black coffee, but once it is mixed with the catalyst, it looks much lighter in color. As shown in Table 25, every experiment showed that just the addition of catalyst to the leachate, prior to any treatment, resulted in a lower color reading than the raw leachate even though the samples were centrifuged at 6000 rpm for 5 minutes.

Table 25: Color concentration change after adding TiO₂ to raw leachate insert a column with percent change

Sample	TiO ₂ (g/L)	Concentration (PCU)	
		Raw Leachate	Leachate w/ TiO ₂
1	4	1175	1125
2	10	950	700
3	16	950	625
4	25	875	625
5	40	925	575
6	30	550	475

The color change from simply adding catalyst ranged from 50 to 350 PCU. Higher doses of catalyst generally resulted in greater initial color change. This is possibly due to immediate adsorption of particles which contribute to the color of leachate when adding the TiO₂. Also, with more catalyst suspended in the leachate, more time may be required in the centrifuge to fully separate it.

If the catalyst does indeed provide a false color removal effect then the variance in the color readings can also be related to the lack of homogeneity between the catalyst and the leachate. Since the TiO₂ nanoparticles are heavy and begin to settle in the leachate rather quickly the ratio of catalyst to leachate can be different in every sample, resulting in a variety of measurement values. The relative degradation rates of color are summarized in Figure 60 and Table 26.

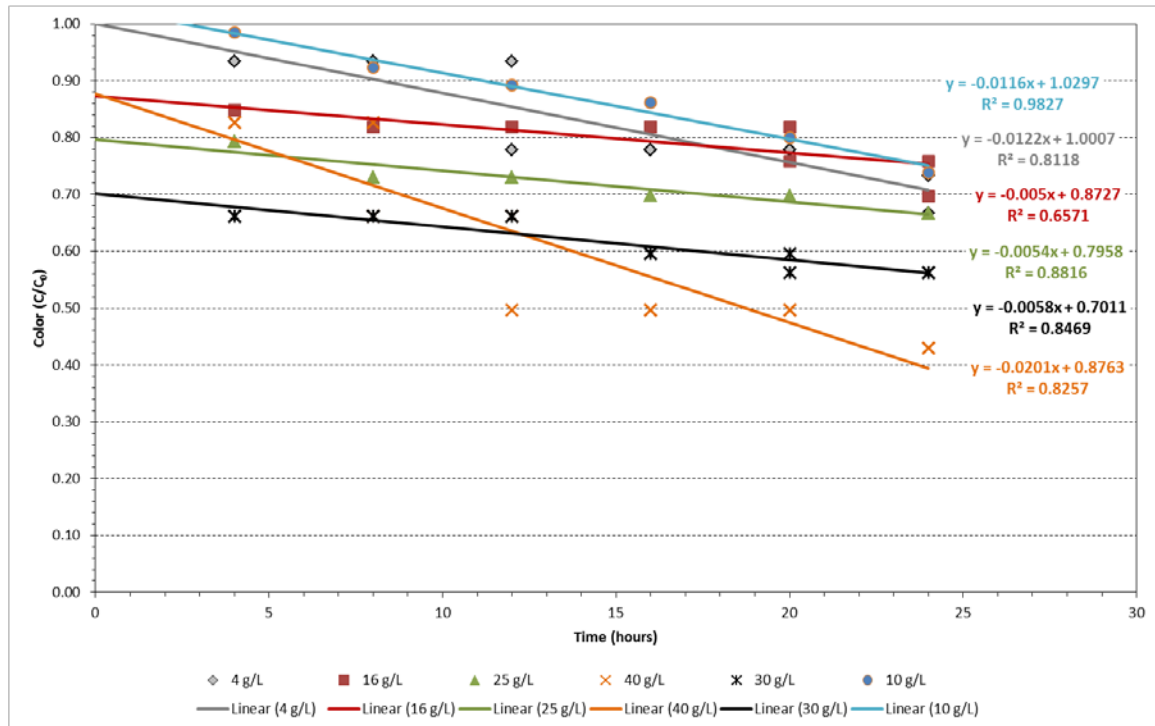


Figure 60: Comparison plot of zero order color removal after 24 hours for the catalyst dosages from six experiments

The data for the color removal does not allow for a good estimate by forcing the comparative trendlines through the point (0, 1.0). Instead, the C/C_0 values were plotted without alteration. To assist in the interpretation of the data the slopes and R^2 values for each experiment were tabulated in Table 26.

Table 26: Slopes and R^2 values for color comparison graph

Exp.	TiO ₂ (g/L)	Slope	R ² value
1	4	-0.0122	0.8118
6	10	-0.0116	0.9827
2	16	-0.0050	0.6571
3	25	-0.0054	0.8816
5	30	-0.0058	0.8469
4	40	-0.0201	0.8257

Figure 60 and Table 26 shows that the highest color removal rate correlates with the highest catalyst dose, showing a slope of -0.0201. The degradation slopes for 4 g/L and 10 g/L are almost identical at -0.0122 and -0.0116, respectively. It is interesting to note that the smallest two catalyst doses showed the second and third largest degradation rates. The “middle” doses (10, 16 and 25 g/L) also had similar slopes in relation to each other, which ranged from -0.0050 to -0.0058. From the data, it is determined that further investigation is needed to better understand the color removal mechanism.

None of the experiments were able to achieve 90% removal of color within the allotted time. As a result, the time necessary to do so had to be predicted from kinetics data. Using the zero order kinetic plots to get a k-value for each experiment, the times to achieve the 90% decolorization were compared in Table 27.

Table 27: Comparison of times to achieve 90% color removal using zero order decay rates from six experiments

Experiment	TiO ₂ (g/L)	k-value (PCU/hr)	C ₀ (PCU)	C _t (PCU)	t (hr)
1	4	-13.735	1125	112.5	73.7
2	16	-3.758	700	70.0	167.6
3	25	-4.257	625	62.5	132.1
4	40	-14.525	625	62.5	38.7
5	30	-5.160	575	57.5	100.3
6	10	-8.817	475	47.5	82.9

Table 27 demonstrates that the catalyst dosage of 40 g/L achieved the fastest degradation rate (k = -14.525 PCU/hr) and therefore had the lowest time (t = 38.7 hours) to reach the 10% of the initial color concentration. The slowest rate of color removal was exhibited by the experimental dosage of 16 g/L TiO₂, resulting in an estimated 168 hours

for target removal. The degradation rates appear to have no significant correlation to the initial concentration.

3.7 Catalyst Optimization

In the investigation of the catalyst dose for the destruction of COD at 24 hours based on first order kinetics for all six experiments, a catalyst optimization plot was created (Figure 61).

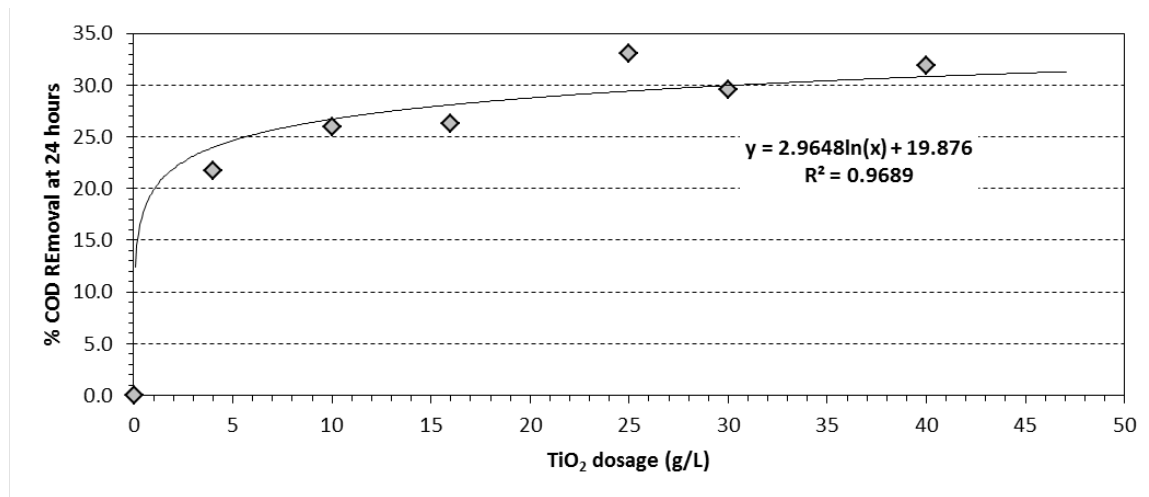


Figure 61: Catalyst optimization curve for COD removal at 24 hours for six experiments

The data from experiments 1 (4 g/L) and 2 (16 g/L) supported the theory that more catalyst generated a higher COD destruction rate. So, for the third experiment the catalyst dose was increased to 25 g/L, which again showed higher COD removal (34%) than the lower doses. Again, the catalyst dose was increased to 40 g/L for the fourth experiment. The degradation that took place in the fourth experiment was not the increase which was expected; only 34% of the COD was mineralized. The removal was increasing

to the point of 25 g/L and 40 g/L exhibited the same removal efficiency. This led to the expectation of a peak in between 25 and 40 g/L TiO₂ and the use of 30 g/L in experiment 5. The results of the 5th experiment were unexpected. The COD destruction from a catalyst dose of 30 g/L only reached 30% mineralization. This is when the development of an asymptotic curve occurred. The data seemed to follow the asymptotic curve pretty closely $R^2 = 0.9697$ (prior to the sixth experiment). Proceeding from there, 10 g/L TiO₂ was tested to be sure it fell on the curve as well. The results of the sixth experiment were as expected and the data point landed on the existing curve, which barely changed once the sixth experiment data was included in the graph as seen in Figure 61.

The optimum catalyst dosage range was deduced from this curve to be between 4 – 10 g/L. At TiO₂ levels higher than 10 g/L there is a large increase in catalyst amount without a correspondingly large increase in removal efficiency. Both alkalinity and ammonia exhibited their two highest levels of degradation from 4 and 10 g/L TiO₂ as well. This amount of catalyst corresponds to a ratio of 0.6-1.5 TiO₂:COD

3.8 Catalyst Recovery

A secondary experiment was run in an attempt to recover the catalyst utilizing nylon monofilament filter bags. The three bag sizes to be tested were 5-micron, 10-micron and 20-micron. Prior to attempting to recover the catalyst using this method, a preliminary test was performed to see how water flows through the bag and if noticeable filtration of the catalyst takes place. The 10-micron bag was used to filter 100 mL of tap water containing 0.73 g of TiO₂. When the water was poured into the filter bag, it collected in the bottom of bag and dripped out slowly. The filtered water appeared just as

cloudy as it did before filtering. The average primary size of Aeroxide P25 TiO₂ nanoparticles is reported to be 21 nm on Aerosil's specifications sheet (Appendix D, Figure 70). This fact prompted the use of the 5 micron filter bag for the recovery trial with actual leachate. The results of attempting to collect the TiO₂ from the treated leachate are summarized in Table 28.

Table 28: Summary of results from catalyst recovery experiment

	Weight (g)
TiO ₂ added to leachate	40.084
Filter bag (empty)	38.036
Filter bag (full)	91.929
Estimated TiO ₂ captured	56.634
Recovery (%)	141.3

The recovery experiment using the nylon monofilament filter bag did not provide usable data results. The leachate did not flow through the bag at a rate that would allow the machine to keep running. The filter bag filled up with leachate and slowly dripped into the reservoir (Figure 62).



Figure 62: 5 micron nylon monofilament filter bag filled with treated leachate

As the head pressure in the bag diminished and the leachate levels went down, so did the flow. After just over an hour of allowing the bag to hang and drip, manual pressure had to be applied to remove the leachate from the filtration bag. During the application of pressure, it was noted that the outside of the filter bag was covered in TiO_2 . Visual inspection revealed that the catalyst particles had the ability to pass through the bag with ease. However, the filtered leachate in the reservoir still had a chocolate milk appearance compared to the coffee appearance of raw leachate. Also, some colored particles, possibly in the form of organics adsorbed onto the catalyst surface were on the inside and outside surfaces of the bag. These particles could also be leachate TSS. Every surface the filter bag touched had remnants of catalyst on it. It appears the catalyst may have a charge affinity for the bag or settled out due to the slowing of the flow conditions

caused by the bag itself. The filter bag was put in a drying oven at 100° C for approximately 75 minutes and then into a desiccator for one hour. The weight of the recovered catalyst was found to be 56.634 grams, which was greater than the amount of catalyst added to the leachate (40.084 g). This showed greater than 100% recovery, which obviously shows that the bag retained more than just TiO₂. The extra material is likely native leachate TSS, which must be measured and subtracted out. By visual inspection, it was observed that the filter bag did not in fact retain 100% of the catalyst. The testing method had no way of accounting for additional particles that may have been caught in filtration. The catalyst has a heavy molecular weight which allows the particles to settle quickly in water or leachate. Recovery of the catalyst should incorporate a sedimentation system to collect the catalyst rather than filtration. The amount of energy required to filter out particles averaging 21 nm would not be cost efficient. Suryaman and Hasegawa (2010) recovered the TiO₂ by adding a separate sedimentation tank to the treatment cycle. The overflow of the tank was the treated effluent while the settled particles were pumped back into the mixing tank for reuse. Cho et al. (2004) used a centrifuge to recover the catalyst from their samples for reuse. After which, the catalyst was washed with deionized water and dried. Washing the catalyst may have been a good technique to purge any other compounds adsorbed to the catalyst surface. In this experiment, removing the catalyst from the filter bag and washing the TiO₂ may have eliminated the excess weight and given a true weight of catalyst recovery. Although, collecting the catalyst from the surface of the filter bag for washing seems challenging.

To develop a sedimentation system to recover the catalyst it was necessary to determine the surface area required. The settling behavior of the catalyst was determined

using a sedimentation test. Assuming discrete settling (Type 1) using Stoke's Law, an initial settling velocity (v_s) was calculated as follows:

$$v_s = \frac{gd^2(\rho_s - \rho)}{18\mu} = \frac{9.81 \times 0.000000021^2(3800 - 995.7)}{18 \times 0.000798} = 8.4 \times 10^{-10} \text{ m/s}$$

where g = acceleration due to gravity (m/s^2), d = particle diameter (m), ρ_s = density of catalyst (kg/m^3), ρ = density of water (kg/m^3), and μ = absolute viscosity ($\text{kg/s}\cdot\text{m}$)

Since Stoke's Law is highly dependent on the average catalyst particle size (21 nm) the settling velocity was found to be extremely low. To be sure Stoke's Law could be used as opposed to Newton's Law the Reynold's number (N_R) was calculated as follows:

$$N_R = \frac{v_s \rho d}{\mu} = \frac{8.446 \times 10^{-10} \times 995.7 \times 0.000000021}{0.000798} = 2.21 \times 10^{-11} < 1$$

Reynold's number was found to be less than 1, indicating laminar flow which is a requirement for Stoke's Law. Using the settling velocity obtained from Stoke's Law, the area of the tank necessary to settle out the catalyst was calculated using the 300 L/hr flow of the reactor and found to be approximately 350,000,000 m^2 . This result shows that the catalyst clearly does not follow simple discrete settling. A small experiment was run to test hindered settling (Type 3) using the Talmadge and Fitch method. Fifty milliliters of leachate with 5 g/L TiO_2 was added to a graduated cylinder and the height of the clearwater interface was recorded at ten-minute intervals. The results were plotted in Figure 63.

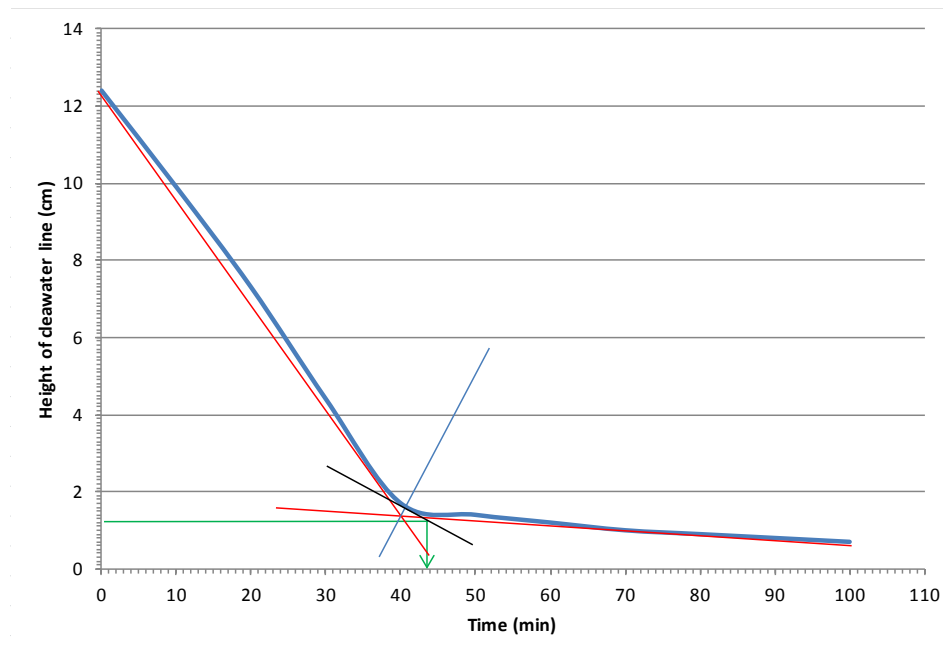


Figure 63: Interface height vs. Time plot for Talmadge and Fitch method

The resulting time (t_u) to the desired underflow concentration ($C_u = 10C_0$) was found to be 43.3 minutes as seen in Figure 63. The calculated area required for thickening based on the 300 L/hr flow of the reactor was found to be 1.74 m². This result proved to be more reasonable than Stoke's Law and indicates that the catalyst may more closely follow Type 3 hindered settling behavior, although it is difficult to confirm this due to factors that affect the settling of the catalyst particles. For example, alkalinity is reported to promote aggregation of the catalyst particles, thereby increasing the effective particle diameter. Also, the adsorption of particles onto the catalyst surface increases the weight and the diameter, which in turn increases the settling velocity. Further investigation is necessary to develop more accurate predictions of the catalyst's settling dynamics. It would also help to determine the particle size distribution of the photocatalyst.

4.0 CONCLUSIONS AND RECOMMENDATIONS

4.1 Summary of Findings

Landfill leachate is highly polluted water that, if released into the environment, can have deleterious effects on groundwater and soil and therefore must be managed properly. Multiple methods of leachate management have been reviewed, revealing a number of issues. One important concern is the biological, chemical and physical contaminants in the leachate, such as ammonia, COD, BOD, heavy metals, TSS and TDS. Also, the variability of the volume and constituent concentrations cannot be governed, since they are dependent on precipitation, landfill area, landfill age and design, waste composition, etc. Alternative methods of dealing with landfill leachate in the future must be able to destroy different types of constituents, many of which are present in very high concentrations, simultaneously and inexpensively, to be able to safely discharge this water back to the environment.

Advanced oxidation processes, especially those which harness the oxidation potential of the hydroxyl radical, have shown promising results in research performed at laboratory and pilot scales. TiO₂ photocatalytic oxidation is among these emerging techniques. The process involves the generation of hydroxyl radicals and superoxide anions which have the capacity to decontaminate wastewaters by removing ammonia, organics, common inorganics, color and heavy metals simultaneously, as explained in detail in Chapter 1.

The purpose of this study was to follow up batch scale testing performed by McBarnette (2011) with the testing of a pilot scale falling film reactor utilizing TiO₂ photocatalysis to treat landfill leachate. The main objective was to determine an optimum dosage of catalyst without the use of any chemical addition or pretreatment with the goal of meeting the Broward County sewer use limitations for COD (<800 mg/L s O₂) and ammonia (<25 mg/L as NH₃-N).

The previous batch scale studies achieved 100% mineralization of COD, 79% removal of copper and 50% degradation of ammonia in simulated leachate using 4 g/L TiO₂ (3.88 TiO₂/COD). This catalyst dose became the starting point for pilot studies. TiO₂ dosages were tested from 4 – 40 g/L (0.64 – 5.73 TiO₂/COD). No pH control was implemented and thus ranged from 7.5 – 9.3 throughout the duration of all experiments. The mean pH for all experiments ranged from 8.72 – 8.89. The consistency of the average pH demonstrated that the pH had minimal effect on the varying removal efficiencies for all parameters. Overall, treatment in the ambient pH conditions resulted in higher degradation of ammonia compared to COD for all experiments, as expected. Maximum COD mineralization (34%) was carried out at catalyst doses of 25 and 40 g/L after 24 hours of treatment. Ammonia reached maximum removal (82%) with 4 g/L TiO₂ after 24 hours of treatment. The greatest alkalinity destruction in 24 hours was 84% occurring with a catalyst dosage of 10 g/L. Maximum color removal in 24 hours was 57% with a catalyst dose of 40 g/L. To find the optimum amount of catalyst, balancing the removal percentages of COD versus ammonia and alkalinity was necessary. It was found that catalyst dosages above 10 g/L reduced ammonia removal 32 – 38% and alkalinity removal by 9 – 12% below their respective maximum degradations. For COD, catalyst

doses less than 25 g/L exhibited only 8 – 12% less removal than the maximum. Since large increases in catalyst provided minimal increases in COD mineralization and great decreases in ammonia and alkalinity degradation, optimization of the catalyst resulted in a preferred dose range of 4 – 10 g/L TiO₂. In this optimum range at 24 hours, 22 – 26% of COD, 72 – 82% of ammonia, 81 – 84% of alkalinity, and 26 – 30% of color was removed from the leachate. The parameters that incurred the most exceedance fees for the Monarch Hill landfill were COD and ammonia, which in the optimum range degrade to the target levels in 160 – 200 hours and 55 – 75 hours of treatment, respectively.

The study of reaction kinetics is very complicated with advanced oxidation processes. A chain of reactions is set in motion by the UV radiation and the TiO₂ photocatalyst. The kinetic studies within this manuscript did not monitor the individual processes occurring, but the overall reaction order, which is defined by the slowest reaction in the matrix (the rate limiting step). The results determined that the photocatalytic degradation of COD followed first order closer than zero or second order. Using the optimum range of catalyst (4 – 10 g/L) the decay rates of COD ranged from -0.0102 to -0.0127 hr⁻¹. Based on the data and literature, ammonia and alkalinity were recommended to also be modeled as overall first order reactions at ambient pH levels. The optimum range of catalyst gave decay rates for ammonia ranging from -0.0580 to -0.0726 hr⁻¹ and alkalinity ranging from -0.0780 to -0.0794. From the data analysis and literature review, it was suggested to model color removal as an overall zero order reaction. Under the optimum range of TiO₂ (4 – 10 g/L) color was degraded at -13.735 to -8.817 PCU/hr. At these rates and these conditions, the goal of meeting the Broward County sewer use limitations is not met.

The attempts to recover the used catalyst after 8 hours of treatment using nylon monofilament filter bags were unsuccessful. The average primary size of Aeroxide P25 TiO₂ nanoparticles is reported to be 21 nm. It was expected that this size would increase due to adsorption of organics and other compounds. The 5-micron bag did not catch many catalyst particles as the filtered leachate clearly still contained a large amount of TiO₂. Some catalyst particles, among other constituents, did adsorb to the inner and outer surfaces of the filter bag. The addition of the other non-TiO₂ particles on the bag surface resulted in a larger estimate (141.3 % recovery) of the catalyst recovered when weighed on a scale. The test method did not have a way to account for additional particles caught in the filtration. Also, the amount of energy required to filter out catalyst particles averaging 21 nm would not be cost efficient and thus, the bag filter system was determined to not be an efficient method catalyst recovery.

4.2 Preliminary Cost Analysis

The Monarch Hill Landfill currently pays disposal fees based on annual volumetric flow rates and constituent concentrations above a certain threshold. It was reported that the average leachate production is 42 – 96 million gallons per year (Meeroff and McBarnette 2011), with the first 12 million gallons per year being free of charge. The high constituent concentrations (i.e. COD > 800 mg/L and NH₃-N > 25 mg/L) of the leachate also add on exceedance fees averaging \$350,000 per year. A goal of the photocatalytic study is to develop a leachate treatment process that can achieve operating costs lower than exceedance fees. Therefore, an attempt will now be made to speculate the cost of the leachate treatment unit at full scale.

Assuming that the sewer disposal costs will remain the same between the current option and the proposed photocatalytic oxidation treatment option, the current disposal option cost is calculated by the exceedance fees and the leachate generation as follows:

$$\frac{\$350,000}{96,000,000 \text{ gal}} = \frac{\$3.65 \times 10^{-3}}{\text{gal}} = \frac{\$3.65}{1000 \text{ gal}}$$

and,

$$\frac{\$350,000}{42,000,000 \text{ gal}} = \frac{\$8.33 \times 10^{-3}}{\text{gal}} = \frac{\$8.33}{1000 \text{ gal}}$$

So, the current cost ranges from \$3.65 – \$8.33 per 1000 gallons plus the cost of sewer disposal. This value will be compared to an estimated cost of the reactor operated at full scale.

By conversion, the leachate generation rates are 115,000 to 262,000 gallons of leachate per day, on average. At the optimum dosage, a treatment cycle of 200 hours is needed, which means the reactor volume would need to be on the order of 960,000 – 2,200,000 gallons. Currently a 10 kg bag of TiO₂ costs \$600. The lower dose of catalyst is 4 g/L of TiO₂. Therefore the amount of TiO₂ needed would be on the order 14,500 – 33,200 kg. Without factoring in the economies of scale, the total cost of photocatalyst is \$870,000 – \$1,990,000. Since the catalyst is reusable, this can be taken as a one-time expenditure.

Further estimates are needed regarding the reservoir size, UV lamps and pumps in order to establish a capital cost. To account for a 200 hour treatment cycle, the daily tank

volume should be on the order of 1.0 – 2.5 MG to account for the worst case scenario. Currently the UV lamp in the pilot reactor produces 120 watts. The wattage of the lamp for a full scale operation was determined based on the assumption that the system will treat the amount of leachate produced per day. After adding in all of the pumps, blowers, and appurtenances, the capital cost is amortized at 6% interest per year for 20 years. The preliminary cost analysis is summarized in Table 29.

Table 29: Preliminary cost analysis based on pilot reactor optimal catalyst dose

Costs	42 MG/year	96 MG/year
TiO ₂ chemical costs (one time only)	\$871,068	\$1,991,014
2 x 1.0 MG tanks	\$1,736,020	
2 x 2.5 MG tanks		\$3,088,180
UV lamps/ballast/power supply	\$250,000	\$500,000
Pumps/blowers/plumbing/etc.	\$89,000	\$136,000
Total capital cost	\$2,946,088	\$5,715,194
Annualized (6%, 20 years)	\$256,899	\$498,365
O&M costs (est. 10% of capital)	\$294,609	\$571,519
Total annual costs	\$551,508	\$1,069,884
Cost per 1000 gallons	\$13.13	\$11.14

A similar cost analysis was made for the batch scale treatment process using optimum batch scale conditions of 13.3 g/L TiO₂ and a 20 hour treatment process (Table 30).

Table 30: Preliminary cost estimate based on batch reactor conditions

Costs	42 MG/year	96 MG/year
TiO ₂ chemical costs (one time only)	\$289,630	\$662,013
2 x 0.2 MG tanks	\$90,000	
2 x 0.3 MG tanks		\$140,000
UV lamps/ballast/power supply	\$40,000	\$70,000
Pumps/blowers/plumbing/etc.	\$21,000	\$36,000
Total capital cost	\$440,630	\$908,013
Annualized (6%, 20 years)	\$38,423	\$79,179
O&M costs (est. 10% of capital)	\$44,063	\$90,801
Total annual costs	\$82,486	\$169,980
Cost per 1000 gallons	\$1.96	\$1.77

The resulting cost analysis shows that the batch scale process provided a cost efficient option while the scale up of the current pilot process currently does not. While the falling film reactor showed promising results, the pilot scale treatment still needs to be further developed in order to be practical in the real world. The main goal in the effort to keep the cost down is to reduce the treatment time, which is the main difference between the two cost estimates. This is because reducing the treatment will reduce the size of the tanks needed, the amount of UV lamps necessary, the quantity of pumps, blowers and plumbing needs, and even the operations costs. This study provides a baseline for the further development in the pilot scale research. The optimal catalyst dosage has been narrowed down, so that further testing and process modifications can be implemented to reduce the treatment costs and increase overall efficiency.

4.3 Recommendations

The following recommendations can be made from this completed study:

- The pilot reactor lamp emits most of its power between 250 – 260 nm. Obtain a UV sensor which measures wavelengths between 250 – 260 nm (UV-C) to develop a better understanding of the radiation intensity applied to the leachate. Also, this will allow tests to be performed on the germicidal irradiation range and the effects it has on parameter removal.
- There was a significant difference in the UV intensity between the batch scale and pilot scale reactors (130 mW/cm² vs. 1.8 mW/cm², respectively). An investigation should be conducted on methods to increase the lamp power in the pilot scale reactor. Subsequently, experiments should be conducted to investigate UV intensity effects by varying the lamp power. The results of these experiments must be used to optimize the UV intensity because the higher the energy output required, the higher the cost of the system.
- The UV lamp in the pilot reactor emits most of its intensity in the UV-C range, which is not received at the earth's surface from the sun. The use of a lamp which mimics the wavelengths of solar radiation received at the surface should be investigated. The efficiencies between both lamps should be compared.
- The most cost effective source of UV is solar radiation as opposed to UV lamps which burn out over time, contain mercury and must be treated as hazardous waste. The use of a narrow range wavelength sensor is inefficient to compare various sources of UV intensity. A more efficient means of detecting a wider range of UV radiation is needed to compare the intensity of UV lamps to wavelengths of radiation.

- Once the optimal UV intensity is found and compared to solar radiation along a wide scale of wavelengths, the research and development of a means to focus the solar energy should begin. The sole use of solar radiation provides a sustainable resource that produces no waste and requires no additional energy. This is a main attraction of photocatalytic processes.
- This study found that an increase in TiO_2 led to a decrease in ammonia removal. Investigation of the effect of the catalyst concentration on ammonia removal should be performed. In this experiment, escape of gaseous ammonia should be monitored, as well.
- Further investigation of the pH effects should be conducted. Experiments should be run at multiple pH values to compare the removal efficiencies of COD, ammonia and/or other parameters of interest with pH adjustment.
- Further studies should be conducted on the catalyst dosage to find the minimal amount of TiO_2 necessary for acceptable removal efficiency in less than 20 hours of reaction time, if possible. Also, the TiO_2/COD ratio should be studied as a means in determining the most effective catalyst dose.
- Based on the results of the catalyst recovery trial, a new recovery study should be conducted. Due to the weight of the TiO_2 particles, the use of a sedimentation process should provide adequate recovery percentages. A size distribution analysis of the photocatalytic particles should be obtained or measured to better understand the sedimentation dynamics.
- Studies should be performed on the reuse of TiO_2 . These studies will help determine the lifetime of the catalyst or the point to which a regeneration process

in necessary. In addition, types of catalyst regeneration methods would need to be studied.

- Since adequate temperature control has been achieved, tests can be run for longer than 4 hour increments. Studies on the removal efficiency after 24 consecutive hours of treatment should be conducted and compared to the 24 hour studies performed in increments.
- Investigate the photo-inhibitory effect of alkalinity and pH so as to determine the optimum values for maximum decomposition.
- Process modifications such as the addition of hydrogen peroxide and/or potassium persulfate to increase the production of radical species and the addition of sulfuric acid to control the pH should be investigated to increase the efficiency of the photocatalytic process.
- Develop a system to catch and measure gases being released from the pilot scale reactor. Determination of the amount of CO₂ being released can provide insight to the degradation kinetics of COD. Determining the volume of H₂ and N₂ can provide valuable information on the photocatalytic breakdown of ammonia.
- Further investigation of COD removal should be performed by measuring the BOD/COD ratio during testing. The change in the BOD/COD ratio will provide insight to the type of oxygen demand present in the leachate.
- Since the composition of landfill leachate varies with time and location, experiments should be conducted to study concentration dependence on COD, ammonia, and other parameters of interest (such as BOD, color, TDS, TSS, TKN, phosphorus, heavy metals, etc.). The determination of concentration dependence

for these parameters, among others, will provide valuable information on the overall reaction kinetics, which can be used to optimize the removal efficiency of said parameter(s). The knowledge of the reaction kinetics for individual parameters can be used to develop more efficient congruent treatments for multiple parameter destruction. Without viable reaction order kinetics tests, it is not possible at this time to develop accurate cost estimates, process footprint, pre-treatment requirements, and operation and maintenance issues.

APPENDIX A: Data for Experiments 1 – 6

Table 31: Data for Experiment 1 (4 g/L TiO₂)

Experiment #1					
Date Leachate Collected:	9/30/2011				
Volume of Leachate:	8 Liters				
Catalyst Dose:	4 g/L TiO ₂				
Maximum Temperature:	36.7 °C				
Time (hr)	pH (pH units)	COD (mg/L as O ₂)	Ammonia (mg/L as NH ₃ -N)	Alkalinity (mg/L as CaCO ₃)	Color (PCU)
0	8.35	6246.25	1712.50	4625.0	1125
4	9.20	5996.67	1205.00	4000.0	1050
4	9.04	5946.67	1275.00	4000.0	1050
8	8.98	5706.67	853.00	2875.0	1050
8	9.23	5935.00	892.50	2750.0	1050
12	9.10	5700.00	681.25	2062.5	1050
12	9.22	5770.00	645.83	1750.0	875
16	9.03	5520.00	455.00	1250.0	875
16	9.18	5370.00	448.75	1250.0	875
20	8.91	5126.67	372.50	1000.0	875
20	9.09	5040.00	371.00	1000.0	875
24	8.91	4866.67	306.25	850.0	825
24	8.94	4890.00	306.00	875.0	750
28	8.72	4636.67	258.00	750.0	625
28	8.77	4640.00	253.33	700.0	625
32	8.69	4295.00	188.00	600.0	625
32	8.67	4410.00	228.50	700.0	625
36	8.62	4286.67	216.33	600.0	625
36	8.65	4215.00	205.00	600.0	525
40	8.62	4113.33	188.50	600.0	525
40	8.63	4215.00	167.00	500.0	525
44	8.61	3910.00	171.50	500.0	525
Removal	N/A	37.40%	89.99%	89.19%	53.33%

Table 32: Data for Experiment 2 (16 g/L TiO₂)

Experiment #2					
Date Leachate Collected:	3/09/2012				
Volume of Leachate:	8 Liters				
Catalyst Dose:	16 g/L TiO ₂				
Maximum Temperature:	35.7 °C				
Time (hr)	pH (pH units)	COD (mg/L as O ₂)	Ammonia (mg/L as NH ₃ -N)	Alkalinity (mg/L as CaCO ₃)	Color (PCU)
0	7.63	5268	1306	3563	825
4	8.85	5000	1250	3500	700
4	8.97	4860	1203	3000	700
8	8.88	4850	1148	2500	675
8	9.01	4810	1092	2500	675
12	8.99	4490	985	2375	675
12	9.16	4410	944	2000	675
16	9.02	4250	862	2000	675
16	9.12	4160	868	2000	675
20	9.01	4120	753	1875	675
20	9.18	4020	738	2250	625
24	9.01	3990	662	1750	625
24	8.97	3780	602	1375	575
28	8.65	3570	573	1250	625
28	8.84	3570	627	1500	500
32	8.61	3540	554	1500	500
32	8.84	3390	513	1375	450
36	8.56	3350	502	1125	438
36	8.79	3180	463	1000	425
40	8.66	3160	433	1000	425
Removal	N/A	40.02%	66.85%	71.93%	48.48%

Table 33: Data for Experiment 3 (25 g/L TiO₂)

Experiment #3					
Date Leachate Collected:	3/09/2012				
Volume of Leachate:	8 Liters				
Catalyst Dose:	25 g/L TiO ₂				
Maximum Temperature:	36.0 °C				
Time (hr)	pH (pH units)	COD (mg/L as O ₂)	Ammonia (mg/L as NH ₃ -N)	Alkalinity (mg/L as CaCO ₃)	Color (PCU)
0	7.54	5360	1380	3562.5	787.5
4	8.59	4920	1280	3330.0	625.0
4	8.86	4650	1270	3500.0	625.0
8	8.84	4620	940	2500.0	575.0
8	8.89	4330	1090	3000.0	575.0
12	8.88	4290	820	2380.0	575.0
12	8.91	4140	980	2750.0	575.0
16	8.79	3940	900	2630.0	550.0
16	8.96	3730	890	2500.0	550.0
20	8.78	3730	820	2500.0	550.0
20	8.86	3590	770	2380.0	550.0
24	8.73	3540	710	2000.0	525.0
24	8.85	3540	700	1875.0	525.0
Removal	N/A	33.96%	49.28%	47.37%	33.33%

Table 34: Data for Experiment 4 (40 g/L TiO₂)

Experiment #4					
Date Leachate Collected:	7/18/2012				
Volume of Leachate:	8 Liters				
Catalyst Dose:	40 g/L TiO ₂				
Maximum Temperature:	37.7 °C				
Time (hr)	pH (pH units)	COD (mg/L as O ₂)	Ammonia (mg/L as NH ₃ -N)	Alkalinity (mg/L as CaCO ₃)	Color (PCU)
0	7.59	6990	1523	4312.5	756
4	8.63	6190	1370	3380.0	625
4	8.84	6140	1300	3000.0	625
8	8.65	5870	1140	2380.0	625
8	9.06	5740	1180	2130.0	500
12	8.83	5470	1050	1880.0	500
12	9.05	5310	1060	1880.0	375
16	8.82	5350	1030	1630.0	375
16	9.01	5060	1020	1630.0	375
20	8.62	4940	938	1500.0	375
20	8.96	4670	908	1380.0	375
24	8.72	4650	849	1250.0	325
24	8.90	4530	842	1130.0	325
Removal	N/A	35.19%	44.71%	73.80%	57.01%

Table 35: Data for Experiment 5 (30 g/L TiO₂)

Experiment #5					
Date Leachate Collected:	7/18/2012				
Volume of Leachate:	8 Liters				
Catalyst Dose:	30 g/L TiO ₂				
Maximum Temperature:	36.8 °C				
Time (hr)	pH (pH units)	COD (mg/L as O ₂)	Ammonia (mg/L as NH ₃ -N)	Alkalinity (mg/L as CaCO ₃)	Color (PCU)
0	7.70	6135	1635	4125	756
4	9.02	5790	1460	2875	500
4	9.19	5660	1450	3125	500
8	8.96	5450	1330	2625	500
8	9.20	5290	1320	2750	500
12	9.01	5260	1190	2000	500
12	8.98	5040	1120	1750	500
16	8.92	4800	1065	1625	450
16	9.08	4767	1020	1605	450
20	8.94	4660	980	1357	450
20	9.06	4590	933	1277	425
24	8.83	4418	855	1110	425
24	9.01	4322	845	1013	425
Removal	N/A	29.55%	48.32%	75.44%	43.78%

Table 36: Data for Experiment 6 (10 g/L TiO₂)

Experiment #6					
Date Leachate Collected:	11/26/2012				
Volume of Leachate:	8 Liters				
Catalyst Dose:	10 g/L TiO ₂				
Maximum Temperature:	37.1 °C				
Time (hr)	pH (pH units)	COD (mg/L as O ₂)	Ammonia (mg/L as NH ₃ -N)	Alkalinity (mg/L as CaCO ₃)	Color (PCU)
0	7.71	5947.5	1670	4375	813
4	9.07	5343.3	1380	3750	800
8	9.04	5080.0	1040	2750	750
12	9.05	5036.7	721	1750	750
12	9.14	4686.7	698	1750	700
16	8.94	4560.0	546	1000	700
16	9.08	4466.7	531	1150	700
20	8.61	4473.3	511	1100	650
24	8.62	4323.3	470	700	600
24	8.89	4327.2	412	600	450
Removal	N/A	27.24%	75.33%	86.29%	44.65%

APPENDIX B: Typical Temperature Recordings

Table 37: Experiment 1 Day 8 Temperature recordings

Time (min)	Temp. (°C)
0	14.3
10	17.3
20	20.0
30	22.4
40	24.5
50	26.3
60	27.8
70	29.1
80	30.3
90	31.6
100	32.5
110	33.3
120	33.9
130	34.5
140	35.0
150	35.4
160	35.7
170	35.9
180	36.1
190	36.2
200	36.3
210	36.4
220	36.5
230	36.6
240	36.7

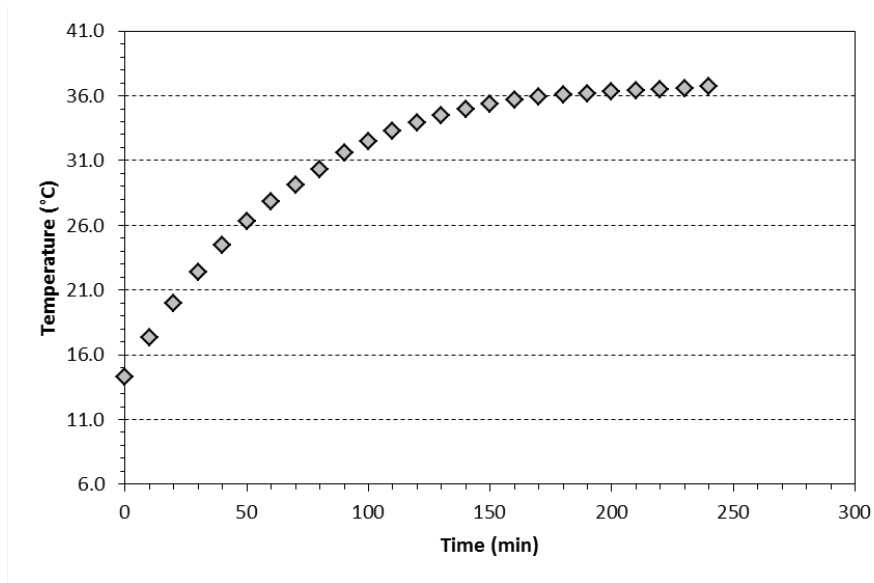


Figure 64: Temperature curve for Experiment 1 Day 8

Table 38: Experiment 2 Day 5 Temperature recordings

Time (min)	Temp. (°C)
0	14.0
10	16.8
20	19.3
30	21.5
40	23.4
50	25.1
60	26.6
70	27.8
80	29.0
90	30.0
100	30.9
110	31.6
120	32.3
130	32.8
140	33.3
150	33.7
160	34.0
170	34.3
180	34.5
190	34.7
200	34.9
210	35.1
220	35.3
230	35.6
240	35.7

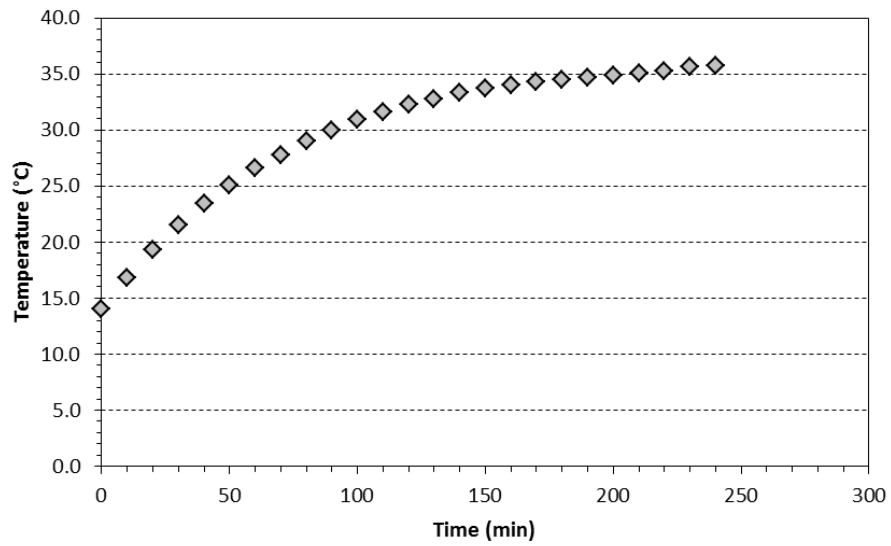


Figure 65: Temperature curve for Experiment 2 Day 5

Table 39: Experiment 3 Day 5 Temperature recordings

Time (min)	Temp. (°C)
0	11.1
10	14.2
20	17.3
30	19.6
40	21.6
50	23.5
60	25.1
70	26.7
80	27.9
90	28.9
100	30.1
110	30.8
120	31.4
130	32.1
140	32.7
150	33.0
160	33.6
170	33.9
180	34.2
190	34.5
200	34.8
210	35.0
220	35.3
230	35.7
240	35.8

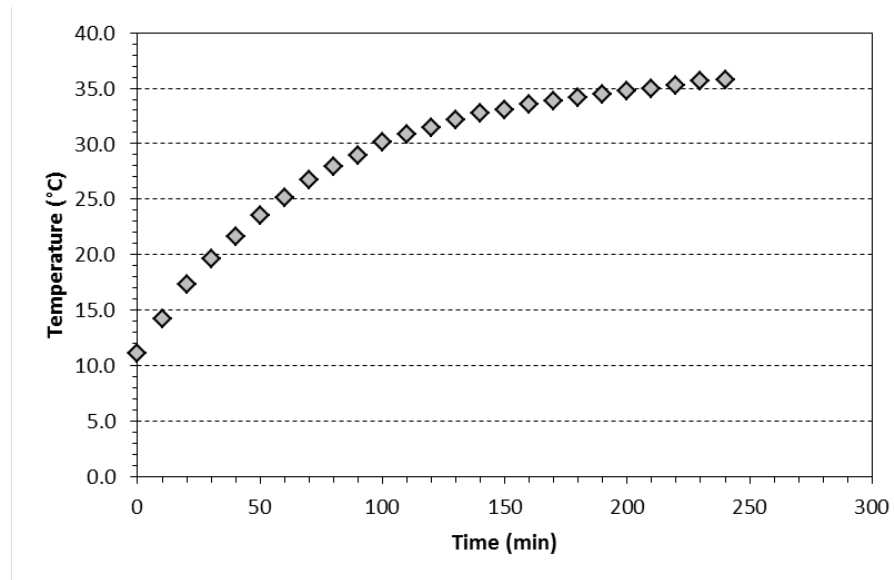


Figure 66: Temperature curve for Experiment 3 Day 5

Table 40: Experiment 4 Day 2 Temperature recordings

Time (min)	Temp. (°C)
0	11.2
10	14.7
20	18.2
30	21.1
40	23.9
50	26.5
60	28.0
70	29.6
80	30.9
90	31.9
100	32.7
110	33.3
120	33.9
130	34.4
140	34.9
150	35.3
160	35.9
170	36.0
180	35.9
190	35.7
200	35.9
210	36.0
220	36.2
230	36.6
240	36.7

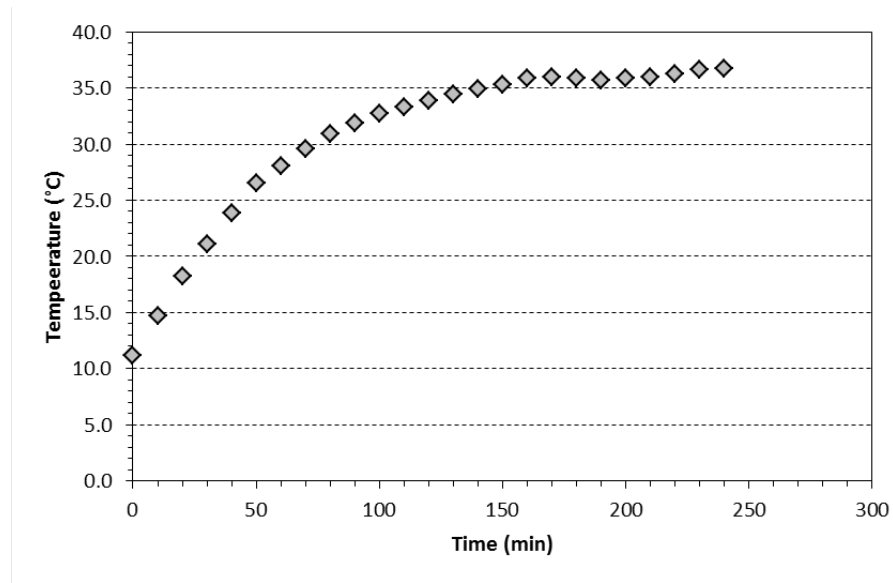


Figure 67: Temperature curve for Experiment 4 Day 2

Table 41: Experiment 5 Day 4 Temperature recordings

Time (min)	Temp. (°C)
0	13.5
10	17.0
20	20.0
30	22.1
40	24.0
50	25.8
60	27.5
70	28.9
80	30.1
90	31.0
100	31.8
110	32.5
120	33.2
130	33.7
140	34.2
150	34.6
160	34.9
170	35.2
180	35.4
190	35.6
200	35.8
210	36.0
220	36.2
230	36.3
240	36.3

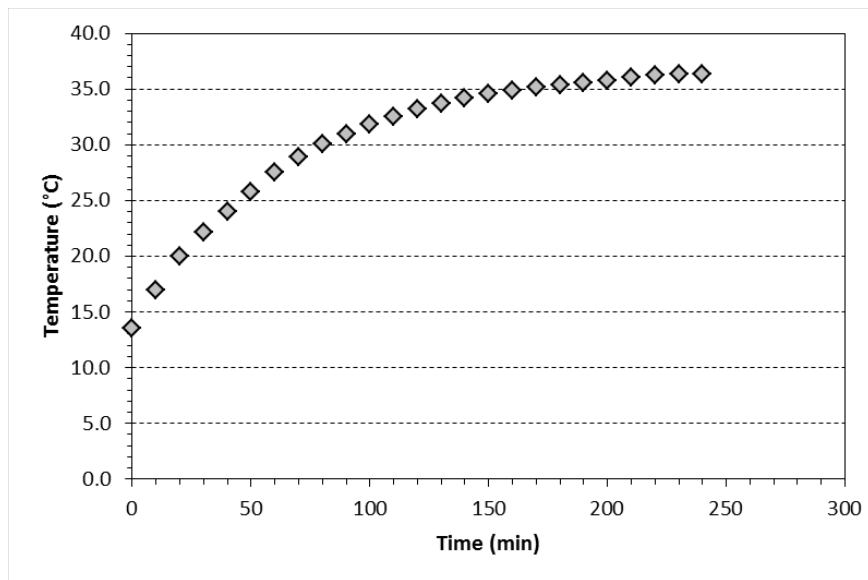


Figure 68: Temperature curve for Experiment 5 Day 4

Table 42: Experiment 6 Day 1 Temperature recordings

Time (min)	Temp. °C
0	11.2
10	14.7
20	18.2
30	21.1
40	23.9
50	26.5
60	28.0
70	29.6
80	30.9
90	31.9
100	32.7
110	33.3
120	33.9
130	34.4
140	34.9
150	35.3
160	35.9
170	36.1
180	35.9
190	35.7
200	35.9
210	36.0
220	36.4
230	36.6
240	36.7
250	36.8
260	36.9
270	37.0
280	37.0
290	37.0
300	37.0
310	37.0
320	37.0
330	37.0
340	37.0
350	37.1
360	37.1
370	37.1
380	37.1
390	37.1
400	37.1
410	37.1

420	37.1
430	37.1
440	37.1
450	37.2
460	37.2
470	37.2
480	37.2
490	37.1
500	37.1
510	37.1
520	37.1
530	37.1
540	37.1
550	37.1
560	37.1
570	37.1
580	37.1
590	37.2
600	37.2
610	37.2
620	37.2
630	37.3
640	37.2
650	37.2
660	37.2
670	37.1
680	37.1
690	37.1
700	37.1
710	37.1
720	37.1

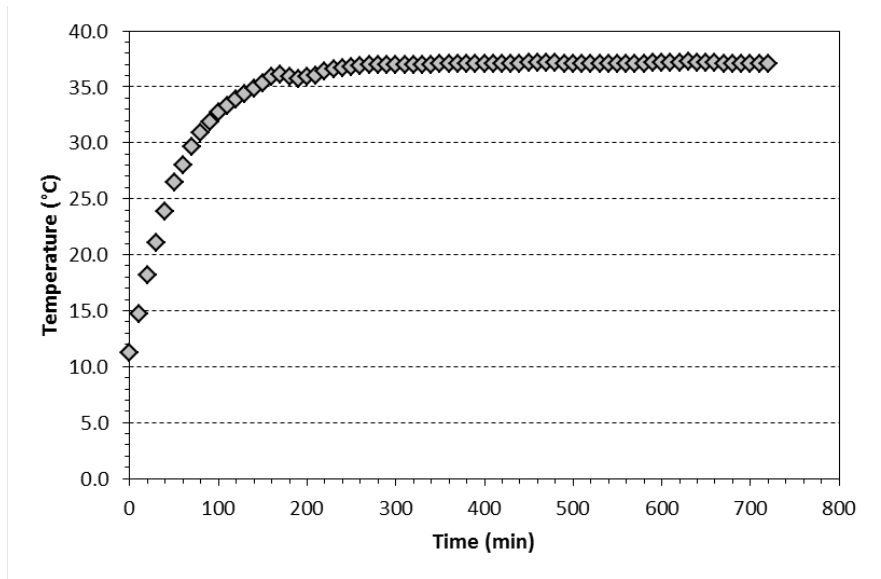


Figure 69: Temperature curve for Experiment 6 Day 1

APPENDIX C: Prediction Tables

Table 43: Alkalinity removal predictions for experiments 1 and 2 using 24 hour k-values from first order kinetics

TiO ₂ (g/L)	k-value (hr ⁻¹)	C ₀ (mg/L as CaCO ₃)	t (hr)	Concentration (mg/L)		% Removal		% error
				calculated	actual	calculated	actual	
4	-0.0780	4625	44	149.5	500	96.7	89.2	70.1
16	-0.0319	3560	40	993.8	1000	72.1	71.9	0.62

Table 44: Ammonia removal predictions for experiments 1 and 2 using 24 hour k-values from first order kinetics

TiO ₂ (g/L)	k-value (hr ⁻¹)	C ₀ (mg/L as NH ₃ -N)	t (hr)	Concentration (mg/L)		% Removal		% error
				calculated	actual	calculated	actual	
4	-0.0726	1713	44	70.2	171.5	95.9	90.0	59.1
16	-0.0316	1310	40	370.1	433.0	71.7	66.9	14.5

Table 45: Color removal predictions for experiments 1 and 2 using 24 hour k-values from zero order kinetics

TiO ₂ (g/L)	k-value (PCU/hr)	C ₀ (PCU)	t (hr)	Concentration (PCU)		% Removal		% error
				calculated	actual	calculated	actual	
4	-0.0780	1125	44	520.7	525	53.7	53.3	0.83
16	-0.0319	700	40	462.5	425	33.9	39.3	8.81

APPENDIX D: UV data recordings

Table 46: Trial 1 of UV measurements

Trial 1	
Distance from UV lamp:	1.844''
Angle of sensor to UV source:	0°
Time (min)	UV intensity (mW/cm ²)
0	0.004
1	0.208
2	0.293
3	0.328
4	0.336
5	0.338
6	0.338
7	0.338
8	0.338
9	0.336
10	0.337

Table 47: Trail 2 of UV measurements

Trial 2	
Distance from UV lamp:	1.844''
Angle of sensor to UV source:	0°
Time (min)	UV intensity (mW/cm ²)
0	0.009
1	0.145
2	0.302
3	0.352
4	0.361
5	0.365
6	0.364
7	0.365
8	0.365
9	0.365
10	0.365

Table 48: Trial 3 of UV measurements, taken at 45° angle

Trial 3	
Distance from UV lamp:	1.844''
Angle of sensor to UV source:	45°
Time (min)	UV intensity (mW/cm ²)
0	0.001
1	0.158
2	0.258
3	0.287
4	0.293
5	0.293
6	0.293
7	0.293
8	0.293
9	0.293
10	0.293

Table 49: Trial 4 of UV measurements, taken at 5.38'' from source

Trial 4	
Distance from UV lamp:	5.38''
Angle of sensor to UV source:	0°
Time (min)	UV intensity (mW/cm ²)
0	0.001
1	0.049
2	0.109
3	0.129
4	0.135
5	0.138
6	0.138
7	0.138
8	0.138
9	0.138
10	0.138

APPENDIX E: MSDS

SAFETY DATA SHEET (EC 1907/2006)**AEROXIDE® TiO2 P 25**

Material no.		Version	3.8 / REG_EU
Specification	132843	Revision date	29.08.2008
VA-Nr		Print Date	30.08.2008
		Page	1 / 6

1. IDENTIFICATION OF THE SUBSTANCE/PREPARATION AND OF THE COMPANY/UNDERTAKING**Product information**

Trade name	:	AEROXIDE® TiO2 P 25
Company	:	Evonik Degussa GmbH Inorganic Materials Produktsicherheit IM-IM-PS Postfach 1345 D-63403 Hanau
Telephone	:	+49 (0)6181 59-4787
Telefax	:	+49 (0)6181 59-4205
Email address	:	sds.asfp@evonik.com
Emergency telephone number	:	+49 (0)7623-919191
Use of the Substance / Preparation	:	Catalyst support Stabilizer UV-filters

2. HAZARDS IDENTIFICATION**Additional safety information for humans and the environment**

On the basis of our data the product is not a hazardous substance as defined by the Chemicals Act or Hazardous Substance Ordinance in the currently valid versions.

3. COMPOSITION/INFORMATION ON INGREDIENTS**Information on ingredients / Hazardous components**

• Titanium dioxide			
CAS-No.	13463-67-7	EC-No.	236-675-5

See chapter 16 for text of risk phrases

4. FIRST AID MEASURES**Inhalation**

In case product dust is released:
Possible discomfort: cough, sneezing
Move victims into fresh air.

Skin contact

Wash off with plenty of water and soap.

Eye contact

Possible discomfort is due to foreign substance effect.
Rinse thoroughly with plenty of water keeping eyelid open.
In case of persistent discomfort: Consult an ophthalmologist.

SAFETY DATA SHEET (EC 1907/2006)**AEROXIDE® TiO2 P 25**

Material no.		Version	3.8 / REG_EU
Specification	132843	Revision date	29.08.2008
VA-Nr		Print Date	30.08.2008
		Page	2 / 6

Ingestion

Clean mouth with water and drink afterwards plenty of water.
After absorbing large amounts of substance / In case of discomfort: Supply with medical care.

Notes to physician

No hazards which require special first aid measures.

5. FIRE-FIGHTING MEASURES**Suitable extinguishing media**

All extinguishing substances suitable.

Specific hazards during fire fighting

None known

Further information

Water used to extinguish fire should not enter drainage systems, soil or stretches of water.
Ensure there are sufficient retaining facilities for water used to extinguish fire.
Fire residues and contaminated fire extinguishing water must be disposed of in accordance with local regulations.

6. ACCIDENTAL RELEASE MEASURES**Personal precautions**

Wear personal protective equipment.

Environmental precautions

Do not allow entrance in sewage water, soil stretches of water, groundwater, drainage systems.

Methods for cleaning up

Sweep up or vacuum up spillage and collect in suitable container for disposal.
Avoid dust formation.

7. HANDLING AND STORAGE**Handling****Safe handling advice**

If necessary: Local ventilation.

Advice on protection against fire and explosion

Take precautionary measures against static discharges.

Storage**Requirements for storage areas and containers**

Keep in a dry place.

SAFETY DATA SHEET (EC 1907/2006)**AEROXIDE® TiO2 P 25**

Material no.		Version	3.8 / REG_EU
Specification	132843	Revision date	29.08.2008
VA-Nr		Print Date	30.08.2008
		Page	3 / 6

8. EXPOSURE CONTROLS / PERSONAL PROTECTION**Components with workplace control parameters****Personal protective equipment****Respiratory protection**

No special protective equipment required.
If dust occurs: Dust mask with P2 particle filter

Hand protection

Wear protective gloves made of the following materials: nitrile rubber (NBR), butyl rubber, PVC.
The material thickness and rupture time data do not apply to non-solute solids / dusts.

Eye protection

Safety glasses with side-shields
If dust occurs: basket-shaped glasses

Skin and body protection

No special protective equipment required.
preventive skin protection
Cleanse and apply cream to skin after work.

Hygiene measures

When using, do not eat, drink or smoke. Wash face and/or hands before break and end of work.
Avoid contaminating clothes with product. Wash contaminated clothing after use.

Protective measures

Handle in accordance with good industrial hygiene and safety practices.
If there is the possibility of skin/eye contact, the indicated hand/eye/body protection should be used.
If the limits at the workplace are exceeded and/or larger amounts are released (leakage, spilling, dust) the indicated respiratory protection should be used.

9. PHYSICAL AND CHEMICAL PROPERTIES**Appearance**

Form	powder
Colour	white
Odour	odourless

Safety data

pH	3.5 - 4.5	(40 g / l)	(20 °C)
Melting point/range	ca. 1850 °C		
Boiling point/range	not applicable		
Flash point	not applicable		
Flammability	not applicable		
Ignition temperature	not applicable		
Autoinflammability	not applicable		

SAFETY DATA SHEET (EC 1907/2006)**AEROXIDE® TiO2 P 25**

Material no.		Version	3.8 / REG_EU
Specification	132843	Revision date	29.08.2008
VA-Nr		Print Date	30.08.2008
		Page	4 / 6

Lower explosion limit	not applicable
Upper explosion limit	not applicable
Minimum ignition energy	> 10 Joule
Vapour pressure	not applicable
Density	ca. 3.8 g/cm ³ (20 °C)
Tapped density	ca. 130 g / l Method: DIN 53 194
Water solubility	insoluble
Partition coefficient (n-octanol/water)	not applicable
Viscosity, dynamic	not applicable

10. STABILITY AND REACTIVITY

Hazardous decomposition products	None known
Thermal decomposition	> 2000 °C

11. TOXICOLOGICAL INFORMATION

Acute oral toxicity	LD50 Rat: > 10000 mg/kg Method: literature (limit test)
Acute dermal toxicity	LD50 Rabbit: >= 10000 mg/kg Method: literature
Skin irritation	Rabbit / literature not irritating
Eye irritation	Rabbit / literature not irritating
Sensitization	Optimizations-test guinea pig: not sensitizing Method: literature Patch test : not sensitizing Method: literature
Genotoxicity in vitro	Microorganisms, cell cultures Shown no mutagenic/genotoxic effect., literature
Genotoxicity in vivo	Microorganisms, cell cultures Shown no mutagenic/genotoxic effect., literature
Carcinogenicity	Oral rat, mouse: 103 weeks

SAFETY DATA SHEET (EC 1907/2006)**AEROXIDE® TiO2 P 25**

Material no.		Version	3.8 / REG_EU
Specification	132843	Revision date	29.08.2008
VA-Nr		Print Date	30.08.2008
		Page	5 / 6

no evidence that cancer may be caused, literature.
Feeding experiments

inhalative Rat: 2 years
Method: literature
Increased incidence of lung tumors.

The scientific discussion of the tumorigenic effect of sparingly soluble inorganic particles (fine dusts)- such as titanium dioxide - is ongoing. It is the opinion of many inhalation toxicologists that the tumor formation observed in rats results from a species-specific mechanism involving overloading of the rat lung (overload phenomenon). Corresponding findings resulting from exposure of humans have not been observed to date. On the other hand, the International Agency for Research on Cancer (IARC) assessed, in February of 2006, the available rat model studies as constituting sufficient proof of the carcinogenicity of titanium dioxide in animal models. For humans, the IARC does not see sufficient evidence of a carcinogenic effect of titanium dioxide. However, the IARC evaluation scheme results in an overall assessment of titanium dioxide as "possibly carcinogenic to humans" (Group 2B).

inhalative (mouse): 2 years
no evidence that cancer may be caused, literature.

Human experience

Epidemiological studies to date have not revealed any evidence of a relation between exposure to titanium dioxide and diseases of the respiratory tract beyond general effects of dust.

12. ECOLOGICAL INFORMATION**Elimination information (persistence and degradability)****Behaviour in environmental compartments****Ecotoxicity effects**


Toxicity to fish	LC50 <i>Fundulus heteroclitus</i> : > 1000 mg/l / 96 h Method: literature
Toxicity to daphnia	EC0 <i>Daphnia magna</i> : 1000 mg/l / 48 h Method: literature
Toxicity to bacteria	EC0 <i>Pseudomonas fluorescens</i> : 10000 mg/l / 24 h Method: DEV, DIN 38412, T. 8 (modified).

13. DISPOSAL CONSIDERATIONS**Product**

Disposal according to local authority regulations.

Uncleaned packaging

Offer rinsed packaging material to local recycling facilities.
Other countries: observe the national regulations.

SAFETY DATA SHEET (EC 1907/2006)			
AEROXIDE® TiO2 P 25			
Material no.		Version	3.8 / REG_EU
Specification	132843	Revision date	29.08.2008
VA-Nr		Print Date	30.08.2008
		Page	6 / 6

Waste Key Number

No waste key number as per the European Waste Types List can be assigned to this product, since such classification is based on the (as yet undetermined) use to which the product is put by the consumer.

The waste key number must be determined as per the European Waste Types List (decision on EU Waste Types List 2000/532/EC) in cooperation with the disposal firm / producing firm / official authority.

14. TRANSPORT INFORMATION

Transport/further information

Not classified as dangerous in the meaning of transport regulations.

15. REGULATORY INFORMATION

Labelling according to EC Directives

Other data

On the basis of our data the product is not a hazardous substance as defined by the Chemicals Act or Hazardous Substance Ordinance in the currently valid versions.

National legislation

16. OTHER INFORMATION

Risk phrase (R phrase) texts

Further information

Changes since the last version are highlighted in the margin. This version replaces all previous versions.

The information provided in this Safety Data Sheet is correct to the best of our knowledge, information and belief at the date of its publication. The information given is designed only as a guidance for safe handling, use, processing, storage, transportation, disposal and release and is not to be considered a warranty or quality specification. The information relates only to the specific material designated and may not be valid for such material used in combination with any other materials or in any process, unless specified in the text.

Figure 70: MSDS for Titanium Dioxide

MATERIAL SAFETY DATA SHEET

1. CHEMICAL PRODUCT AND COMPANY IDENTIFICATION

Product Name: Digestion Solution for COD 20-1500 mg/l Range
Catalog Number: 2125915

Hach Company
P.O.Box 389
Loveland, CO USA 80539
(970) 669-3050

Emergency Telephone Numbers:
(Medical and Transportation)
(303) 623-5716 24 Hour Service
(515)232-2533 8am - 4pm CST

MSDS Number: M00485
Chemical Name: Not applicable
CAS Number: Not applicable
Additional CAS No. (for hydrated forms): Not applicable
Chemical Formula: Not applicable
Chemical Family: Not applicable
Intended Use: Laboratory Use Determination of Chemical Oxygen Demand

2. HAZARDS IDENTIFICATION

GHS Classification:

Hazard categories: Acute Toxicity: Acute Tox. 4-Orl Acute Toxicity: Acute Tox. 3-Derm Skin Corrosion/Irritation: Skin Corr. 1A Germ Cell Mutagenicity: Muta. 1B Carcinogenicity: Carc. 1A Specific Target Organ Toxicity - Repeated Exposure: STOT RE. 2 Hazardous to the Aquatic Environment: Aquatic Chronic 1

GHS Label Elements:



Hazard statements: May be corrosive to metals. Harmful if swallowed. Toxic in contact with skin. Causes severe skin burns and eye damage. May cause genetic defects. May cause cancer. May cause damage to organs through prolonged or repeated exposure. Very toxic to aquatic life with long lasting effects.

Precautionary statements: Obtain special instructions before use. Wear protective gloves / protective clothing / eye protection / face protection. IF SWALLOWED: rinse mouth. Do NOT induce vomiting. IF ON SKIN (or hair): Remove/Take off immediately all contaminated clothing. Rinse skin with water/shower. IF IN EYES: Rinse cautiously with water for several minutes. Remove contact lenses, if present and easy to do. Continue rinsing. IF exposed or if you feel unwell: Call a POISON CENTER or doctor/physician.

HMIS:

Health: 3*
Flammability: 0
Reactivity: 2
Protective Equipment: X - See protective equipment, Section 8.

NFPA:

Health: 3
Flammability: 0
Reactivity: 2
Symbol: Water Reactive

3. COMPOSITION / INFORMATION ON INGREDIENTS

Hazardous Components according to GHS:

Sulfuric Acid

CAS Number: 7664-93-9
Chemical Formula: H₂SO₄
GHS Classification: Met. Corr. 1 H290; Skin Corr. 1A, H314
Percent Range: 80.0 - 90.0
Percent Range Units: weight / weight
PEL: 1 mg/m³
TLV: 1 mg/m³ (TWA); 3 mg/m³ (STEL)

Silver Sulfate

CAS Number: 10294-26-5
Chemical Formula: Ag₂SO₄
GHS Classification: Eye Dam.1, H318; Aquatic Acute 1, H400
Percent Range: 0.5 - 3.0
Percent Range Units: weight / volume
PEL: 0.01 mg/m³ (Ag)
TLV: 0.01 mg/m³ (Ag)

Mercuric Sulfate

CAS Number: 7783-35-9
Chemical Formula: HgSO₄
GHS Classification: Acute Tox. Inh. 2, H330; Acute Tox Der. 1, H310; Acute Tox. Or. 2, H300; STOT RE 2, H373X, Aquatic Acute 1, H400; Aquatic Chron. 1, H410
Percent Range: 0.1 - 1.0
Percent Range Units: weight / weight
PEL: 0.1 mg/m³ (Hg)
TLV: 0.05 mg/m³ (Hg)

Chromic Acid

CAS Number: 13530-68-2
Chemical Formula: H₂Cr₂O₇
GHS Classification: Ox. Sol.2,H272; Carc.1B,H350; Muta.1B, H340; Repr.1B, H360FD; Acute Tox.2-Inh, H330; Acute Tox.3-Orl, H301; Acute Tox.4-Derm, H312; STOT RE 1, H372; Skin Corr.1B, H314; Resp. Sens.1, H334; Skin Sens.1, H317; Aquatic Acute 1, H400; Aquatic Chronic 1, H410
Percent Range: 0.1 - 1.0
Percent Range Units: weight / volume
PEL: 5 µg/m³ (0.00235 ppm Cr⁺⁶), 8 Hr TWA; Action Level is 2.5 µg/m³ (0.00117 ppm), 8 Hr TWA
TLV: 0.05 mg/m³ (0.0235 ppm as Cr⁺⁶)

Hazardous Components according to GHS: No

Demineralized Water

CAS Number: 7732-18-5
Chemical Formula: H₂O
GHS Classification: Not applicable
Percent Range: 10.0 - 20.0
Percent Range Units: weight / weight
PEL: Not established
TLV: Not established

4. FIRST AID MEASURES

General Information: In the event of exposure, show this Material Safety Data Sheet and label (where possible) to a doctor.

Advice to doctor: Treat symptomatically.

Eye Contact: Immediately flush eyes with water for 15 minutes. Call physician.

Skin Contact (First Aid): Wash skin with plenty of water for 15 minutes. Remove contaminated clothing. Call physician immediately.

Inhalation: Remove to fresh air. Give artificial respiration if necessary. Call physician.

Ingestion (First Aid): Do not induce vomiting. Give large quantities of water. Never give anything by mouth to an unconscious person. Call physician immediately.

5. FIRE FIGHTING MEASURES

Flammable Properties: Not Flammable, but reacts with most metals to form flammable hydrogen gas. During a fire, corrosive and toxic gases may be generated by thermal decomposition.

Fire Fighting Instruction: As in any fire, wear self-contained breathing apparatus pressure-demand and full protective gear. Evacuate area and fight fire from a safe distance. Water runoff can cause environmental damage. Dike and collect water used to fight fire.

Extinguishing Media: Use media appropriate to surrounding fire conditions

Extinguishing Media NOT To Be Used: Not applicable

Fire / Explosion Hazards: Contact with metals gives off hydrogen gas which is flammable. May react violently with: strong bases water

Hazardous Combustion Products: This material will not burn.

6. ACCIDENTAL RELEASE MEASURES

Spill Response Notice:

Only persons properly qualified to respond to an emergency involving hazardous substances may respond to a spill according to federal regulations (OSHA 29 CFR 1910.120(a)(v)) and per your company's emergency response plan and guidelines/procedures. See Section 13, Special Instructions for disposal assistance. Outside of the US, only persons properly qualified according to state or local regulations should respond to a spill involving chemicals.

Containment Technique: Releases of this material may contaminate the environment. Absorb spilled liquid with non-reactive sorbent material. Stop spilled material from being released to the environment. Dike the spill to contain material for later disposal.

Clean-up Technique: Mercury and its compounds are extremely toxic! Be extremely careful not to contact the spill or breathe any vapors. Absorb spilled liquid with non-reactive sorbent material. Dispose of all mercury contaminated material at a government approved hazardous waste facility. Dispose of material in government approved hazardous waste facility. Decontaminate area with commercially available mercury absorbing compounds.

Evacuation Procedure: Evacuate general area (50 foot radius or as directed by your facility's emergency response plan) when: any quantity is spilled. Deny access to unnecessary and unprotected personnel. Remain up-wind from spilled material. If conditions warrant, increase the size of the evacuation.

DOT Emergency Response Guide Number: 137

7. HANDLING AND STORAGE

Handling: Avoid contact with eyes skin clothing Do not breathe mist or vapors. Use with adequate ventilation. Maintain general industrial hygiene practices when using this product.

Storage: Protect from: light contamination by organic materials (will affect product stability) heat

Flammability Class: Not applicable

8. EXPOSURE CONTROLS / PERSONAL PROTECTION

Engineering Controls: Use a fume hood to avoid exposure to dust, mist or vapor. Maintain general industrial hygiene practices when using this product. Maintain adequate ventilation to keep vapor level below TWA for chemicals in this product. Refer to the OSHA Standard at 29CFR1910.1026 for Cr (VI) (See Federal Register 28 February 2006 Page 10100.)

Personal Protective Equipment:

Eye Protection: chemical splash goggles

Skin Protection: disposable latex gloves lab coat

Inhalation Protection: laboratory fume hood

Precautionary Measures: Avoid contact with: eyes skin clothing Do not breathe: mist/vapor Wash thoroughly after handling. Use with adequate ventilation. Protect from: heat light organic materials Keep away from: alkalis metals other combustible materials oxidizers reducers

TLV: Not established. 0.05 mg/m³ (0.0235 ppm as Cr⁺⁶).

PEL: Not established. 5 µg/m³ (0,00235 ppm Cr⁶⁺), 8 Hr TWA; Action Level is 2,5 µg/m³ (0,00117 ppm), 8 Hr TWA
For Occupational Exposure Limits (OEL) for ingredients, see section 3 - Composition/Information on Ingredients.:

9. PHYSICAL AND CHEMICAL PROPERTIES

Appearance: Turbid, light orange liquid
Physical State: Liquid
Molecular Weight: Not applicable
Odor: Not determined
Odor Threshold: Not applicable
pH: < 0.5
Metal Corrosivity:
Corrosivity Classification: Classified as corrosive to metals.
Steel: Corrosive
Aluminum: Corrosive
Specific Gravity/Relative Density (water = 1; air =1): > 1.0
Viscosity: Not determined
Solubility:
Water: Miscible
Acid: Not determined
Other: Not determined
Partition Coefficient (n-octanol / water): Not applicable
Coefficient of Water / Oil: Not applicable
Melting Point: Not applicable
Decomposition Temperature: Not determined
Boiling Point: > 100°C (> 212°F)
Vapor Pressure: Not determined
Vapor Density (air = 1): Not determined
Evaporation Rate (water = 1): Not determined
Volatile Organic Compounds Content: Not applicable
Flammable Properties: Not Flammable, but reacts with most metals to form flammable hydrogen gas. During a fire, corrosive and toxic gases may be generated by thermal decomposition.
Flash Point: Not applicable
Method: Not applicable
Flammability Limits:
Lower Explosion Limits: Not applicable
Upper Explosion Limits: Not applicable
Autoignition Temperature: Not applicable
Explosive Properties:
Not classified according to GHS criteria.
Oxidizing Properties:
Not classified according to GHS criteria.
Reactivity Properties:
Not classified as self-reactive, pyrophoric, self-heating or emitting flammable gases in contact with water according to GHS criteria.
Gas under Pressure:
Not classified as gas under pressure according to GHS.

10. STABILITY AND REACTIVITY

Chemical Stability: Stable when stored under proper conditions.
Mechanical Impact: None reported
Static Discharge: None reported.
Reactivity / Incompatibility: May react violently in contact with: caustics
Hazardous Decomposition: Heating to decomposition releases toxic and/or corrosive fumes of: mercury compounds sulfur oxides
Conditions to Avoid: Exposure to light or contamination by organic materials will affect this product's stability.

11. TOXICOLOGICAL INFORMATION

Toxicokinetics, Metabolism and Distribution: No information available

Toxicologically Synergistic Products: None reported

Acute Toxicity:

Oral rat LD50 = 496 mg/kg.

Dermal LD50 = 614 mg/kg.

Inhalation LC50 = 32 mg/L.

Specific Target Organ Toxicity - Single Exposure (STOT-SE): Based on classification principles, the classification criteria are not met.

Specific Target Organ Toxicity - Repeat Exposure (STOT-RE): Target Organs Respiratory Tract Kidneys Liver
Reproductive system Central nervous system

Skin Corrosion/Irritation: Corrosive to skin.

Eye Damage: Corrosive to eyes.

Sensitization: Based on classification principles, the classification criteria are not met.

CMR Effects/Properties (carcinogenic, mutagenic or toxic to reproduction): Contains Listed Carcinogen Data supporting mutagenicity was found.

An ingredient of this mixture is: NTP Listed Group 1: Recognized Carcinogen

Hexavalent Chromium Compounds

An ingredient of this product is an OSHA listed carcinogen.

Hexavalent chromium (Cr⁶⁺) compounds

Symptoms/Effects:

Ingestion: Causes: severe burns May cause: abdominal pain circulatory disturbances diarrhea loosening of the teeth
nausea vomiting rapid pulse and respirations toxic nephritis (inflammation of the kidneys) shock collapse kidney
damage death Toxic

Inhalation: Causes: severe burns May cause: difficult breathing mouth soreness teeth erosion Effects similar to those
of ingestion. Toxic

Skin Absorption: Toxic Will be absorbed through the skin. Effects similar to those of ingestion

Chronic Effects: Chronic overexposure may cause destruction of any tissue contacted difficult breathing mouth
soreness erosion of the teeth accumulation of silver in body tissues which causes a slate-gray to bluish discoloration.
cancer Chromate and dichromate salts may cause ulceration and perforation of the nasal septum, severe liver damage,
central nervous system effects, and lung cancer. Mercury is a general protoplasmic poison; it circulates in the blood and
is stored in the liver, kidneys, spleen and bones. Main symptoms are sore mouth, tremors and psychic disturbances.

Medical Conditions Aggravated: Pre-existing: Respiratory conditions Eye conditions Skin conditions Allergies or
sensitivity to chromates or chromic acid. Allergies or sensitivity to mercury.

12. ECOLOGICAL INFORMATION

Product Ecological Information: Calculated: Crustacea 48 hr EC50 = 0.0045 mg/L.

Mobility in soil: No data available

Method Used for Estimation of Aquatic Toxicity of Mixture M-factor (Multiplier) for highly toxic ingredients: 100

Ingredient Ecological Information: Silver sulfate: Crustacea 48 hr EC50 = 0.0045 mg/L; mercuric sulfate: Algae: EC50 -
Pseudokirchneriella subcapitata - 0.033 mg/L - 14 d; chromic acid: Daphnia magna (Water flea) 48 hr EC50 = 0.8 mg/L.

13. DISPOSAL CONSIDERATIONS

EPA Waste ID Number: D002 D007 D009 D011

Special Instructions (Disposal): Dispose of all mercury contaminated material at an E.P.A. hazardous waste facility.

Dispose of material in an E.P.A. approved hazardous waste facility.

Empty Containers: Rinse three times with an appropriate solvent. Dispose of empty container as normal trash. Rinsate
from empty containers may contain sufficient product to require disposal as hazardous waste.

NOTICE (Disposal): These disposal guidelines are based on federal regulations and may be superseded by more stringent
state or local requirements. Please consult your local environmental regulators for more information. In Europe: Chemical
and analysis solutions must be disposed of in compliance with the respective national regulations. Product packaging must
be disposed of in compliance with the country-specific regulations or must be passed to a packaging return system.

14. TRANSPORT INFORMATION

D.O.T.:

D.O.T. Proper Shipping Name: Sulphuric Acid

--

Hazard Class: 8

Subsidiary Risk: NA

ID Number: UN1830

Packing Group: II
I.D.G.:
Proper Shipping Name: Sulphuric Acid
--
Hazard Class: 8
Subsidiary Risk: NA
UN Number/PIN: 1830
Packing Group: II
I.C.A.O.:
I.C.A.O. Proper Shipping Name: Sulphuric Acid
--
Hazard Class: 8
Subsidiary Risk: NA
ID Number: UN1830
Packing Group: II
I.M.O.:
Proper Shipping Name: Sulphuric Acid
--
Hazard Class: 8
Subsidiary Risk: NA
ID Number: UN1830
Packing Group: II

Additional Information: There is a possibility that this product could be contained in a reagent set or kit composed of various compatible dangerous goods. If the item is NOT in a set or kit, the classification given above applies. If the item IS part of a set or kit, the classification would change to the following: UN3316 Chemical Kit, Class 9, PG II or III. If the item is not regulated, the Chemical Kit classification does not apply.

15. REGULATORY INFORMATION

U.S. Federal Regulations:

O.S.H.A.: This product meets the criteria for a hazardous substance as defined in the Hazard Communication Standard. (29 CFR 1910.1200)

E.P.A.:

S.A.R.A. Title III Section 311/312 Categorization (40 CFR 370): Immédiat (aigu) Danger pour la santé Delayed (Chronic) Health Hazard Reactive

S.A.R.A. Title III Section 313 (40 CFR 372): This product contains a chemical(s) subject to the reporting requirements of Section 313 of Title III of SARA.

Mercury compounds, Silver compounds, Chromium Compounds, Sulfuric acid (acid aerosols including mists, vapors, gas, fog and other airborne forms).

302 (EHS) TPQ (40 CFR 355): Sulfuric Acid 1000 lbs.

304 CERCLA RQ (40 CFR 302.4): Chromic acid and Mercuric sulfate (each) = 10 lbs. Sulfuric Acid 1000 lbs.

304 EHS RQ (40 CFR 355): Sulfuric Acid - RQ 1000 lbs.

Clean Water Act (40 CFR 116.4): Chromic acid - RQ 10 lbs. Mercuric sulfate - RQ = 10 lbs. (4.54 kgs.) Sulfuric acid - RQ 1000 lbs.

RCRA: Contains RCRA regulated substances. See Section 13, EPA Waste ID Number.

State Regulations:

California Prop. 65: WARNING - This product contains a chemical known to the State of California to cause cancer.

WARNING - This product contains a chemical known to the State of California to cause birth defects or other reproductive harm.

Identification of Prop. 65 Ingredient(s): Chromium (hexavalent compounds); Mercury and mercury compounds.

California Perchlorate Rule CCR Title 22 Chap 33: Not applicable

Trade Secret Registry: Not applicable

National Inventories:

U.S. Inventory Status: All ingredients in this product are listed on the TSCA 8(b) Inventory (40 CFR 710).

CAS Number: Not applicable

Canadian Inventory Status: All ingredients of this product are DSL Listed.

EEC Inventory Status: All ingredients used to make this product are listed on EINECS / ELINCS.

Australian Inventory (AICS) Status: All ingredients are listed.

New Zealand Inventory (NZIoC) Status: All components either listed or exempt.

Korean Inventory (KECI) Status: All components of this product are either listed, listed as the anhydrous compound or exempt.

Japan (ENCS) Inventory Status: All components either listed or exempt.

China (PRC) Inventory (MEP) Status: All components either listed or exempt.

16. OTHER INFORMATION

References: 29 CFR 1900 - 1910 (Code of Federal Regulations - Labor). Air Contaminants, Federal Register, Vol. 54, No. 12. Thursday, January 19, 1989. pp. 2332-2983. CCINFO RTECS. Canadian Centre for Occupational Health and Safety. Hamilton, Ontario Canada: 30 June 1993. Fire Protection Guide on Hazardous Materials, 10th Ed. Quincy, MA: National Fire Protection Association, 1991. IARC Monographs on the Evaluation of the Carcinogenic Risks to Humans. World Health Organization (Volumes 1-42) Supplement 7. France: 1987. List of Dangerous Substances Classified in Annex I of the EEC Directive (67/548) - Classification, Packaging and Labeling of Dangerous Substances, Amended July 1992. Outside Testing. Sixth Annual Report on Carcinogens, 1991. U.S. Department of Health and Human Services. Rockville, MD: Technical Resources, Inc. 1991. Technical Judgment. Verschuieren, Karel. Handbook of Environmental Data on Organic Chemicals. New York: Van Nostrand Reinhold Co., 1977.

Complete Text of H phrases referred to in Section 3: H290 May be corrosive to metals. H302 Harmful if swallowed. H311 Toxic in contact with skin. H314 Causes severe skin burns and eye damage. H340 May cause genetic defects. H350 May cause cancer. H373 May cause damage to organs through prolonged or repeated exposure. H410 Very toxic to aquatic life with long lasting effects.

Revision Summary: Substantial revision to comply with EU Reg 1272/2008, Reg 1907/2006 and UN GHS (ST/SG/AC.10/36/Add.3).

Date of MSDS Preparation:

Day: 08

Month: October

Year: 2012

MSDS Prepared: MSDS prepared by Product Compliance Department extension 3350

CCOHS Evaluation Note: This product has been classified and labeled in accordance with the requirements of GHS (ST/SG/AC.10/36/Add.3). It is offered under the interim policy that was established by Health Canada permitting use of GHS-formatted safety data sheets in Canada prior to revision of CPR to GHS. It is offered under exemption from WHMIS labeling as specified in the Controlled Products Regulation (CPR) Section 17.

Legend:

NA - Not Applicable

ND - Not Determined

NV - Not Available

w/w - weight/weight

w/v - weight/volume

v/v - volume/volume

USER RESPONSIBILITY: Each user should read and understand this information and incorporate it in individual site safety programs in accordance with applicable hazard communication standards and regulations.

THE INFORMATION CONTAINED HEREIN IS BASED ON DATA CONSIDERED TO BE ACCURATE. HOWEVER, NO WARRANTY IS EXPRESSED OR IMPLIED REGARDING THE ACCURACY OF THESE DATA OR THE RESULTS TO BE OBTAINED FROM THE USE THEREOF.

HACH COMPANY ©2013

Figure 71: MSDS for COD digestion vials

REFERENCES

- Abu Amr, S. S., and Aziz, H. A., (2012). New treatment of stabilized leachate by ozone/Fenton in the advanced oxidation process. *Waste Management*.
- Adlan, M.N., Palaniandy, P., Aziz, H.A. (2011). Optimization of coagulation and dissolved air flotation (DAF) treatment of semi-aerobic landfill leachate using response surface methodology (RSM). *Desalination* 277: 74-82.
- Altomare, M., Chiarello, G.L., Costa, A., Guarino, M., Selli, E. (2012). Photocatalytic abatement of ammonia in nitrogen-containing effluents. *Chemical Engineering Journal* 191: 394-401.
- Aman, N., Mishra, T., Hait, J., Jana, R.K. (2011). Simultaneous photoreductive removal of copper (II) and selenium (IV) under visible light over spherical binary oxide photocatalyst. *Journal of Hazardous Materials* 186: 360-366.
- Anglada, A., Urtiaga, A., Ortiz, I., Mantzavinos, D., Diamadopoulos, E. (2011). Treatment of municipal landfill leachate by catalytic wet air oxidation: Assessment of the role of operating parameters by factorial design. *Waste Management* 31: 1833–1840.
- Autin, O., Hart, J., Jarvis, P., MacAdam, J, Parsons, S.A., Jefferson, B. (2013). The impact of background organic matter and alkalinity on the degradation of the

pesticide metaldehyde by two advanced oxidation processes: UV/H₂O₂ and UV/TiO₂. *Water Research* 47: 2041-2049.

Aziz, H.A., Ling, T.J., Haque, A.A.M., Umar, M., Adlan, M.N. (2011). Leachate treatment by swim-bed bio fringe technology. *Desalination* 276: 278–286.

Baransi, K., Dubowski, Y., Sabbah, I. (2012). Synergetic effect between photocatalytic degradation and adsorption processes on the removal of phenolic compounds from olive mill wastewater. *Water Research* 46: 789-798.

Bashir, M.J.K., Aziz, H.A., Yusoff, M.S., Aziz, S.Q., Mohajeri, S. (2010). Stabilized sanitary landfill leachate treatment using anionic resin: Treatment optimization by response surface methodology. *Journal of Hazardous Materials* 182: 115–122.

Bekbolet, M. and Araz, C.V. (1996). Inactivation of *Escherichia coli* by photocatalytic oxidation. *Chemosphere* 32: 959-965.

Birchler, D. R., Milke, M. W., Marks, A. L., Luthy, R. G. (1994). Landfill Leachate Treatment by Evaporation. *Journal of Environmental Engineering* 120:1109-1131.

Blandford, L.K. (2011). St. Lucie's new way of getting rid of leachate costs less, is environmentally friendly. *TCPalm News*.
<<http://www.tcpalm.com/news/2011/oct/18/st-lucies-new-way-of-getting-rid-of-leachate-is>> (Nov. 18, 2012).

- Bouhezila, F., Hariti, M., Lounici, H., Mameri, N. (2011). Treatment of the OUED SMAR town landfill leachate by an electrochemical reactor. *Desalination* 280: 347–353.
- Brown, L.S., Holme, T.A. (2011). *Chemistry for Engineering Students*. Brooks/Cole, Cengage Learning, Belmont, California.
- Buxton, G.V., Greenstock, C.L, Helman, W. P., Ross, A.B. (1988). Critical Review of Rate Constants for Reactions of Hydrated Electrons, Hydrogen Atoms and Hydroxyl Radicals ($\cdot\text{OH}/\text{O}^{\cdot}$) in Aqueous Solution. *Journal of Physical and Chemical Reference Data* 17 issue 2: 513-534.
- California MTBE Research Partnership. (2000). *Treatment Technologies for Removal of Methyl Tertiary Butyl Ether (MTBE) from Drinking Water: Air Stripping, Advanced Oxidation Processes, Granular Activated Carbon, Synthetic Resin Sorbents; Second Edition*. Center for Groundwater Restoration and Protection and National Water Research Institute, Fountain Valley.
- Carneiro, J.T., Moulijn, J.A., Mul, G. (2010). Photocatalytic oxidation of cyclohexane by titanium dioxide: Catalyst deactivation and regeneration. *Journal of Catalysis* 273: 199-210.
- Chemlal, R., Abdi, N., Drouiche, N., Lounici, H., Paus, A., Mameri, N. (2013). Rehabilitation of Oued Smar landfill into a recreation park: Treatment of the contaminated waters. *Ecological Engineering* 51: 244-248.

- Cho, S.P., Hong, S.C., Hong, S.-I. (2004). Study of the end point of photocatalytic degradation of landfill leachate containing refractory matter. *Chemical Engineering Journal* 98: 245-253.
- Chong, M.N., Jin, B., Chow, C.W.K., Saint, C. (2010). Recent developments in photocatalytic water treatment technology: A review. *Water Research* 44: 2997-3027.
- Commonwealth of Australia. (2010). "Ammonia (total): Overview." <<http://www.npi.gov.au/substances/ammonia/index.html>> (September 13, 2012).
- Deng, Y., and Ezyske, C. M. (2011). Sulfate radical-advanced oxidation process (SR-AOP) for simultaneous removal of refractory organic contaminants and ammonia in landfill leachate. *Water Research* 45: 6189-6194.
- Department of Human Health and Services (2011). Occupational Exposure to Titanium Dioxide. *Current Intelligence Bulletin* 63: April 2011.
- Dincer, A.R., Karakaya, N., Gunes, E., Gunes, Y. (2008). Removal of COD from oil recovery industry wastewater by the advanced oxidation processes (AOP) based on H₂O₂. *Global NEST Journal* 10 No.1: 31-38.
- Dutta, P.K., Ray, A.K., Sharma, V.K., Millero, F.J. (2004). Adsorption of arsenate and arsenite on titanium dioxide suspensions. *Journal of Colloid and Interface Science* 278: 270-275.

- Eddy, F.B. (2005). Ammonia in estuaries and effects on fish. *Journal of Fish Biology* 67(6): 1495-1513.
- Evonik Industries. (2008). Safety Data Sheet: Aeroxide[®] TiO₂ P 25 Version 3.8.
- Faure, B., Lindelov, J.S., Wahlberg, M., Adkins, N., Jackson, P., Bergstrom, L. (2010). Spray drying of TiO₂ nanoparticles into redispersible granules. *Powder Technology* 203: 384-388.
- Frank, S.N. and Bard, A.J. (1977). Heterogeneous Photocatalytic Oxidation of Cyanide Ion in Aqueous Solutions at TiO₂ Powder. *Journal of the American Chemical Society* 99:1 303-304.
- Gandhi, V.G., Mishra, M.K., Joshi, P.A. (2012). A study on deactivation and regeneration of titanium dioxide during photocatalytic degradation of phthalic acid. *Journal of Industrial and Engineering Chemistry* 18: 1902-1907.
- Gernjak, W., Maldonado, M.I., Malato, S., Caceres, J., Krutzler, T., Glaser, A., Bauer, R. (2004). Pilot-plant treatment of olive mill wastewater (OMW) by solar TiO₂ photocatalysis and solar photo-Fenton. *Solar Energy* 77: 567-572.
- Ghaly, M.Y., Jamil, T.S., El-Seesy, I.E., Souaya, E.R., Nasr, R.A. (2011). Treatment of highly polluted paper mill wastewater by solar photocatalytic oxidation with synthesized nano TiO₂. *Chemical Engineering Journal* 168: 446-454.

- Gorska, P., Zaleska, A., Hupka, J. (2009). Photodegradation of phenol by UV/TiO₂ and Vis/N,C-TiO₂ processes: Comparative mechanistic and kinetic studies. *Separation and Purification Technology* 68: 90-96.
- Grabowska, E., Reszczyńska, J., Zaleska, A. (2012). Mechanism of phenol photodegradation in the presence of pure and modified-TiO₂: A review. *Water Research* 46: 5453-5471.
- Hammer, M.J., Hammer, M.J. Jr. (2011). *Water and Wastewater Technology*. Pearson Education, Inc., Upper Saddle River, New Jersey.
- Hapeshi, E. Achilleos, A., Vasquez, M.I., Michael, C., Xekoukoulotakis, N.P., Mantzavinos, D., Kassinos, D. (2010). Drugs degrading photocatalytically: Kinetics and mechanisms of ofloxacin and atenolol removal on titania suspensions. *Water Research* 44: 1737-1746.
- Hazime, R., Nguyen, Q.H., Ferronato, C., Huynh, T.K.X., Jaber, F., Chovelon, J.-M. (2013). Optimization of imazalil removal in the system UV/TiO₂/K₂S₂O₈ using a response surface methodology (RSM). *Applied Catalysis B: Environmental* 132-133: 519-526.
- Helali, S., Dappozze, F., Horishoki, S., Bui, T.H., Perol, N., Guillard, C. (2013). Kinetics of the photocatalytic degradation of methylamine: Influence of pH and of UV-A/UV-B radiant fluxes. *Journal of Photochemistry and Photobiology A: Chemistry* 2013.

- Hemond, H.F., Fechner-Levy, E.J. (2000). *Chemical Fate and Transport in the Environment*. Academic Press, San Diego, California.
- Holmes, F.R. (2003). "The performance of a reactor using photocatalysis to degrade a mixture of organic contaminants in aqueous solution." MS Thesis, University of Florida, Gainesville, FL.
- Hong, X., Wang, Z., Cai, W., Lu, F., Zhang, J., Yang, Y., Ma, N., Liu, Y. (2005). Visible-Light-Activated Nanoparticle Photocatalyst of Iodine-Doped Titanium Dioxide. *Chemistry of Materials* 17: 1548-1552.
- Iaconi, C. D., Pagano, M., Ramadori, R., Lopez, A. (2010). Nitrogen recovery from a stabilized municipal landfill leachate. *Bioresource Technology* 101: 1732–1736.
- Jegadeesan, G., Al-Abed, S.R., Sundaram, V., Choi, H., Scheckel, K.G., Dionysiou, D.D. (2010). Arsenic sorption on TiO₂ nanoparticles: Size and crystallinity effects. *Water Research* 44: 965-973.
- Jia, C., Wang, Y., Zhang, C., Qin, Q. (2011). UV-TiO₂ Photocatalytic Degradation of Landfill Leachate. *Water Air Soil Pollution* 217:375–385.
- Jia, C., Zhu, J., Qin, Q. (2013). "Variation Characteristics of Different Fractions of Dissolved Organic Matter in Landfill Leachate during UV-TiO₂ Photocatalytic Degradation" Report for the 2013 Third International Conference on Intelligent System Design and Engineering Applications.

- Kebir, M., Chabani, M., Nasrallah, N., Bensmaili, A., Trari, M. (2011). Coupling adsorption with photocatalysis process for the Cr(VI) removal. *Desalination* 270: 166-173.
- Kima, D., Ryua, H., Kim, M., Kima, J., Lee, S. (2007). Enhancing struvite precipitation potential for ammonia nitrogen removal in municipal landfill leachate. *Journal of Hazardous Materials* 146: 81–85.
- Kishimoto, N., Yasuda, Y., Mitzutani, H., Ono, Y. (2007). Applicability of Ozonation Combined with Electrolysis to 1,4-Dioxane Removal from Wastewater Containing Radical Scavengers. *Ozone: Science and Engineering* 29: 13-22.
- Kominami, H., Nishimune, H., Ohta, Y., Arakawa, Y., Inaba, T. (2012). Photocatalytic hydrogen formation from ammonia and methyl amine in an aqueous suspension of metal-loaded titanium(IV) oxide particles. *Applied Catalysts B: Environmental* 111-112: 297-302.
- Kosmulski, M., Prochniak, P., Rosenholm, J.B. (2009). Electrokinetic study of adsorption of ionic surfactants on titania from organic solvents. *Colloids and Surfaces A: Physicochemical and Engineering Aspects* 348: 298-300.
- Kurniawan, T.A. and Lo, W. (2009). Removal of refractory compounds from stabilized landfill leachate using an integrated H₂O₂ oxidation and granular activated carbon (GAC) adsorption treatment. *Water Research* 43: 4079–4091.

- Kwon, B.G., Ryu, S., Yoon, J. (2009). Determination of hydroxyl radical rate constants in a continuous flow system using competition kinetics. *Journal of Industrial and Engineering chemistry* 15: 809-812.
- Li, H., Zhoua, S., Sun, Y., Feng, P., Li, J. (2009). Advanced treatment of landfill leachate by a new combination process in a full-scale plant. *Journal of Hazardous Materials* 172: 408–415.
- Liu, C., Yang, Y., Wang, Q., Kim, M., Zhu, Q., Li, D., Zhang, Z. (2012). Photocatalytic degradation of waste activated sludge using a circulating bed photocatalytic reactor for improving biohydrogen production. *Bioresource Technology* 125: 30-36.
- Ma, C.M., Lee, Y.W., Hong, G.B., Su, T.L., Shie, J.L., Chang, C.T. (2011). Effect of platinum on the photocatalytic degradation of chlorinated organic compound. *Journal of Environmental Sciences* 23(4): 687-692.
- Mahmud, K., Hossain, Md. D., Shams, S. (2011). Different treatment strategies for highly polluted landfill leachate in developing countries. *Waste Management*.
- Manahan, S. E. (2005). *Environmental Chemistry*, 8th ed., CRC Press, Boca Raton, FL.
- Mandal, T., Maity, S., Dasgupta, D., Datta, S. (2010). Advanced oxidation process and biotreatment: Their roles in combined industrial wastewater treatment. *Desalination* 250: 87 – 94.

- Marugan, J., van Grieken, R., Pablos, C., Satuf, M.L., Cassano, A.E., Alfano, O.M. (2012). Modeling of a bench-scale photocatalytic reactor for water disinfection from laboratory-scale kinetic data. *Chemical Engineering Journal*.
- Masters, G.M. and Ela, W.P. (2008). Introduction to Environmental Engineering and Science. Pearson Education, Inc., Upper Saddle River, NJ.
- Meeroff, D.E., Gasnier, F., Tsai, C.T. (2008). "Investigation Of Energized Options For Leachate Management: Year Two Tests of Advanced Oxidation Processes for Treatment of Landfill Leachate" Final Report for the William W. "Bill" Hinkley Center for Solid and Hazardous Waste Management, Gainesville, FL. Report # 0632018.
- Meeroff, D.E. and Teegavarapu, R. (2010). "Interactive Decision Support Tool For Leachate Management," Final Report for the William W. "Bill" Hinkley Center for Solid and Hazardous Waste Management, Gainesville, FL. Report # 0832028.
- Meeroff, D.E. and McBarnette, A. (2011). "Energized Processes for Onsite Treatment of Leachate," Final Report for the William W. "Bill" Hinkley Center for Solid and Hazardous Waste Management, Gainesville, FL. Report # 0932015.
- Meeroff, D.E., Bloetscher, F., Reddy, D.V., Gasnier, F., Jain, S., McBarnette, A., Hamaguchi, H. (2012). Application of photochemical technologies for treatment of landfill leachate. *Journal of Hazardous Materials* 209-210: 299-307.

- Mehrjouei, M., Muller, S., Moller, D. (2012). Removal of fuel oxygenates from water using advanced oxidation technologies by means of falling film reactor. *Chemical Engineering Journal* 211-212: 353-359.
- Mohajeri, S., Aziz, H.A., Isa, M.H., Zaheda, M.A., Adlana, M.N. (2010). Statistical optimization of process parameters for landfill leachate treatment using electro-Fenton technique. *Journal of Hazardous Materials* 176: 749–758.
- Naumczyk, J., Prokurat, I., Marcinowski, P. (2012). Landfill Leachates Treatment by H₂O₂/UV, O₃/ H₂O₂, Modified Fenton, and Modified Photo-Fenton Methods. *International Journal of Photoenergy* Volume 2012, Article ID 909157.
- Ohtani, B., Prieto-Mahaney, O.O., Li, D., Abe, R. (2010). What is Degussa (Evonik) P25? Crystalline composition analysis, reconstruction from isolated pure particles and photocatalytic activity test. *Journal of Photochemistry and Photobiology A: Chemistry* 216(2-3): 179-182.
- Pan, L., Zou, J.J., Wang, S., Huang, Z.F., Zhang, X., Wang, L. (2013). Enhancement of visible-light-induced photodegradation over hierarchical porous TiO₂ by nonmetal doping and water-mediated dye sensitization. *Applied Surface Science* 268: 252-258.
- Pelaez, M., Nolan, N.T., Pillai, S.C., Seery, M.K., Falaras, P., Kontos, A.G., Dunlop, P.S.M., Hamilton, J.W.J., Byrne, J.A., O’Shea, K., Entezari, M.H., Dionysiou, D.D. (2012). A review on the visible light active titanium dioxide photocatalysts

for environmental applications. *Applied Catalysts B: Environmental* 125: 331-349.

Poblete, R., Prieto-Rodríguez, L., Oller, I., Maldonado, M.I., Malato, S., Ota, E., Vilches, L.F., Fernández-Pereira, C. (2012). Solar photocatalytic treatment of landfill leachate using a solid mineral by-product as a catalyst. *Chemosphere* 88: 1090–1096.

Qasim, S.R. and Chiang, W. (1994). *Sanitary landfill leachate – Generation, Control and Treatment*. CRC Press, Boca Raton, FL.

Qasim, S.R., Motley, E.M., Zhu, G. (2000). *Water Works Engineering: Planning, Design and Operation*. Pearson Education, Inc., Upper Saddle River, NJ.

Renou, S., Givaudan, J.G., Poulain, S., Dirassouyan, F., Moulin, P. (2008). Landfill leachate treatment: Review and opportunity. *Journal of Hazardous Materials* 150: 468–493.

Rocha, E.M.R., Vilar, V.J.P., Fonseca, A., Saraiva, I., Boaventura, R.A.R. (2011). Landfill leachate treatment by solar-driven AOPs. *Solar Energy* 85: 46-56.

Salem, Z., Hamouri, K., Djemaa, R., Allia, K. (2008). Evaluation of landfill leachate pollution and treatment. *Desalination* 220: 108–114.

Sangchay, W., Sikong, L., Kooptarnond, K. (2012). Comparison of photocatalytic reaction of commercial P25 and synthetic TiO₂-AgCl nanoparticles. *Procedia Engineering* 32: 590-596.

- Sanphoti, N., Towprayoon, S., Chaiprasert, P., Nopharatana, A. (2006). The effects of leachate recirculation with supplemental water addition on methane production and waste decomposition in a simulated tropical landfill. *Journal of Environmental Management* 81: 27–35.
- Selvam, K., Muruganandham, M., Sobana, N., Swaminathan, M. (2007). Enhancement of UV-assisted photo-Fenton degradation of reactive orange 4 using TiO₂-P25 nanoparticles. *Separation and Purification Technology* 54: 241-247.
- Shephard, G.S., Stockenstrom, S., de Villiers, D., Engelbrecht, W.J., Wessels, G.F.S. (2002). Degradation of microcystin toxins in a falling film photocatalytic reactor with immobilized titanium dioxide catalyst. *Water Research* 36: 140-146.
- State Water Resources Control Board (SWRCB). (2010). <http://www.swrcb.ca.gov/water_issues/programs/swamp/docs/cwt/guidance/3159.pdf> (Dec. 15, 2012).
- Suryaman, D., Hasegawa, K. (2010). Color of Water Fact Sheet. *Journal of Hazardous Materials* 183: 490-496.
- Tamrat, M., Costa, C., Márquez, M.C. (2012). Biological treatment of leachate from solid wastes: Kinetic study and simulation. *Biochemical Engineering Journal* 66: 46–51.
- Teh, C.M. and Mohamed, A.R. (2011). Roles of titanium dioxide and ion-doped titanium dioxide on photocatalytic degradation of organic pollutants (phenolic compounds

and dyes) in aqueous solutions: A review. *Journal of Alloys and Compounds* 509: 1648-1660.

United States Environmental Protection Agency (USEPA). (1985). Ambient Water Quality Criteria for Ammonia - 1984 *EPA* 440/5-85-O1.

U.S. Environmental Protection Agency (USEPA). (1999). U.S. Methane Emissions 1990 – 2020: Inventories, Projections, and Opportunities for Reductions. Chapter 2: Landfills. *USEPA*.

U.S. Environmental Protection Agency (USEPA). (2012). “National Recommended Water Quality Criteria.” <<http://water.epa.gov/scitech/swguidance/standards/criteria/current/index.cfm#cm>> (Sept. 13, 2012).

U.S. Environmental Protection Agency (USEPA). (2012). “Secondary Drinking Water Regulations: Guidance for Nuisance Chemicals” <<http://water.epa.gov/drink/contaminants/secondarystandards.cfm>> (Sept. 14, 2012).

U.S. Environmental Protection Agency (USEPA). (2012). “Managing Nonhazardous Solid Waste” <<http://www.epa.gov/osw/inforesources/pubs/orientat/rom2.pdf>> (Dec. 14, 2012).

United States Geological Survey (USGS). (2012). Titanium and Titanium Dioxide. *Mineral Commodity Summaries* January 2012.

- Valencia, S., Catano, F., Rios, L., Restrepo, G., Marin, J. (2011). A new kinetic model for heterogeneous photocatalysis with titanium dioxide: Case of non-specific adsorption considering back reaction. *Applied Catalysis B: Environmental* 104: 300-304.
- Vedrenne, M., Vasquez-Medrano, R., Prato-Garcia, D., Frontana-Uribe, B., Ibanez, J.G. (2012). Characterization and detoxification of a mature landfill leachate using a combined coagulation–flocculation/photo Fenton treatment. *Journal of Hazardous Materials* 205-206: 208-215.
- Vilar, V. J.P., Rocha, E. M.R., Mota, F. S., Fonseca, A., Saraiva, I., Boaventura, R. A.R. (2011). Treatment of a sanitary landfill leachate using combined solar photo-Fenton and biological immobilized biomass reactor at a pilot scale. *Water Research* 45: 2647-2658.
- Vineetha, M.N., Matheswaran, M., Sheeba, K.N. (2012). Photocatalytic colour and COD removal in the distillery effluent by solar radiation. *Solar Energy*.
- Wang, J.L. and Xu, L.J. (2012). Advanced Oxidation Processes for Wastewater Treatment: Formation of Hydroxyl Radical and Application. *Critical Reviews in Environmental Science and Technology* 42:3: 251-325.
- Wang, Q., Chen, X., Yu, K., Zhang, Y., Cong, Y. (2013). Synergistic photosensitized removal of Cr(VI) and Rhodamine B dye on amorphous TiO₂ under visible light irradiation. *Journal of Hazardous Materials* 246-247: 135-144.

- Wenjen, L., Di, W., Xin, S., Lixiong, W., Lei, S. (2012). Removal of Organic Matter and Ammonia Nitrogen in Azodicarbonamide Wastewater by a Combination of Power Ultrasound Radiation and Hydrogen Peroxide. *Chinese Journal of Chemical Engineering* 20(4): 754-759.
- Westlake, K. and M. Phil. (1995). *Landfill Waste Pollution and Control*. Albion Publishing, Chichester, West Sussex, England.
- World Health Organization (WHO). (2003). Ammonia in drinking-water. Background document for preparation of WHO Guidelines for drinking-water quality. Geneva, World Health Organization (WHO/SDE/WSH/03.04/1).
- Xing, W., Lu, W., Zhao, Y., Deng, W., Christensen, T. H. (2012). Environmental impact assessment of leachate recirculation in landfill of municipal solid waste by comparing with evaporation and discharge (EASEWASTE). *Waste Management*.
- Yahiat, S., Fourcade, F., Brosillon, S., Amrane, A. (2011). Photocatalysis as a pre-treatment prior to a biological degradation of cyproconazole. *Desalination* 281: 61-67.
- Zhang, H., Wu, X., Li, X. (2012). Oxidation and coagulation removal of COD from landfill leachate by Fered–Fenton process. *Chemical Engineering Journal* 210: 188-194.
- Zhao, J., Yang, X. (2003). Photocatalytic oxidation for indoor air purification: a literature review. *Building and Environment* 38: 645-654.

Zhao, R., Huang, T., McGuire, M. (2012). From a Literature Review to an Alternative Treatment System for Landfill Gas and Leachate. *Challenges* 3: 278-289.

Zhao, X., Qu, J., Liu, H., Wang, C., Xiao, S., Liu, R., Liu, P., Lan, H., Hu, C. (2010). Photoelectrochemical treatment of landfill leachate in a continuous flow reactor. *Bioresource Technology* 101: 865–869.